# University of Alberta

Effect of Chlorine on the Melting of the Subcratonic Lithospheric Mantle

by

Linglin Chu

A thesis submitted to the Faculty of Graduate Studies and Research
in partial fulfillment of the requirements for the degree of

Master of Science

Department of Earth & Atmospheric Sciences



Spring 2010
Edmonton, Alberta

## Examining Committee

Jeff Gu, Department of Physics

Tom Chacko, Department of Earth & Atmospheric Sciences

Robert W. Luth, Department of Earth & Atmospheric Sciences

## Abstract

The presence of chlorine in the subcratonic lithospheric mantle (SCLM) has been evaluated by compiling the compositional data of fluid inclusions in fibrous diamonds. Chlorine associates with potassium, dissolving in water and forming a KCl-bearing brine with the $Cl/(Cl+H_2O)$ molar ratio of 0.05-0.68.

To examine the effect of such a KCl-bearing brine on the melting behavior of the SCLM, we conducted experiments in the $Mg_2SiO_4$-$MgSiO_3$-$H_2O$ and $Mg_2SiO_4$-$MgSiO_3$-KCl-$H_2O$ systems at 5 GPa and 1100-1700 ℃. In the $Mg_2SiO_4$-$MgSiO_3$-$H_2O$ system, the solidus temperature of forsterite+enstatite is ~1230 ℃. In the $Mg_2SiO_4$-$MgSiO_3$-KCl-$H_2O$ systems with molar $Cl/(Cl+H_2O)$ ratios of 0.2, 0.4 and 0.6, the solidus temperatures are ~1430 ℃, ~1530 ℃ and ~1580 ℃, respectively. The increase in the temperature of the solidus demonstrates that KCl elevates the solidus of the $Mg_2SiO_4$-$MgSiO_3$-$H_2O$ system. Therefore, KCl in the SCLM can prevent melting at the $H_2O$-saturated solidus, and a KCl-bearing fluid can be a robust agent for mantle metasomatism.

**Acknowledgment**

Establishing the method of study and writing this thesis were not easy tasks, and I would like to express thanks to my supervisor, Dr. Robert W. Luth, a professor of Igneous Petrology and Experimental Geochemistry in the Department of Earth & Atmospheric Sciences at the University of Alberta, for giving me his continuous guidance, supervision and advice on this research. I am grateful for his wisdom and academic strength, and I will carry the knowledge gained into future studies.

I would like to acknowledge Diane Caird, the Superpress and X-ray Technician in the Department of Earth & Atmospheric Sciences at the University of Alberta, for teaching me sample assembly and how to operate the Superpress. But more than that, I'd like to express appreciation for her motherly care while I was in the lab.

I would like to acknowledge Dr. Sergi Matveev, the Microprobe Technician in the Department of Earth & Atmospheric Sciences at the University of Alberta, and Dr. Tom Chacko, a professor in the Department of Earth & Atmospheric Sciences at the University of Alberta, for helping me develop skills and solve problems when using the microprobe.

Finally, I would like to thank my buddies, Andreas Enggist and Xianmin Hu. "A friend in need is a friend indeed."

## Table of Contents

## List of Tables

## List of Figures

## Abbreviations

| | |
|---|---|
| ℃ | degree celsius |
| cm | centimeter |
| GPa | gigapascal |
| h | hour |
| km | kilometer |
| kV | kilovolt |
| min | minute |
| mm | millimeter |
| mol% | molar percent |
| nA | nanoampere |
| P | pressure |
| ppm | part per million |
| s | second |
| T | temperature |
| wt% | weight percent |

## Chapter 1. Introduction

"Volatiles" in the petrological literature are constituents that are liquid or gaseous at normal Earth's surface conditions, and they mainly include $H_2O$, $CO_2$ and sulfur-bearing and halogen-bearing species (Luth, 2003). Present in the Earth's mantle, these constituents can have significant effects on the stability and physical-chemical properties of partial melts and the mantle (Dasgupta and Dixon, 2009; and references therein). Of these volatiles, halogens are rarely studied from mantle samples, and their effects on mantle processes are poorly constrained by experiments. Based on studies of fluid inclusions in fibrous diamonds (Johnson et al., 2000; Burgess et al., 2002; Burgess et al., 2009), chlorine has much higher concentrations than other halogens in the mantle-derived fluids, which indicates that chlorine is the dominant halogen in the upper mantle and may play a more significant role than fluorine, bromine or iodine.

The existence of chlorine in the upper mantle has been documented in different tectonic settings over the past 30 years. In subduction zones, chlorine exists as solutes in subduction-related magmas (Perfit *et al.*, 1980; Poorter *et al.*, 1989; Kent et al., 2002) and as highly saline fluid inclusions in subduction zone metasediments (Philippot, 1993) and eclogite-facies rocks (Scambelluri and Philippot, 2001). In cratonic areas, the existence of chlorine in the upper mantle is evidenced by alkali chlorides in kimberlite groundmass (Kamenetsky *et al.*, 2004), chlorine-rich fluids trapped in fibrous diamonds (Izraeli et al., 2001; Tomlinson et al., 2006; Klein-BenDavid et al., 2007) and chlorine-bearing apatite and mica in mantle xenoliths (Smith *et al.*, 1981; Smith, 1981). In a Group I

kimberlite described as “exceptionally fresh” from the Udachnaya-East pipe in Siberia, alkali chlorides, alkali carbonates and sulfates (ratio 5:3:1) were found as >8 wt% of the groundmass (Kamenetsky *et al.*, 2004). A mantle origin of these chlorides and carbonates has been confirmed by Sr, Nd and Pb isotope studies (Kamenetsky *et al.*, 2004; Maas *et al.*, 2005). In fibrous diamonds from the Diavik mine in Canada, fluid inclusions can have chlorine contents up to 34.2 wt% (Klein-BenDavid *et al.*, 2007). In mantle xenoliths, chlorine content can be up to 1.0 wt% in apatite and 0.05 wt% in mica (Smith, 1981; Smith *et al.*, 1981).

If widespread in the upper mantle, chlorine could potentially play important roles in affecting partial melting and metasomatism of the mantle and also in affecting physical-chemical properties of resulting melts or fluids. Experiments at pressures of <0.9 GPa show that chlorine reduces the activity of water in hydrous systems and increases the melting temperature of albite relative to the pure water case (Shmulovich and Graham, 1996). If this reduction of water activity still happens under high-pressure conditions, we anticipate that chlorine will increase the vapor-saturated solidus of hydrous peridotites and thereby prevent melting and stabilize water-rich fluids, which are effective agents for mantle metasomatism. Moreover, Keppler (1996) proposed that chloride would favor complexing with ions, such as $Rb^{2+}$, $Ba^{2+}$, $Sr^{2+}$ and $Pb^{2+}$, rather than with more highly charged cations, such as $Nb^{5+}$ and $Ta^{5+}$. Chemical transport by the chlorine-rich fluid will generate the relative enrichment of large ionic lithophile elements, such as Pb and U, and the relative depletion in high field strength elements, such as Nb and Ta, which has been invoked to explain the trace element pattern for calc-alkaline

magmas in subduction zones where chlorine can be transported by subducted slab into the mantle and then released to the mantle wedge.

This thesis is composed of two sections. The first section (Chapter 2) compiles compositional data of fluid inclusions in fibrous diamonds in order to evaluate the composition of chlorine-bearing fluids in the subcratonic lithospheric mantle. The second section (Chapter 3) reports the results of high pressure and temperature experiments in the $Mg_2SiO_4$-$MgSiO_3$-$H_2O$ and $Mg_2SiO_4$-$MgSiO_3$-KCl-$H_2O$ systems to reveal the effects of chlorine on the melting of the hydrous Earth's mantle.

**References**

Burgess, R., Layzelle, E., Turner, G. and Harris, J.W., 2002, Constraints on the age and halogen composition of mantle fluids in Siberian coated diamonds: Earth and Planetary Science Letters, v. 197, p. 193-203.

Burgess, R., Cartigny, P., Harrison, D., Hobson, E. and Harris, J., 2009, Volatile composition of microinclusions in diamonds from the Panda kimberlite, Canada: Implications for chemical and isotopic heterogeneity in the mantle: Geochimica et Cosmochimica Acta, v. 73, p. 1779-1794.

Dasgupta, R., and Dixon, J.E., 2009, Volatiles and volatile-bearing melts in the Earth's interior: Chemical Geology, v. 262, p.1-3.

Izraeli, E.S., Harris, J.W. and Navon, O., 2001, Brine inclusions in diamonds: a new upper mantle fluid: Earth and Planetary Science Letters, v. 187, p. 323-332.

Johnson, L.H., Burgess, R., Turner, G., Hariss, J.H. and Milledge, H.J., 2000, Noble gas and halogen geochemistry of mantle fluids in diamonds: comparison of African and Canadian stones: Geochimica et Cosmochimica Acta, v. 64, p. 717-732.

Kamenetsky, M.B., Sobolev, A.V., Kamenetsky, V.S., Maas, R., Danyushevsky, L.V., Thomas, R., Pokhilenko, N.P. and Sobolev, N.V., 2004, Kimberlite melts rich in alkali chlorides and carbonates: A potent metasomatic agent in the mantle: Geology, v 32, p. 845-848.

Kent, A.J.R., Peate, D.W., Newman, S., Stolper, E.M. and Pearce, J.A., 2002, Chlorine in submarine glasses from the Lau Basin: seawater contamination and

constraints on the composition of slab-derived fluids: Earth and Planetary Science Letters, v. 202, p. 361-377.

Keppler, H., 1996, Constraints from partitioning experiments on the composition of subduction-zone fluids: Nature, v. 380, p. 237-240.

Klein-BenDavid, O., Izraeli, E.S., Hauri, E. and Navon, O., 2007, Fluid inclusions in diamonds from the Diavik mine, Canada and the evolution of diamond-forming fluids: Geochimica et Cosmochimica Acta, v. 71, p. 723-744.

Luth, R.W., 2003, Mantle volatiles-distribution and consequences. *in* Carlson R.W., Holland, H.D. and Turekian, K.K., ed., The mantle and core: Treatise on Geochemistry, v. 2, p. 319-361.

Maas, R., Kamenetsky, M.B., Sobolev, A.V., Kamenetsky, V.S., and Sobolev, N.V., 2005, Sr, Nd and Pb isotope evidence for a mantle origin of alkali chlorides and carbonates in the Udachnaya kimberlite, Siberia: Geology, v. 33, p. 549-552.

Perfit, M.R., Gust, D.A., Bence, A.E., Arculus, R.J. and Taylor, S.R., 1980, Chemical characteristics of island-arc basalts: Implications for mantle sources: Chemical Geology, v. 30, p. 227-265.

Philippot, P., 1993, Fluid-melt-rock interaction in mafic eclogites and coesite-bearing metasediments: Constraints on volatile recycling during subduction: Chemical Geology, v. 108, p. 93-112.

Poorter, R.P.E., Varekamp, J.C., Vanbergen, M.J., Kreulen, R., Sriwana, T., Vroon, P.Z. and Wirakusumah, A.D., 1989, The Sirung volcanic boiling spring: An extreme chloride-rich, acid brine on Pantar (Lesser Sunda Islands, Indonesia): Chemical Geology, v. 76, p. 215-228.

Scambelluri, M. and Philippot, P., 2001, Deep fluids in subduction zones: Lithos, v. 55, p. 213-227.

Shmulovich, K.I. and Graham, C.M., 1996, Melting of albite and dehydration of brucite in $H_2O$-NaCl fluids to 9 kbars and 700-900°C: implications for partial melting and water activities during high pressure metamorphism: Contributions to Mineralogy and Petrology, v. 124, p. 370-382.

Smith, J.V., 1981, Halogen and phosphorus storage in the Earth: Nature, v. 289, p. 762-765.

Smith, J.V., Delaney, J.S., Herving, R.L. and Dawson, J.B., 1981, Storage of F and Cl in the upper mantle: geochemical implications: Lithos, v. 14, p. 133-147.

Tomlinson, E.L., Jones, A.P. and Harris, J.W., 2006, Co-existing fluid and silicate inclusions in mantle diamond: Earth and Planetary Science Letters, v. 250, p. 581-595.

## Chapter 2. Chlorine-bearing fluids in the subcratonic lithospheric mantle

### Introduction

The presence of chlorine-bearing fluids in the subcratonic lithospheric mantle (SCLM) has been documented by fluid inclusions in fibrous diamonds (Izraeli et al., 2001; Tomlinson et al., 2006; Klein-BenDavid et al., 2007). Because of their mechanical strength and chemical inertness, diamonds are probably the best material for transporting pristine fluid samples from the mantle to the surface (Navon et al., 1988). According to studies of syngenetic mineral inclusions in fibrous diamonds from both Koffiefontein in South Africa (Izraeli et al., 2004) and the Panda mine in Canada (Tomlinson et al., 2006), fibrous diamonds formed mainly at the pressure of 4-6 GPa and the temperature of 900-1200 ℃. Therefore, the fluids trapped in the diamonds can represent fluids at depths of 130-200 km in the SCLM.

Compositions of the trapped fluids in the fibrous diamonds from different cratons have been reported by Schrauder and Navon (1994), Izraeli et al. (2001), Shiryaev et al. (2005), Tomlinson et al. (2006), Klein-BenDavid et al. (2006), Klein-BenDavid et al.(2007) and Klein-BenDavid et al. (2009). In the reported compositions, some components were analyzed but others were calculated based on various assumptions. Therefore, these data incorporate both analytical uncertainties and uncertainties associated with the assumptions inherent to the calculations, which introduces limitations in applying these data to reveal the compositions of fluids in the SCLM. Moreover, both $H_2O$ and Cl have been found as common components in the trapped fluids and the $Cl/(Cl+H_2O)$ molar ratio

may control the compositions of the trapped fluids, however, this $Cl/(Cl+H_2O)$ molar ratio has not been calculated in the previous studies.

This chapter compiles the reported compositional data of fluid inclusions in fibrous diamonds and examines their limitations, with the aim to achieve a more accurate understanding of the compositions of chlorine-bearing fluids in the SCLM. Based on the more accurate understanding of compositions, the range of $Cl/(Cl+H_2O)$ molar ratio for the fluids is calculated in this chapter, which will guide the preparation of starting materials in the next chapter (Chapter 3).

**Data compilation**

The compositions of sub-micrometer fluid inclusions have been reported in cubic fibrous diamonds, fibrous coats of octahedral diamonds and some undefined diamond fragments from Jwaneng in Botswana (Schrauder and Navon, 1994), Koffiefontein in South Africa (Izraeli et al., 2001), Brazil (Shiryaev et al., 2005), Diavik and Panda mines in Canada (Tomlinson et al., 2006; Klein-BenDavid et al., 2006; Klein-BenDavid et al., 2007) and Yakutia diamond field in Russia (Klein-BenDavid et al., 2006; Klein-BenDavid et al., 2009). Elements such as Si, Ti, Al, Cr, Fe, Mg, Ca, Ba, Sr, Na, K, P, S and Cl, were analyzed by electron probe microanalysis (EPMA) for individual inclusions. Volumes activated by the electron beam are bigger than inclusion volumes, and therefore the totals of the analyses are significantly lower than 100%. Schrauder and Navon (1994), being aware of the uncertainty arising from variable inclusion depths and the assumption of a uniform matrix, estimated precision of 10-40% for the various oxides in individual analyses and less than 10% for the sample averages. They

also estimated that the accuracy of the results obtained by EPMA is in the range of 10-15% by comparing the EPMA data with proton-probe and neutron activation data of the same diamonds. Izraeli et al. (2004) estimated the EPMA precision and accuracy by examination of olivine microinclusions in clouds of fibrous diamonds. They estimated the precision to be better than ~15% by analyzing the same mineral inclusions at different dates and with different EDS systems, and they estimated the accuracy to be in the range of only a few percent for the most abundant elements by comparing the range of Mg/(Mg+Fe) molar ratio and Si/(Mg+Fe) molar ratio of olivine microinclusions with those of large olivine inclusions in diamonds.

Infrared absorption spectra of the fibrous diamonds were collected with Fourier transform infrared spectroscopy (FTIR). The absorption of the trapped materials in fluid inclusions was obtained after correcting the spectrum for baseline and diamond absorption. The most common bands after the corrections are those of carbonate and water. The $[CO_3]^{2-}/([CO_3]^{2-}+H_2O)$ molar ratio was estimated from the maximum height of net absorption bands of carbonate and water at ~1430 and ~3420 $cm^{-1}$ and Beer's law. The entire wafer thickness of diamond was sampled by IR spectroscopy, but it can be cancelled in calculating the $[CO_3]^{2-}/([CO_3]^{2-}+H_2O)$ molar ratio, because the thickness is the same for both $[CO_3]^{2-}$ and $H_2O$ for each analysis if assuming that $H_2O$ and $[CO_3]^{2-}$ are in same inclusions. Because different absorption coefficients were used in the different studies, the $[CO_3]^{2-}/([CO_3]^{2-}+H_2O)$ molar ratio has been recalculated in this thesis using consistent absorption coefficients ($\varepsilon_{calcite}$ = 250 L/mol $cm^{-1}$ (~1430 $cm^{-1}$)

(Navon et al., 1988), $\varepsilon_{\text{liquid water}}$ = 80 L/mol cm$^{-1}$ (3420 cm$^{-1}$) (Thompson, 1965), which are believed by Navon et al. (1988) to be representative of the absorption by the carbonate and hydrous species in the inclusions). As stated by Navon et al. (1988), absorption coefficients of other carbonates (for example, $Na_2CO_3$, gaylucite) differ from that of calcite by less than 30%, and the water absorption coefficient is accurate to ~30%[1].

Based on results of a transmission electron microscopy study on four diamonds from Canada and Siberia, together with the tight range of composition detected by EPMA and the volatiles detected by FTIR, Klein-BenDavid et al. (2006) suggested that the fluids trapped in inclusions were uniform, dense and supercritical and then evolved to secondary phases, including crystallized minerals and low-density fluids, during cooling. Most elements in fluid inclusions are hosted in the crystallized minerals such as silicates, carbonates, phosphate, sulfates and chlorides, which is supported by the agreement of the composition of the whole inclusion to that of its daughter crystals (Klein-BenDavid et al., 2006). Based on these observations, Klein-BenDavid et al. (2006) postulated that $Ca^{2+}$, $Mg^{2+}$, $Fe^{2+}$, $Ba^{2+}$, $Na^{+}$ and $K^{+}$ were balanced by $[Cl]^{-}$, $[PO_4]^{3-}$ and $[CO_3]^{2-}$ to form chloride, phosphate and carbonate and that $Si^{4+}$, $Ti^{4+}$ and $Al^{3+}$ were balanced by $O^{2-}$ to form silicates, and they calculated the $[CO_3]^{2-}$ content by the formula: $[CO_3]^{2-} = Ca^{2+} + Mg^{2+} + Fe^{2+} + Ba^{2+} + 0.5Na^{+} + 0.5K^{+} - 0.5[Cl]^{-} - 1.5[PO_4]^{3-}$. Based on studies of minerals crystallized from trapped fluids in more fibrous

[1] The original paper states this accuracy to be "-30%". The assignment of accuracy as a negative percentage makes no sense; I believe the authors meant "~30%".

diamonds, Klein-BenDavid et al. (2007) assumed that $Ti^{4+}$, $Ca^{2+}$, $Mg^{2+}$, $Fe^{2+}$, $Ba^{2+}$, $Na^{+}$ and $K^{+}$ were balanced by $[Cl]^{-}$, $[PO_4]^{3-}$, $[CO_3]^{2-}$ and $[SiO_4]^{4-}$ and that $Si^{4+}$ and $Al^{3+}$ were associated with $Mg^{2+}$, $Fe^{2+}$ and $K^{+}$ in proportions to form mica, and they changed the formula to be $[CO_3]^{2-} = 2Ti^{4+} + Ca^{2+} + Mg^{2+} + Fe^{2+} + Ba^{2+} + 0.5Na^{+} + 0.5K^{+} - 0.5[Cl]^{-} - 1.5[PO_4]^{3-} - [SiO_4]^{4-}$. In this formula, $[SiO_4]^{4-}$ is subtracted with the factor of 1, which implies for the silicates with the (2Ti + Ca + Mg + Fe + Ba + 0.5Na + 0.5K)/Si molar ratio of 1, such as pyroxenes. Following the calculation of the $[CO_3]^{2-}$ content, the $H_2O$ content can be calculated by using the $[CO_3]^{2-}$ content and the $[CO_3]^{2-}/([CO_3]^{2-}+H_2O)$ molar ratio.

In this thesis, only Si, Al, Fe, Mg, Ca, Na, K and Cl are considered (Table 2-1) because the other elements such as Ti, Cr, Ba, Sr, P and S are minor (<5mol% for each) and not always reported. These elements, together with the $[CO_3]^{2-}/([CO_3]^{2-}+H_2O)$ molar ratio, are calculated into four components with a total of 100 mol%, including silica tetrahedron ($[SiO_4]^{4-}$), carbonate ion ($[CO_3]^{2-}$), chloride ion ($[Cl]^{-}$) and water molecule ($H_2O$) , where $[SiO_4]^{4-} = Si^{4+}$, $[CO_3]^{2-} = Ca^{2+} + Mg^{2+} + Fe^{2+} + 0.5Na^{+} + 0.5K^{+} – 0.5[Cl]^{-}$, $[Cl]^{-} = [Cl]^{-}$, and $H_2O = [CO_3]^{2-}(1/\alpha–1)$ where $\alpha = [CO_3]^{2-}/([CO_3]^{2-}+H_2O)$ from FTIR.

Table 2-1. Original compositional data of fluid inclusions in fibrous diamonds.

| Sample | Location | Num | wt% | | | | | | | | C/CH | References |
|---|---|---|---|---|---|---|---|---|---|---|---|---|
| | | | $SiO_2$ | $Al_2O_3$ | FeO | MgO | CaO | $Na_2O$ | $K_2O$ | Cl | tot | |
| ON-DVK-269 | Diavik, Canada | 12 | 4.1 | 0.7 | 6.1 | 2.3 | 4.8 | 9.5 | 31.9 | 34.2 | 3.1 | 0.15 | Klein-BenDavid et al., 2007 |
| ON-DVK-272 | Diavik, Canada | 18 | 3.8 | 0.9 | 7.5 | 3.9 | 7.5 | 8.3 | 29.1 | 3.8 | 3.5 | 0.21 | Klein-BenDavid et al., 2007 |
| ON-DVK-275 | Diavik, Canada | 19 | 5.2 | 0.7 | 5.9 | 4.5 | 6.4 | 11.8 | 24.7 | 30.7 | 3.6 | 0.13 | Klein-BenDavid et al., 2007 |
| ON-DVK-276 | Diavik, Canada | 11 | 2.8 | 0.5 | 7.1 | 3.83 | 2.5 | 11.1 | 27.1 | 32.4 | 4.4 | 0.27 | Klein-BenDavid et al., 2007 |
| ON-DVK-280 | Diavik, Canada | 33 | 3.8 | 3 | 5.5 | 2.2 | 4 | 13 | 23.7 | 32.1 | 3.7 | 0.33 | Klein-BenDavid et al., 2007 |
| ON-DVK-282 | Diavik, Canada | 13 | 2.9 | 0.7 | 6.6 | 3 | 4.8 | 8.8 | 29.9 | 32.8 | 4.1 | 0.3 | Klein-BenDavid et al., 2007 |
| ON-DVK-283 | Diavik, Canada | 20 | 4.2 | 0.5 | 5.9 | 4 | 5.6 | 11.5 | 27.5 | 30 | 3.6 | 0.39 | Klein-BenDavid et al., 2007 |
| ON-DVK-286 | Diavik, Canada | 23 | 3.4 | 0.8 | 6.8 | 3.8 | 5.8 | 12.8 | 24.7 | 31.8 | 5.4 | 0.22 | Klein-BenDavid et al., 2007 |
| ON-DVK-287 | Diavik, Canada | 20 | 3.5 | 0.5 | 5.3 | 5.9 | 7.3 | 13.9 | 25.4 | 28.9 | 4.2 | 0.36 | Klein-BenDavid et al., 2007 |
| ON-DVK-288 | Diavik, Canada | 20 | 5 | 0.6 | 5.2 | 5.2 | 6.7 | 10.2 | 26.8 | 30.3 | 3.4 | 0.19 | Klein-BenDavid et al., 2007 |
| ON-DVK-281 | Diavik, Canada | 48 | 27.5 | 3.6 | 12.6 | 6.2 | 14.3 | 3.2 | 22.5 | 1.6 | 3.4 | 0.27 | Klein-BenDavid et al., 2007 |
| PAN2 | Panda, Canada | 43 | 4.6 | 1.4 | 12.2 | 5.7 | 7.1 | 3.9 | 22.4 | 21.3 | 13.5 | 0.34 | Tomlinson et al., 2006 |
| PAN3 | Panda, Canada | 17 | 3.1 | 0.8 | 6.9 | 3.3 | 4.9 | 4.6 | 27.9 | 29.2 | 6.1 | 0.35 | Tomlinson et al., 2006 |
| PAN4 | Panda, Canada | 13 | 15.1 | 1.7 | 9.8 | 1.2 | 4.9 | 4.1 | 26 | 22.2 | 8 | 0.30 | Tomlinson et al., 2006 |
| PAN5 | Panda, Canada | 22 | 5.8 | 1.9 | 26.8 | 7.8 | 12.7 | 5.9 | 12.7 | 13.1 | 7.9 | 0.39 | Tomlinson et al., 2006 |
| PAN6 | Panda, Canada | 27 | 4 | 1.3 | 16.9 | 4.6 | 7.6 | 7.6 | 21.9 | 23.4 | 7.9 | 0.41 | Tomlinson et al., 2006 |
| PAN7 | Panda, Canada | 28 | 3.5 | 0.8 | 18.9 | 4.9 | 9 | 9 | 19.9 | 21.4 | 23.2 | 0.42 | Tomlinson et al., 2006 |
| PAN8 | Panda, Canada | 17 | 4.5 | | 13.6 | 5.5 | 7.4 | 11.8 | 22.4 | 26.6 | 5.1 | 0.41 | Tomlinson et al., 2006 |
| JWN90 | Jwaneng, Botswana | 50 | 25.1 | 2.5 | 16.1 | 10.1 | 15.6 | 2.6 | 18.3 | 1.3 | | 0.7 | Schrauder and Navon, 1994 |
| JWN87 | Jwaneng, Botswana | 92 | 25.6 | 2 | 17.5 | 10.8 | 16.3 | 2.2 | 15.4 | 1 | | 0.5 | Schrauder and Navon, 1994 |
| JWN106 | Jwaneng, Botswana | 16 | 28.4 | 2.2 | 14.9 | 10.6 | 12.6 | 3 | 18.4 | 1.7 | | 0.4 | Schrauder and Navon, 1994 |
| JWN89 | Jwaneng, Botswana | 27 | 29.4 | 2.9 | 16.1 | 8.2 | 13.4 | 2.3 | 18.1 | 0.9 | | 0.6 | Schrauder and Navon, 1994 |
| JWN112 | Jwaneng, Botswana | 70 | 36.5 | 4.2 | 13.5 | 7.8 | 9.1 | 2.5 | 16.9 | 0.7 | | 0.5 | Schrauder and Navon, 1994 |
| JWN110 | Jwaneng, Botswana | 42 | 41.3 | 4.9 | 11.1 | 5.1 | 6.8 | 2.4 | 18.7 | 1.1 | | 0.4 | Schrauder and Navon, 1994 |
| JWN99 | Jwaneng, Botswana | 34 | 44.1 | 4.6 | 10.5 | 5.8 | 5.6 | 2.2 | 17.8 | 1 | | 0.1 | Schrauder and Navon, 1994 |
| JWN91 | Jwaneng, Botswana | 34 | 45.1 | 5.4 | 10.7 | 5.7 | 5.1 | 1.6 | 16.4 | 0.8 | | 0.3 | Schrauder and Navon, 1994 |
| JWN92 | Jwaneng, Botswana | 42 | 47.8 | 5.5 | 9.9 | 4.8 | 4.7 | 3 | 15.3 | 0.8 | | 0.4 | Schrauder and Navon, 1994 |
| JWN88 | Jwaneng, Botswana | 12 | 50.1 | 6.2 | 9.8 | 4.6 | 3.2 | 0.3 | 15.9 | 1.4 | | 0.2 | Schrauder and Navon, 1994 |
| JWN115 | Jwaneng, Botswana | 76 | 50.3 | 5.3 | 12.2 | 4.4 | 3.3 | 2.8 | 12.1 | 1.2 | | 0.2 | Schrauder and Navon, 1994 |
| JWN93 | Jwaneng, Botswana | 36 | 52.3 | 5.6 | 8.8 | 5.1 | 5.5 | 2 | 11.5 | 0.7 | | 0.2 | Schrauder and Navon, 1994 |
| 155 | Koffiefontein, South Africa | 2 | 5.1 | 0 | 20.6 | 1.7 | 7.7 | 5.2 | 26.8 | 27.8 | 3.5 | 0.08 | Izraeli et al., 2001 |

Note: C/CH represents $[CO_3]^{2-}/([CO_3]^{2-}+H_2O)$ molar ratio.

Table 2-1 (continued). Original compositional data of fluid inclusions in fibrous diamonds.

| Sample | Location | Num | wt% | | | | | | | | C/CH | References |
|---|---|---|---|---|---|---|---|---|---|---|---|---|
| | | | $SiO_2$ | $Al_2O_3$ | FeO | MgO | CaO | $Na_2O$ | $K_2O$ | Cl | tot | |
| 156 | Koffiefontein, South Africa | 15 | 5.1 | 0.5 | 14.5 | 1.1 | 11.1 | 4.6 | 28.8 | 38.5 | 4.2 | 0.09 | Izraeli et al., 2001 |
| 159 | Koffiefontein, South Africa | 7 | 7.2 | 0.7 | 14.2 | 1.8 | 4.7 | 1.1 | 36.5 | 43.2 | 4.1 | 0.02 | Izraeli et al., 2001 |
| 162 | Koffiefontein, South Africa | 13 | 5.9 | 0.3 | 20.3 | 1.8 | 9.6 | 4.4 | 26.7 | 31.2 | 4.3 | 0.23 | Izraeli et al., 2001 |
| 165 | Koffiefontein, South Africa | 31 | 7.1 | 0.5 | 10.1 | 1.1 | 3.7 | 2.8 | 39 | 42.2 | 4.2 | 0.004 | Izraeli et al., 2001 |
| 175 | Koffiefontein, South Africa | 13 | 3.7 | 0.4 | 20 | 2.2 | 7.7 | 2 | 30.6 | 35.7 | 6.4 | 0.18 | Izraeli et al., 2001 |
| 176 | Koffiefontein, South Africa | 11 | 8.9 | 0.6 | 22 | 2 | 7.5 | 4.1 | 25.5 | 29.3 | 3.7 | 0.055 | Izraeli et al., 2001 |
| UB 5-41 | Yakutia, Russia | 2 | 7.3 | 1.5 | 9.5 | 10.6 | 15.3 | 12.1 | 24.5 | 7.8 | 3.6 | 0.56 | Klein-BenDavid et al., 2009 |
| UDC 239 | Yakutia, Russia | 52 | 9.8 | 1.1 | 7.3 | 25.5 | 20.5 | 9.5 | 17.3 | 2.5 | 5.4 | 0.64 | Klein-BenDavid et al., 2009 |
| UDC 241 | Yakutia, Russia | 35 | 8.5 | 0.6 | 7.9 | 19.1 | 17.7 | 10.5 | 24 | 5.4 | 4.4 | 0.64 | Klein-BenDavid et al., 2009 |
| UDC 243 | Yakutia, Russia | 7 | 8.5 | 1.5 | 11.2 | 17.7 | 15.4 | 8.8 | 22 | 4.7 | 2.2 | 0.62 | Klein-BenDavid et al., 2009 |
| UDC 244 | Yakutia, Russia | 27 | 9.2 | 0.7 | 7.1 | 22.8 | 18.8 | 12.1 | 18.6 | 3.7 | 3.3 | 0.67 | Klein-BenDavid et al., 2009 |
| UDC 246 | Yakutia, Russia | 4 | 7.6 | 1.4 | 6.4 | 17.5 | 12.5 | 14.2 | 23.4 | 7.2 | 2.9 | 0.56 | Klein-BenDavid et al., 2009 |
| UDC 252 | Yakutia, Russia | 28 | 8 | 0.6 | 8.5 | 22 | 20.6 | 8.2 | 23.5 | 4 | 4.3 | 0.66 | Klein-BenDavid et al., 2009 |
| ZAR 263 | Yakutia, Russia | 25 | 9.5 | 1.7 | 6.3 | 23.1 | 16.9 | 9.7 | 23 | 5 | 3.3 | 0.68 | Klein-BenDavid et al., 2009 |
| ZAR 265 | Yakutia, Russia | 14 | 8.8 | 1.7 | 8 | 22.6 | 18.6 | 4 | 25.6 | 4.3 | 3 | 0.63 | Klein-BenDavid et al., 2009 |
| UB_81 | Yakutia, Russia | 23 | 8.8 | 0.5 | 7.4 | 24.1 | 18.2 | 9.4 | 20.6 | 4.1 | 5.1 | 0.65 | Klein-BenDavid et al., 2009 |
| FK 925 | Yakutia, Russia | 29 | 8.6 | 0.5 | 10 | 23.6 | 24.9 | 6.9 | 19.8 | 2.4 | | 0.67 | Klein-BenDavid et al., 2009 |
| FK 951 | Yakutia, Russia | 50 | 8.6 | 0.6 | 8.2 | 25.3 | 26.3 | 7.5 | 17.3 | 3.2 | | 0.66 | Klein-BenDavid et al., 2009 |
| FK 952 | Yakutia, Russia | 15 | 9.8 | 0.3 | 10.4 | 21.6 | 16.1 | 6.3 | 27.2 | 5.2 | | 0.49 | Klein-BenDavid et al., 2009 |
| AIK 297 | Yakutia, Russia | 3 | 11.9 | 3.6 | 14 | 10.7 | 21.2 | 8.1 | 18.7 | 1.9 | 4.3 | 0.32 | Klein-BenDavid et al., 2009 |
| EG 133 | Yakutia, Russia | 15 | 9.8 | 1.3 | 17.5 | 12 | 21.3 | 8.3 | 22.5 | 2.7 | | 0.66 | Klein-BenDavid et al., 2009 |
| AIK 298 | Yakutia, Russia | 20 | 16.3 | 3.1 | 11.9 | 10.9 | 17.1 | 7 | 23.6 | 3 | 4.5 | 0.56 | Klein-BenDavid et al., 2009 |
| EG 138 | Yakutia, Russia | 33 | 37.1 | 6.6 | 8.4 | 3.8 | 16.7 | 0.6 | 17.3 | 5.9 | | 0.3 | Klein-BenDavid et al., 2009 |
| FK 927 | Yakutia, Russia | 17 | 62.8 | 12.5 | 2.9 | 1.6 | 3.4 | 0.01 | 15.1 | 0.9 | | 0.09 | Klein-BenDavid et al., 2009 |
| UDC 242 | Yakutia, Russia | 5 | 57.4 | 13 | 3.8 | 1.4 | 5.8 | 0 | 12.8 | 0.7 | 5.6 | 0.28 | Klein-BenDavid et al., 2009 |
| UDC 255 | Yakutia, Russia | 31 | 65.2 | 13.3 | 1.2 | 0.8 | 2.2 | 2.3 | 10.7 | 1 | 14.2 | 0.19 | Klein-BenDavid et al., 2009 |
| Sp.BR-1 | Brazil | 84 | 38.6 | 7.4 | 6.4 | 3 | 11.7 | 3.1 | 16.1 | 4.9 | | 0.28 | Shiryaev et al., 2005 |
| Sp.BR-2 | Brazil | 41 | 25.6 | 2.8 | 13.2 | 7.1 | 16.2 | 3.9 | 15.2 | 4.8 | | 0.56 | Shiryaev et al., 2005 |
| Sp.BR-5inner | Brazil | 45 | 45.4 | 5.2 | 9.7 | 4 | 6.7 | 2.8 | 14.9 | 3.7 | | 0.43 | Shiryaev et al., 2005 |
| Sp.BR-5outer | Brazil | 23 | 25.4 | 2.6 | 13.5 | 7 | 16.9 | 4.5 | 15.7 | 4.8 | | 0.68 | Shiryaev et al., 2005 |

Note: C/CH represents $[CO_3]^{2-}/([CO_3]^{2-}+H_2O)$ molar ratio.

**Limitations**

The calculation of $[CO_3]^{2-}$ in this thesis is based on the assumptions used by Klein-BenDavid et al. (2007) that $Ti^{4+}$, $Ca^{2+}$, $Mg^{2+}$, $Fe^{2+}$, $Ba^{2+}$, $Na^{+}$ and $K^{+}$ are balanced by $[Cl]^{-}$, $[PO_4]^{3-}$, $[CO_3]^{2-}$ and $[SiO_4]^{4-}$ and that $Si^{4+}$ and $Al^{3+}$ are associated with $Mg^{2+}$, $Fe^{2+}$ and $K^{+}$ in proportions to form mica. This assumption considers that $Mg^{2+}$, $Fe^{2+}$ and $K^{+}$ not only combine with $[CO_3]^{2-}$ and $[Cl]^{-}$ but also combine with $[SiO_4]^{4-}$, which is supported by the discovery of silicate minerals such as mica, pyroxenes and olivine in fluid inclusions. According to this assumption, the calculation of $[CO_3]^{2-}$ should include the subtraction of $[SiO_4]^{4-}$ with a factor. In the calculation by Klein-BenDavid et al. (2007), this factor is 1, which is only suitable for the fluid inclusions where the crystallized silicate minerals have the (2Ti + Ca + Mg + Fe + Ba + 0.5Na + 0.5K)/Si molar ratio of 1. However, most crystallized silicate minerals in fluid inclusions do not have this molar ratio of 1. For example, quartz has this molar ratio of 0, and olivine has this molar ratio of 2. For fluid inclusions where the crystallized silicate mineral is only quartz, the calculation by Klein-BenDavid et al. (2007) will generate a negative value for $[CO_3]^{2-}$. Therefore, the calculation of $[CO_3]^{2-}$ in this thesis does not include the subtraction of $[SiO_4]^{4-}$. Besides this, the calculation of $[CO_3]^{2-}$ also does not consider the minor elements such as Ti, Cr, Ba, Sr, P and S.

Without subtracting $[SiO_4]^{4-}$, $[CO_3]^{2-}$ can be overestimated for Si-rich fluid inclusions, and $H_2O$ can also be overestimated because $H_2O$ is calculated from $[CO_3]^{2-}$ using the formula: $H_2O = [CO_3]^{2-}(1/\alpha - 1)$. Therefore, the $[Cl]^{-}/([Cl]^{-} + H_2O)$ molar ratio can be underestimated for Si-rich fluid inclusions because of the

overestimation of $H_2O$, and the $[Cl]^-/([Cl]^- + H_2O)$ molar ratio for Si-rich fluid inclusions cannot represent their actual $Cl/(Cl + H_2O)$ molar ratio. However, the effect of not subtracting $[SiO_4]^{4-}$ is negligible for Si-poor fluid inclusions. Furthermore, the neglect of Ti, Cr, Ba, Sr, P and S could cause uncertainty in the calculated $[CO_3]^{2-}$. For example, neglecting Ti, Cr, Ba and Sr underestimates $[CO_3]^{2-}$, and neglecting P and S overestimates $[CO_3]^{2-}$. Because these elements are minor in fluid inclusions and the underestimation and overestimation of $[CO_3]^{2-}$ can be cancelled by each other to some extent, the uncertainty caused by neglecting these elements is negligible. Therefore, the calculation without subtracting $[SiO_4]^{4-}$ and without considering the minor elements can still yield a relatively accurate $Cl/(Cl + H_2O)$ molar ratio for the Si-poor fluid inclusions.

Table 2-2. Calculated composition of fluid inclusions in fibrous diamonds.

| Sample | Location | mol % | | | | | | | | mol% | | | |
|---|---|---|---|---|---|---|---|---|---|---|---|---|---|
| | | Si | Al | Fe | Mg | Ca | Na | K | Cl | $[SiO_4]^{4-}$ | $[CO_3]^{2-}$ | $[Cl]^-$ | $H_2O$ |
| ON-DVK-269 | Diavik, Canada | 3.0 | 0.6 | 3.8 | 2.5 | 3.8 | 13.6 | 30.0 | 42.7 | 2.61 | 9.07 | 36.90 | 51.41 |
| ON-DVK-272 | Diavik, Canada | 4.5 | 1.3 | 7.4 | 6.9 | 9.5 | 19.0 | 43.9 | 7.6 | 1.75 | 20.01 | 2.96 | 75.28 |
| ON-DVK-275 | Diavik, Canada | 4.0 | 0.6 | 3.8 | 5.1 | 5.2 | 17.5 | 24.1 | 39.7 | 2.49 | 9.43 | 24.94 | 63.13 |
| ON-DVK-276 | Diavik, Canada | 2.2 | 0.5 | 4.6 | 4.4 | 2.1 | 16.7 | 26.9 | 42.7 | 2.48 | 13.21 | 48.61 | 35.70 |
| ON-DVK-280 | Diavik, Canada | 2.9 | 2.7 | 3.6 | 2.5 | 3.3 | 19.5 | 23.4 | 42.1 | 3.93 | 13.13 | 56.29 | 26.65 |
| ON-DVK-282 | Diavik, Canada | 2.2 | 0.6 | 4.3 | 3.4 | 4.0 | 13.2 | 29.4 | 42.9 | 2.68 | 13.80 | 51.33 | 32.20 |
| ON-DVK-283 | Diavik, Canada | 3.2 | 0.5 | 3.8 | 4.6 | 4.6 | 17.2 | 27.0 | 39.1 | 3.93 | 18.89 | 47.63 | 29.55 |
| ON-DVK-286 | Diavik, Canada | 2.6 | 0.7 | 4.3 | 4.3 | 4.7 | 18.8 | 23.8 | 40.8 | 2.38 | 13.17 | 37.77 | 46.68 |
| ON-DVK-287 | Diavik, Canada | 2.6 | 0.4 | 3.3 | 6.6 | 5.9 | 20.2 | 24.3 | 36.7 | 2.79 | 20.93 | 39.07 | 37.21 |
| ON-DVK-288 | Diavik, Canada | 3.8 | 0.5 | 3.3 | 5.9 | 5.5 | 15.2 | 26.2 | 39.4 | 3.04 | 12.50 | 31.18 | 53.29 |
| ON-DVK-281 | Diavik, Canada | 26.3 | 4.1 | 10.1 | 8.8 | 14.7 | 5.9 | 27.5 | 2.6 | 12.51 | 23.29 | 1.23 | 62.97 |
| PAN2 | Panda, Canada | 4.4 | 1.6 | 9.7 | 8.1 | 7.3 | 7.2 | 27.3 | 34.4 | 3.88 | 22.22 | 30.46 | 43.44 |
| PAN3 | Panda, Canada | 2.7 | 0.8 | 5.1 | 4.3 | 4.6 | 7.8 | 31.2 | 43.4 | 3.40 | 14.74 | 54.22 | 27.64 |
| PAN4 | Panda, Canada | 13.6 | 1.8 | 7.4 | 1.6 | 4.7 | 7.2 | 29.9 | 33.9 | 13.83 | 15.55 | 34.46 | 36.16 |
| PAN5 | Panda, Canada | 5.5 | 2.1 | 21.2 | 11.0 | 12.9 | 10.8 | 15.4 | 21.0 | 3.65 | 31.74 | 13.99 | 50.62 |
| PAN6 | Panda, Canada | 3.4 | 1.3 | 12.1 | 5.9 | 7.0 | 12.6 | 23.9 | 33.9 | 3.40 | 26.02 | 33.68 | 36.90 |
| PAN7 | Panda, Canada | 3.0 | 0.8 | 13.6 | 6.3 | 8.3 | 15.0 | 21.8 | 31.2 | 2.80 | 28.84 | 29.02 | 39.34 |
| PAN8 | Panda, Canada | 3.5 | | 8.8 | 6.4 | 6.2 | 17.8 | 22.2 | 35.1 | 3.64 | 24.79 | 36.42 | 35.15 |
| JWN90 | Jwaneng, Botswana | 24.2 | 2.8 | 13.0 | 14.5 | 16.1 | 4.9 | 22.5 | 2.1 | 22.69 | 52.72 | 1.99 | 22.60 |
| JWN87 | Jwaneng, Botswana | 25.2 | 2.3 | 14.4 | 15.8 | 17.2 | 4.2 | 19.3 | 1.7 | 17.54 | 40.65 | 1.16 | 40.65 |
| JWN106 | Jwaneng, Botswana | 27.1 | 2.5 | 11.9 | 15.1 | 12.9 | 5.5 | 22.4 | 2.7 | 16.83 | 32.58 | 1.71 | 48.87 |
| JWN89 | Jwaneng, Botswana | 28.8 | 3.4 | 13.2 | 12.0 | 14.1 | 4.4 | 22.7 | 1.5 | 24.63 | 44.45 | 1.28 | 29.64 |
| JWN112 | Jwaneng, Botswana | 35.9 | 4.9 | 11.1 | 11.4 | 9.6 | 4.8 | 21.2 | 1.2 | 28.46 | 35.31 | 0.93 | 35.31 |
| JWN110 | Jwaneng, Botswana | 40.6 | 5.7 | 9.1 | 7.5 | 7.2 | 4.6 | 23.5 | 1.8 | 30.17 | 27.39 | 1.36 | 41.08 |
| JWN99 | Jwaneng, Botswana | 43.4 | 5.3 | 8.6 | 8.5 | 5.9 | 4.2 | 22.3 | 1.7 | 10.85 | 8.87 | 0.42 | 79.86 |
| JWN91 | Jwaneng, Botswana | 45.2 | 6.4 | 9.0 | 8.5 | 5.5 | 3.1 | 21.0 | 1.4 | 28.08 | 21.32 | 0.84 | 49.75 |
| JWN92 | Jwaneng, Botswana | 47.1 | 6.4 | 8.2 | 7.1 | 5.0 | 5.7 | 19.2 | 1.3 | 36.68 | 24.91 | 1.04 | 37.37 |
| JWN88 | Jwaneng, Botswana | 50.5 | 7.4 | 8.3 | 6.9 | 3.5 | 0.6 | 20.5 | 2.4 | 26.21 | 14.51 | 1.24 | 58.04 |
| JWN115 | Jwaneng, Botswana | 50.4 | 6.3 | 10.2 | 6.6 | 3.5 | 5.4 | 15.5 | 2.0 | 25.04 | 14.79 | 1.01 | 59.16 |
| JWN93 | Jwaneng, Botswana | 52.6 | 6.6 | 7.4 | 7.6 | 5.9 | 3.9 | 14.7 | 1.2 | 26.00 | 14.68 | 0.59 | 58.73 |
| 155 | Koffiefontein, South Africa | 4.1 | 0.0 | 13.8 | 2.0 | 6.6 | 8.1 | 27.5 | 37.8 | 1.33 | 6.91 | 12.25 | 79.51 |

Table 2-2 (continued). Calculated composition of fluid inclusions in fibrous diamonds.

| Sample | Location | mol % | | | | | | | | mol% | | | |
|---|---|---|---|---|---|---|---|---|---|---|---|---|---|
| | | Si | Al | Fe | Mg | Ca | Na | K | Cl | $[SiO_4]^{4+}$ | $[CO_3]^{2-}$ | $[Cl]^-$ | $H_2O$ |
| 156 | Koffiefontein, South Africa | 3.6 | 0.4 | 8.5 | 1.2 | 8.4 | 6.3 | 25.8 | 45.9 | 2.07 | 6.43 | 26.46 | 65.04 |
| 159 | Koffiefontein, South Africa | 4.8 | 0.6 | 7.9 | 1.8 | 3.4 | 1.4 | 31.1 | 49.0 | 1.61 | 1.64 | 16.37 | 80.38 |
| 162 | Koffiefontein, South Africa | 4.5 | 0.3 | 12.9 | 2.0 | 7.8 | 6.5 | 25.9 | 40.2 | 3.54 | 14.89 | 31.73 | 49.84 |
| 165 | Koffiefontein, South Africa | 4.8 | 0.4 | 5.7 | 1.1 | 2.7 | 3.7 | 33.5 | 48.2 | 0.46 | 0.38 | 4.62 | 94.55 |
| 175 | Koffiefontein, South Africa | 2.7 | 0.3 | 12.3 | 2.4 | 6.1 | 2.9 | 28.7 | 44.5 | 2.15 | 11.29 | 35.11 | 51.45 |
| 176 | Koffiefontein, South Africa | 6.9 | 0.5 | 14.2 | 2.3 | 6.2 | 6.2 | 25.2 | 38.4 | 1.75 | 4.87 | 9.74 | 83.65 |
| UB 5-41 | Yakutia, Russia | 6.2 | 1.5 | 6.8 | 13.5 | 14.0 | 20.0 | 26.7 | 11.3 | 5.65 | 47.11 | 10.23 | 37.01 |
| UDC 239 | Yakutia, Russia | 8.0 | 1.1 | 5.0 | 31.2 | 18.0 | 15.1 | 18.1 | 3.5 | 6.73 | 57.83 | 2.91 | 32.53 |
| UDC 241 | Yakutia, Russia | 6.9 | 0.6 | 5.4 | 23.1 | 15.4 | 16.5 | 24.8 | 7.4 | 6.31 | 55.62 | 6.79 | 31.28 |
| UDC 243 | Yakutia, Russia | 7.4 | 1.5 | 8.1 | 22.8 | 14.3 | 14.8 | 24.3 | 6.9 | 6.50 | 54.19 | 6.09 | 33.21 |
| UDC 244 | Yakutia, Russia | 7.4 | 0.7 | 4.8 | 27.5 | 16.3 | 19.0 | 19.2 | 5.1 | 6.78 | 59.36 | 4.62 | 29.24 |
| UDC 246 | Yakutia, Russia | 6.1 | 1.3 | 4.3 | 21.1 | 10.8 | 22.3 | 24.1 | 9.9 | 5.42 | 48.09 | 8.70 | 37.79 |
| UDC 252 | Yakutia, Russia | 6.5 | 0.6 | 5.8 | 26.6 | 17.9 | 12.9 | 24.3 | 5.5 | 5.78 | 58.95 | 4.90 | 30.37 |
| ZAR 263 | Yakutia, Russia | 7.5 | 1.6 | 4.2 | 27.3 | 14.4 | 14.9 | 23.3 | 6.7 | 7.19 | 58.75 | 6.41 | 27.65 |
| ZAR 265 | Yakutia, Russia | 7.4 | 1.7 | 5.6 | 28.4 | 16.8 | 6.5 | 27.5 | 6.1 | 6.37 | 55.66 | 5.28 | 32.69 |
| UB_81 | Yakutia, Russia | 7.2 | 0.5 | 5.1 | 29.3 | 15.9 | 14.9 | 21.5 | 5.7 | 6.31 | 57.66 | 4.98 | 31.05 |
| FK 925 | Yakutia, Russia | 7.0 | 0.5 | 6.8 | 28.8 | 21.8 | 11.0 | 20.7 | 3.3 | 6.00 | 61.08 | 2.84 | 30.08 |
| FK 951 | Yakutia, Russia | 6.9 | 0.6 | 5.5 | 30.4 | 22.7 | 11.7 | 17.8 | 4.4 | 5.82 | 59.74 | 3.67 | 30.78 |
| FK 952 | Yakutia, Russia | 7.9 | 0.3 | 7.0 | 26.0 | 13.9 | 9.8 | 28.0 | 7.1 | 5.56 | 43.82 | 5.00 | 45.61 |
| AIK 297 | Yakutia, Russia | 10.9 | 3.9 | 10.7 | 14.6 | 20.8 | 14.4 | 21.8 | 2.9 | 5.19 | 29.89 | 1.40 | 63.52 |
| EG 133 | Yakutia, Russia | 8.4 | 1.3 | 12.6 | 15.4 | 19.7 | 13.9 | 24.7 | 3.9 | 7.61 | 58.63 | 3.56 | 30.20 |
| AIK 298 | Yakutia, Russia | 14.4 | 3.2 | 8.8 | 14.3 | 16.2 | 12.0 | 26.6 | 4.5 | 12.04 | 47.15 | 3.76 | 37.05 |
| EG 138 | Yakutia, Russia | 34.1 | 7.2 | 6.5 | 5.2 | 16.5 | 1.1 | 20.3 | 9.2 | 21.68 | 21.74 | 5.84 | 50.73 |
| FK 927 | Yakutia, Russia | 58.8 | 13.8 | 2.3 | 2.2 | 3.4 | 0.0 | 18.0 | 1.4 | 24.44 | 6.75 | 0.59 | 68.22 |
| UDC 242 | Yakutia, Russia | 56.4 | 15.1 | 3.1 | 2.1 | 6.1 | 0.0 | 16.1 | 1.2 | 45.33 | 15.05 | 0.94 | 38.69 |
| UDC 255 | Yakutia, Russia | 62.0 | 14.9 | 1.0 | 1.1 | 2.2 | 4.2 | 13.0 | 1.6 | 48.64 | 9.52 | 1.26 | 40.58 |
| Sp.BR-1 | Brazil | 36.9 | 8.3 | 5.1 | 4.3 | 12.0 | 5.7 | 19.6 | 7.9 | 24.48 | 19.97 | 5.27 | 50.29 |
| Sp.BR-2 | Brazil | 24.9 | 3.2 | 10.7 | 10.3 | 16.9 | 7.3 | 18.8 | 7.9 | 21.30 | 40.26 | 6.77 | 31.67 |
| Sp.BR-5inner | Brazil | 43.9 | 5.9 | 7.8 | 5.8 | 6.9 | 5.2 | 18.4 | 6.1 | 37.03 | 24.75 | 5.12 | 33.10 |
| Sp.BR-5outer | Brazil | 24.1 | 2.9 | 10.7 | 9.9 | 17.2 | 8.3 | 19.0 | 7.7 | 23.61 | 46.60 | 7.56 | 22.23 |

**Composition of chlorine-bearing fluids**

Concentrations of the elements Si, Al, Fe, Mg, Ca, Na, K and Cl are calculated into molar percentages and shown in Table 2-2 and Figure 2-1. From the concentration of Cl, fluids in fibrous diamonds divide into high-Cl fluids and low-Cl fluids (Figure 2-1a and 2-1b, respectively), which are shown as the two peaks in the histogram of Cl mol% in Figure 2-2. The high-Cl fluids are rich in Cl and K but poor in Si, Mg and Ca, and they are from Diavik and Panda mines in Canada and Koffiefontein in South Africa. In contrast, the low-Cl fluids are poor in Cl but rich in Si, Mg, Ca and K, and they are from Brazil, the Diavik mine in Canada, Jwaneng in Botswana and Yakutia in Russia. The Cl/(Cl+K) molar ratio is around 0.6 for the high-Cl fluids but <0.35 for the low-Cl fluids, and the K/(K+Na) molar ratio is >0.5 for all fluids (Figure 2-3). Overall, the concentration of elements indicates that fluids trapped in fibrous diamonds can be divided into the high-Cl fluids and the low-Cl fluids, and Cl is mainly associated with K.

The four components $[SiO_4]^{4-}$, $[CO_3]^{2-}$, $[Cl]^-$ and $H_2O$ are calculated and shown in Table 2-2 and projected in Figure 2-4. This projection of the four components shows that the high-Cl fluids, except those in fibrous diamonds from the Panda mine, fall along a line and the low-Cl fluids distribute close to the $[SiO_4]^{4-}$-$[CO_3]^{2-}$-$H_2O$ plane. The fluid inclusions in the fibrous diamonds from the Panda mine fall between the line and the plane, which may be caused by mixing of different types of fluids. As listed in Table 2-2, the $[Cl]^-/([Cl]^-+H_2O)$ molar ratio of the high-Cl fluids is 0.05-0.68, and the $[Cl]^-/([Cl]^-+H_2O)$ molar ratio of the low-Cl fluids is 0.01-0.25. Because the chlorine-rich fluids are poor in Si, the

calculated $[CO_3]^{2-}$ and $H_2O$ are not affected by the calculation without subtracting $[SiO_4]^{4-}$ and therefore, their calculated $[Cl]^-/([Cl]^-+H_2O)$ molar ratio would represent the actual $Cl/(Cl+H_2O)$ molar ratio of fluids. However, because the low-Cl fluids are rich in Si, the calculated $[Cl]^-/([Cl]^-+H_2O)$ molar ratio underestimates the $Cl/(Cl+H_2O)$ molar ratio of the fluids. Therefore, the $Cl/(Cl+H_2O)$ molar ratio of chlorine-bearing fluids in fibrous diamonds is more accurately represented by the $[Cl]^-/([Cl]^-+H_2O)$ molar ratio of 0.05-0.68 for the high-Cl fluids.

In previous works, Klein-BenDavid et al. (2007) concluded that there is a continuous compositional evolution between saline-HDFs and carbonatitic-HDFs by plotting the composition of fluid inclusions on the (Si+Al)-(K+Na)-(Ca+Mg+Fe) triangular diagram, and, similarly, Safonov et al. (2007) also concluded a continuous compositional evolution between the Si-bearing chloride-carbonate brine and the chloride-bearing carbonatitic liquid by plotting compositions of fluid inclusions on the (Si+Al+Ti+P)-Cl-(Ca+Mg+Fe+Ba+Sr) triangular diagram. Because the high-Cl fluids in this thesis are equivalents to the saline-HDFs by Klein-BenDavid et al. (2007) and the Si-bearing chloride-carbonate brine by Safonov et al. (2007) and the low-Cl fluids in this thesis include the carbonatitic-HDFs by Klein-BenDavid et al. (2007) and the chloride-bearing carbonatitic liquid by Safonov et al. (2007), the division of high-Cl fluids and low-Cl fluids in this thesis is opposed to the continuous compositional evolution by Klein-BenDavid et al. (2007) and Safonov et al. (2007).

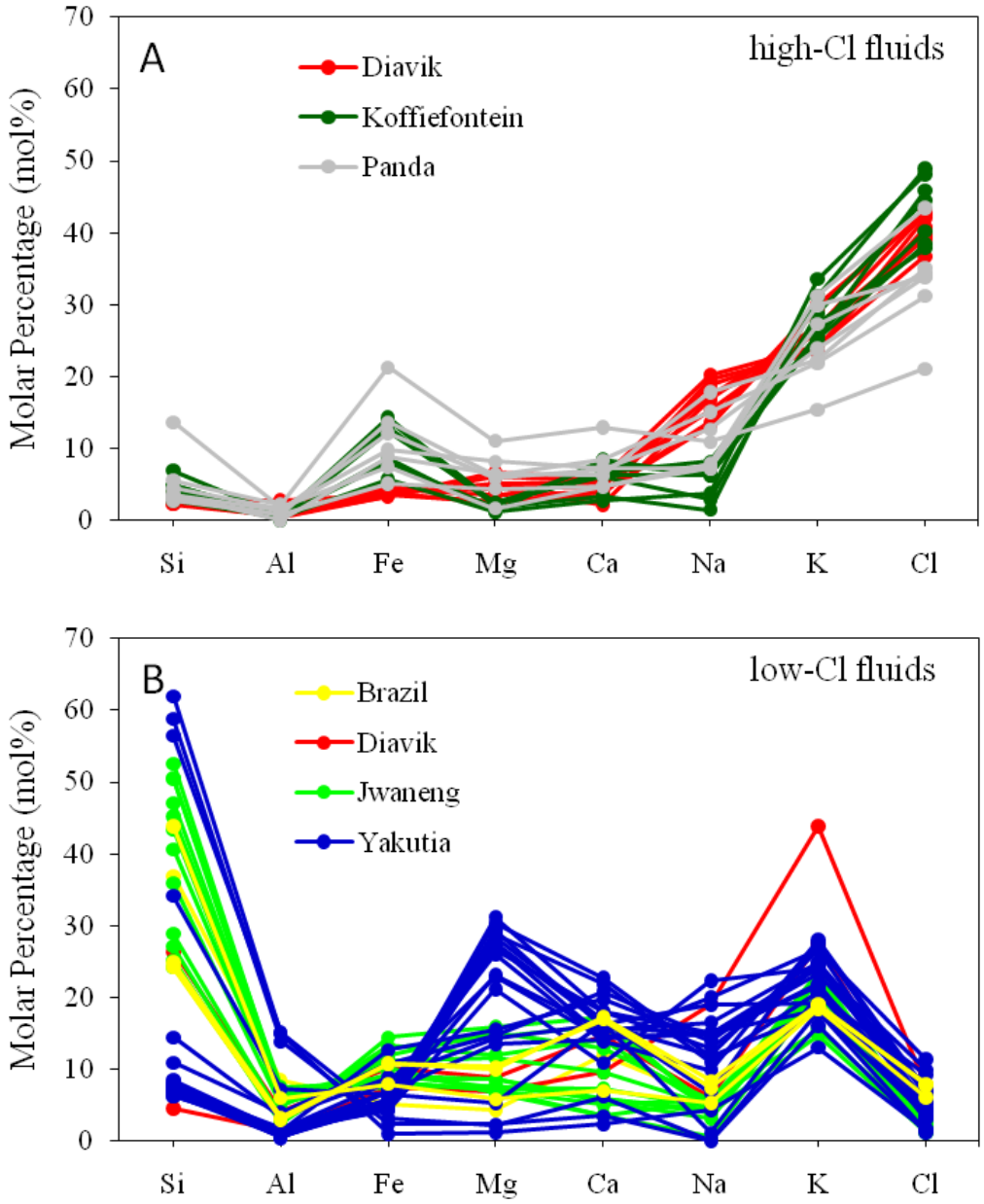


Figure 2-1. Concentrations of elements in fluid inclusions in fibrous diamonds.

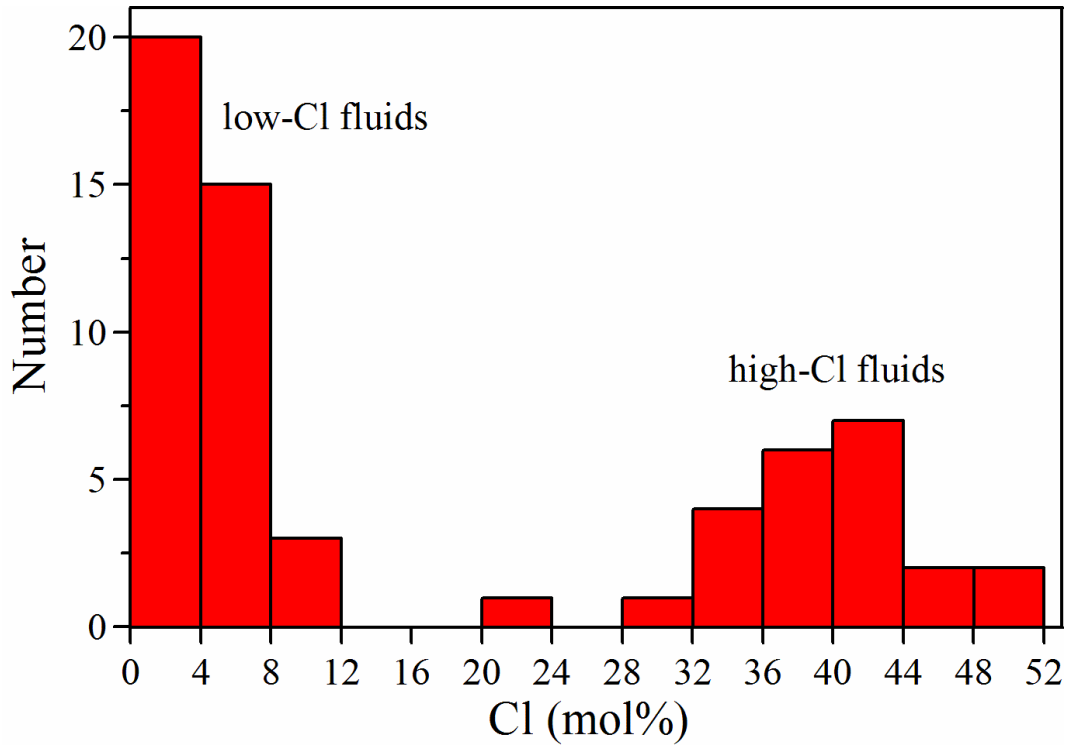


Figure 2-2. Distribution of the concentration of Cl in fluid inclusions in fibrous diamonds.

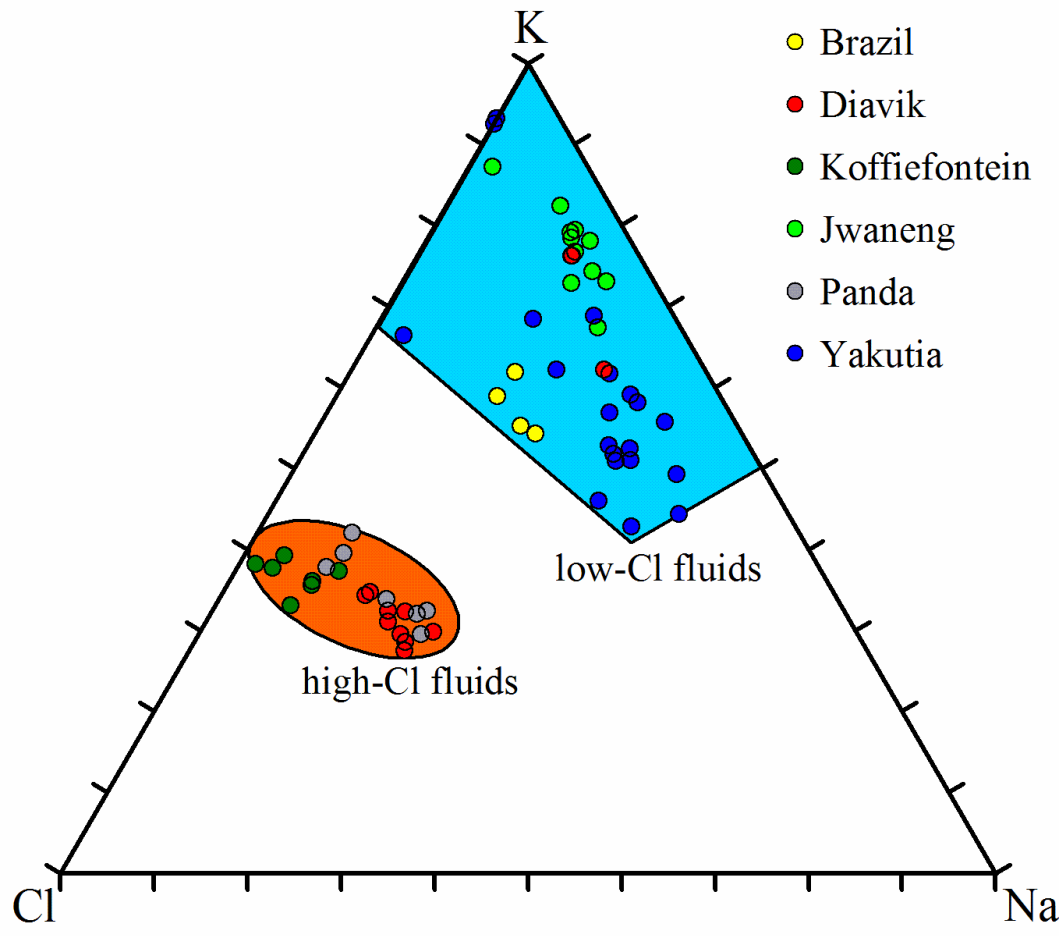


Figure 2-3. Projection of Cl, K and Na in fluid inclusions in fibrous diamonds.

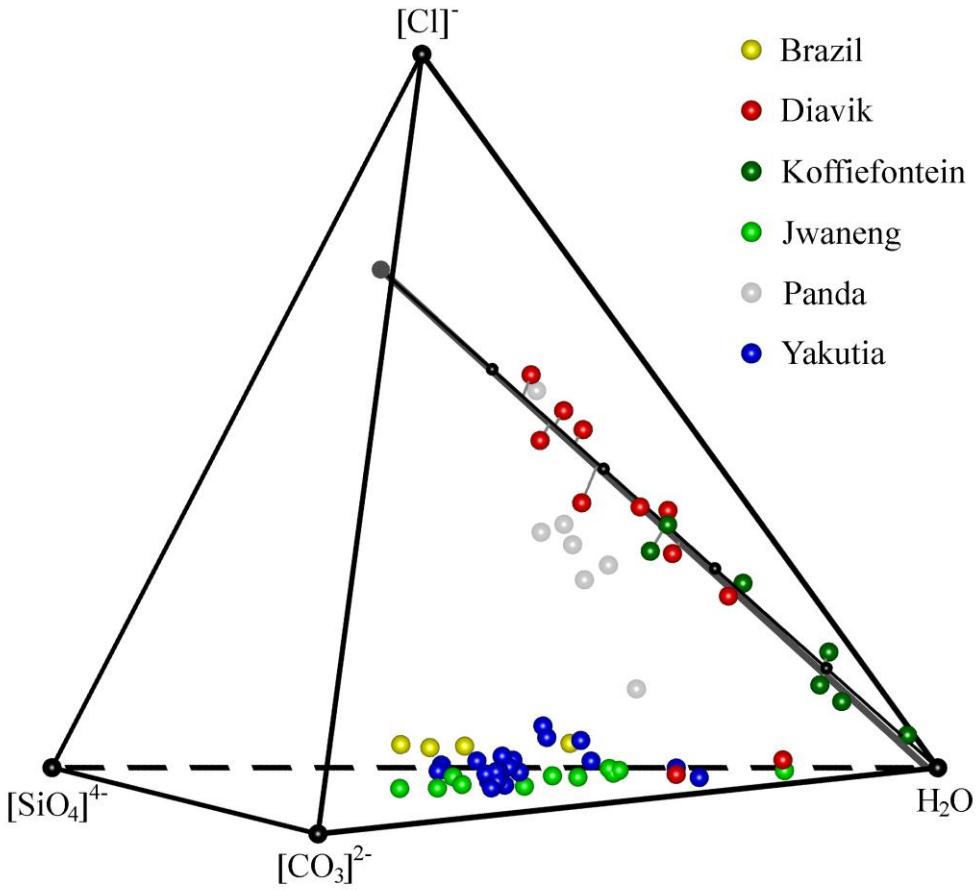


Figure 2-4. Projection of the calculated $[SiO_4]^{4-}$, $[CO_3]^{2-}$, $[Cl]^-$ and $H_2O$ for fluid inclusions in diamonds. Data are in Table 2-2. The formula to calculate $[CO_3]^{2-}$ is in the text. The gray solid line is the regression of chlorine-rich fluid inclusions in diamonds from Diavik and Koffiefontein mines, which can be expressed as the equations: $[SiO_4]^{4-} = -0.0378H_2O + 4.5295$ ($r^2 = 0.73$), $[CO_3]^{2-} = -0.2387H_2O + 23.789$ ($r^2 = 0.78$) and $[Cl]^- = -0.7236H_2O + 71.682$ ($r^2 = 0.97$), and which intersects the $[SiO_4]^{4-}$-$[CO_3]^{2-}$-$[Cl]^-$ plane at the point ($[SiO_4]^{4-}$, $[CO_3]^{2-}$, $[Cl]^-$) = (4.5, 23.8, 71.7). The black solid line ties the point of the intersection and the $H_2O$ vertex, and it almost superposes the gray regressed line. Small black spheres on the black solid line show the water contents of 20, 40, 60, and 80 mol%.

This significant difference is due to considering $H_2O$ as an end member in plotting, in this thesis. Klein-BenDavid et al. (2007) and Safonov et al. (2007) did not consider $H_2O$ as an end member of fluid compositions in plotting, therefore, their results of plotting are equal to that of projecting the compositions of fluid inclusions from the "$H_2O$" vertex to the $[SiO_4]^{4-}$-$[CO_3]^{2-}$-$[Cl]^-$ triangular plane in Figure 2-4. This projection can cause an intersection or connection of the group of high-Cl fluids and the group of low-Cl fluids in the $[SiO_4]^{4-}$-$[CO_3]^{2-}$-$[Cl]^-$ triangular plane. Therefore, the division of high-Cl fluids and low-Cl fluids, revealed by plotting with considering $H_2O$ in compositions of fluid inclusions in this thesis, is more reliable than the continuous compositional evolution of fluids by Klein-BenDavid et al. (2007) and Safonov et al. (2007). This division is possibly caused by fluid immiscibility between the high-Cl fluids and the low-Cl fluids because both of these two kinds of fluid inclusions exist in fibrous diamonds from the Diavik mine in Canada.

**Conclusion**

Fluids trapped in fibrous diamonds represent fluids in the SCLM, and they divide into high-Cl fluids and low-Cl fluids. Chlorine in the fluids is mainly associated with K and dissolves in $H_2O$ with the $Cl/(Cl+H_2O)$ molar ratio of 0.05-0.68.

**References**

Izraeli, E.S., Harris, J.W. and Navon, O., 2004, Fluid and mineral inclusions in cloudy diamonds from Koffiefontein, South Africa: Geochimica et Cosmochimica Acta, v. 68, p. 2561-2575.

Izraeli, E.S., Harris, J.W. and Navon, O., 2001, Brine inclusions in diamonds: a new upper mantle fluid: Earth and Planetary Science Letters, v. 187, p. 323-332.

Klein-BenDavid, O., Izraeli, E.S., Hauri, E.H. and Navon, O., 2007, Fluid inclusions in diamonds from the Diavik Mine, Canada and the evolution of diamond-forming fluids: Geochimica et Cosmochimica Acta, v. 71, p. 723-744.

Klein-BenDavid, O., Logvinova, A.M., Schrauder, M., Spetius, Z.V., Weiss, Y., Hauri, E., Kaminsky, F.V., Sobolev, N.V. and Navon, O., 2009, High-Mg carbonatitic microinclusions in some Yakutian Diamonds- a new type of diamond-forming fluid: Lithos, In Press.

Klein-BenDavid, O., Richard, W. and Navon, O., 2006, TEM imaging and analysis of microinclusions in diamonds; a close look at diamond-growing fluids: American Mineralogist, v. 91, p. 353-365.

Navon, O., Hutcheon, I.D., Rossman, G.R. and Wasserburg, G.J., 1988, Mantle-derived fluids in diamond micro-inclusions: Nature, v. 335, p. 784-789.

Schrauder, M. and Navon, O., 1994, Hydrous and carbonatitic mantle fluids in fibrous diamonds from Jwaneng, Botswana: Geochimica et Cosmochimica Acta, v. 58, p. 761.

Shiryaev, A.A., Izraeli, E.S., Hauri, E.H., Zakharchenko, O.D. and Navon, O., 2005, Chemical, optical and isotopic investigation of fibrous diamonds from Brazil: Russian Geology and Geophysics, v. 46, p. 1185-1201.

Thompson, W.K., 1965， Infra-red spectroscopic studies of aqueous systems. Part 1. Molar extinction coefficients of water, deuterium oxide, deuterium hydrogen oxide, aqueous sodium chloride and carbon disulphide: Transactions of the Faraday Society, v. 61, p. 2635-2640.

Tomlinson, E.L., Jones, A.P. and Harris, J.W., 2006, Co-existing fluid and silicate inclusions in mantle diamond: Earth and Planetary Science Letters, v. 250, p. 581-595.

## Chapter 3. Effect of KCl on melting of the $Mg_2SiO_4$-$MgSiO_3$-$H_2O$ system at 5 GPa

### Introduction

Chlorine has been found as a major constituent in fluids trapped in fibrous diamonds (Navon et al., 1988; Izraeli et al., 2001; Tomlinson et al., 2006; Klein-BenDavid et al., 2006; Klein-BenDavid et al., 2007). It is mainly associated with potassium, forming a KCl-bearing brine with the $Cl/(Cl+H_2O)$ molar ratio of 0.05-0.68 (see Chapter 2). Syngenetic mineral inclusions in the fibrous diamonds from Koffiefontein in South Africa and from the Panda mine in Canada revealed that these fibrous diamonds formed at pressures of 4-6 GPa and temperatures of 900-1200 ℃ (Izraeli et al., 2004; Tomlinson et al., 2006). The high end of this temperature range is above the anticipated water-saturated peridotite solidus of Grove et al. (2006). Because these fibrous diamonds originate from the subcratonic lithospheric mantle (SCLM), the KCl-bearing brine in fluid inclusions of these diamonds indicates the existence of KCl in the SCLM at the depth relevant to the pressure 4-6 GPa. KCl in the brine may reduce the activity of $H_2O$ sufficiently to stabilize a fluid, rather than a melt, under these conditions.

Chlorides have been shown to affect melting behavior at lower pressure. The melting of albite and dehydration of brucite in $H_2O$-NaCl fluids to 0.9 GPa and 700-900 ℃ shows that NaCl increases the solidus temperature of albite+fluid relative to the pure water case by reducing the activity of water in hydrous systems (Shmulovich and Graham, 1996). The $H_2O$ activity measurement in concentrated NaCl, KCl and KCl-NaCl solutions to 1.5 GPa and 550-900 ℃

shows that KCl reduces the activity of water more than NaCl does at the same condition (Aranovich and Newton, 1996; Aranovich and Newton, 1997; Aranovich and Newton, 1998), which means that KCl can increase melting temperature more than the same amount of NaCl. However, whether this effect exists at high pressures, corresponding to the depth of the SCLM, is unknown. This study conducts experiments to examine the effect of KCl on melting of the $Mg_2SiO_4$-$MgSiO_3$-$H_2O$ system, a simple model for $H_2O$-bearing harzburgitic Earth's mantle, at 5 GPa (~160 km).

**Experimental techniques**

Starting materials (Table 3-1) were prepared in four different compositions by mixing $Mg(OH)_2$ (≥95% purity), $SiO_2$ (99.999% purity) and KCl (99.999% purity) that were dried at 120°C for >12 h. Material 1 is a mixture of $Mg(OH)_2$ and $SiO_2$ in 3:2 molar proportion, generating the $Mg_2SiO_4$-$MgSiO_3$-$H_2O$ system with $Mg_2SiO_4$/ $MgSiO_3$ molar ratio of 1 and water content of 18.3 wt%. Materials 2, 3 and 4, generated by mixing Material 1 (Mg:Si=1.5) with KCl in different proportions, have $Cl/(Cl+H_2O)$ molar ratios of 0.2, 0.4 and 0.6, respectively, which are consistent with those of chlorine-rich fluid inclusions in fibrous diamonds from the Diavik mine in Canada (Klein-BenDavid et al., 2007), ranging from 0.05 to 0.68 (see in Chapter 2). All starting materials were ground in an agate mortar under ethanol for 1 h and then dried at 120°C and stored in a desiccator. After this drying, the water content of Material 1 was checked by thermogravimetric analysis (Figure 3-1).

Approximately 3-5 mg of the appropriate starting material was loaded into an open-ended Pt capsule for each experiment. After drying at 120°C for >12 h, the capsule was welded shut quickly, within 3 min, and compressed gently into a cylindrical shape in a steel die. The compressed capsules had a diameter of 1.5 mm and a length ranging from 1.0 to 2.3 mm.

All experiments were run in the 2000 ton uniaxial split-sphere multi-anvil apparatus in the C.M. Scarfe Laboratory for Experimental Petrology at the University of Alberta. The 18mm sample assembly with high-T stepped graphite furnace, described by Walter et al. (1995), was used in all experiments. A semi-sintered MgO-5%$Cr_2O_3$ octahedron was used as a pressure cell, and the sample assembly was inserted in a cylindrical hole in the octahedron. A $W_{95}Re_5$-$W_{74}Re_{26}$ thermocouple was inserted axially into the cylindrical sample assembly, and it was in contact with the Pt capsule. Each sample assembly was dried at 120°C for >10 h, then fired at 1000°C in (2% $H_2$) $N_2$ gas flow for 1 h. The sample capsule was removed from the assembly for this latter step. After firing, the sample capsule was re-inserted in the assembly, and then the assembly was kept in 120°C until use. The dried sample assembly was placed in the octahedral cavity formed by triangular truncations of 11 mm of eight 32.5 mm edge-length WC-cubes. These cubes formed a big cube placed in the cubic cavity formed by six anvils of the uniaxial press. Calibrations of pressure and thermal gradient have been described in detail by Walter et al. (1995). The pressure calibration is accurate to within ±0.5 GPa, and the thermal gradient of the high-T stepped graphite furnace is +25°C $mm^{-1}$, away from the furnace midline (Walter et al.,

1995). Experiments were brought to 5 GPa, and then heated at ~70°C $s^{-1}$ to 1100-1700°C, and maintained at ±5°C. No pressure correction to the emf of the thermocouple was applied. Durations for runs at ≤1600°C were 8-12 h, and those for runs at >1600°C were 2 h. Experiments were quenched by turning off the power to the furnace, resulting in a temperature drop to <300°C in 2-5 s, and then decompressed over 3 h. After the runs, the capsules were weighed and then punctured with a razor blade. The punctured capsules were dried at 120°C for >12 h and then reweighted. If there was no weight loss after the drying, the capsule was presumed to have leaked, and the experiment was repeated. The punctured capsules in successful experiments were boiled in distilled water for 20 min twice to remove water-soluble material, such as chloride, because the presence of this material caused plucking of run products during polishing. The boiled capsules were dried and mounted in an epoxy plug using Petropoxy 154. After mounting, sample mounts were ground, polished with progressively finer suspensions of alumina, ultrasonically washed and then dried at 120°C for >12 h before being coated with carbon.

Table 3-1. Starting materials.

| System | $Mg_2SiO_4$-$MgSiO_3$-$H_2O$ | $Mg_2SiO_4$-$MgSiO_3$-KCl- $H_2O$ | | |
|---|---|---|---|---|
| Starting Material | 1 | 2 | 3 | 4 |
| *(wt%)* | | | | |
| $SiO_2$ | 40.72 | 34.23 | 27.05 | 19.06 |
| $Mg(OH)_2$ | 59.28 | 49.84 | 39.38 | 27.74 |
| KCl | 0 | 15.93 | 33.56 | 53.20 |
| *Calculated molar ratio* | | | | |
| Mg/Si | 1.5 | 1.5 | 1.5 | 1.5 |
| $Cl/(Cl+H_2O)$ | 0 | 0.2 | 0.4 | 0.6 |
| *Calculated water content (wt%)* | | | | |
| $H_2O$ | 18.31 | 15.40 | 12.17 | 8.57 |
| *Calculated KCl content in generated aqueous solutions (wt%)* | | | | |
| KCl | 0 | 50.85 | 73.40 | 86.13 |

Material 1 represents the $Mg_2SiO_4$-$MgSiO_3$-$H_2O$ system. Material 2, 3 and 4 represent the $Mg_2SiO_4$-$MgSiO_3$-KCl- $H_2O$ systems with the $Cl/(Cl+H_2O)$ molar ratio of 0.2, 0.4 and 0.6, respectively.

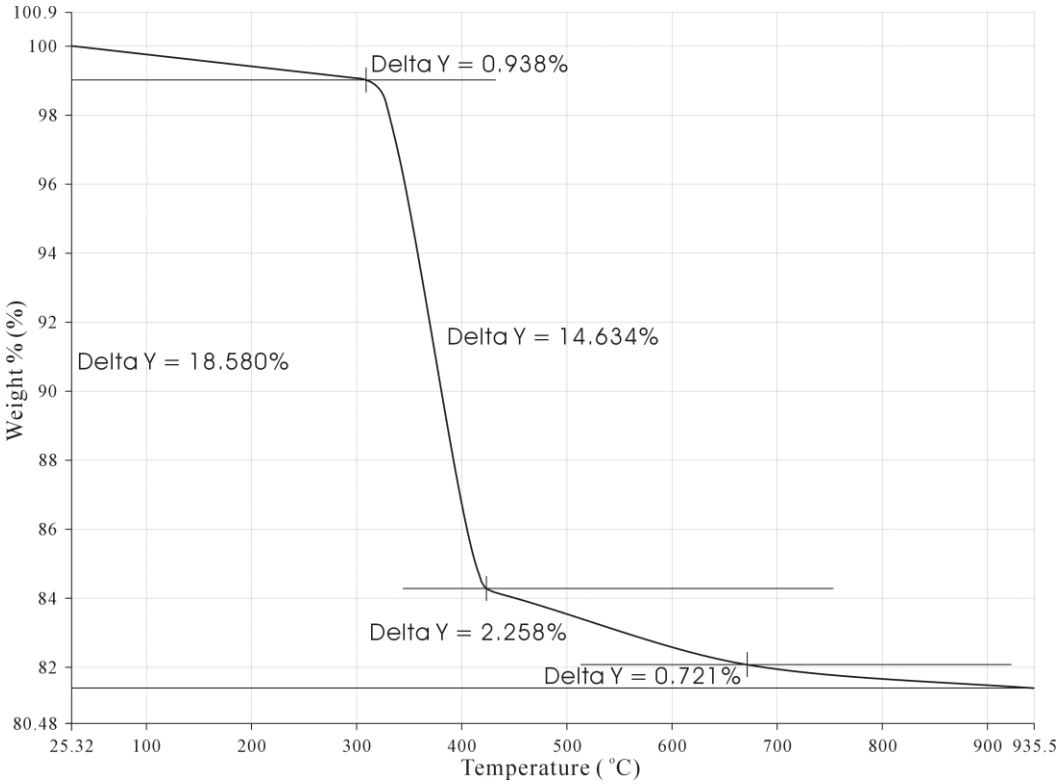


Figure 3-1. Thermogravimetric analysis of starting material of $Mg_2SiO_4$-$MgSiO_3$-$H_2O$ system.

The total weight loss (Delta Y) of 18.58 wt% is close to the calculated water content of 18.31 wt% for the Material 1 in Table 3-1.

Examination and analysis of the run products were carried out with the JEOL 8900R electron microprobe at the University of Alberta. The textural relationships between coexisting phases were examined using backscattered electron (BSE) imaging at least twice by repolishing the mounts. To examine the compositional changes at the solidus, the Ca contents of forsterite and enstatite were analyzed using 20 kV accelerating voltage, and the signal was detected by wavelength dispersive spectrometers with the PETH crystal. Because the Ca contents of forsterite and enstatite were much lower than that of diopside standard, the sample current for the diopside standard was 15 nA, and that for forsterite and enstatite samples was 150 nA. Counting time was 120 s on peaks and 60 s on background at each side. Si and Mg were also analyzed for the ZAF correction. In analyzing Ca, the detection limit and the standard deviation reported by microprobe were 5 ppm and ~10%, respectively. Potts (1986) pointed out that the reported detection limit (2 $\sigma_{background}$) is an over-optimistic estimate of the lower limit of detection and the limit of determination for quantitative measurement is 6 $\sigma_{background}$. Therefore, the limit of determination (6 $\sigma_{background}$) used in this thesis was calculated from the reported counts and counting time using the formula of Scott and Love (1983). The calculated limit of determination (6 $\sigma_{background}$) in analyzing Ca was 15 ppm. The EPMA analysis of run products is listed in the Appendix.

**Results**

Experimental conditions and results are summarized in Table 3-2. Because the fluids and melts are unquenchable, the texture of quenched phases cannot reveal the relationships, such as immiscibility, between the water/brine and

silicate melts under experimental conditions. “Vapor” and “Liquid” are used to describe subsolidus fluids and suprasolidus melts, respectively. The solidus is determined by examining the amount of quenched phases and the change of Ca content in the primary phases. Because of the thermal gradient in the capsule, subsolidus vapor and suprasolidus liquid can appear in one capsule. According to the study of Walter et al., 1995, the thermal gradient for the high-T stepped graphite furnace is +25°C $mm^{-1}$ away from the furnace midline. Based on this thermal gradient, the temperature at the center of the capsule ($T'$) was corrected from the run temperature which was measured by a thermocouple at the top, and the temperature range ($R$) in the capsule was calculated from the inner height of the capsule.

Textures of the run products are shown in Figure 3-2. For all systems, phases interpreted to be primary phases are equant to sub-equant and typically have large grain size, whereas quenched phases are subhedral to euhedral and typically display elongate prismatic habit. The primary phases in the $Mg_2SiO_4$-$MgSiO_3$-$H_2O$ system were typically smaller than those in $Mg_2SiO_4$-$MgSiO_3$-KCl-$H_2O$ systems, and the quenched phases in the $Mg_2SiO_4$-$MgSiO_3$-$H_2O$ system are generally larger than those in $Mg_2SiO_4$-$MgSiO_3$-KCl-$H_2O$ systems. In the $Mg_2SiO_4$-$MgSiO_3$-$H_2O$ system, primary forsterite and enstatite coexist in all runs; the quenched phases have compositions similar to enstatite and forsterite, and their amount increases abruptly at the run temperature of 1250°C. In $Mg_2SiO_4$-$MgSiO_3$-KCl-$H_2O$ systems with Cl/(Cl+$H_2O$) ratio of 0.2, 0.4 and 0.6, the primary phases changes

from coexisting forsterite and enstatite at lower temperatures to only fosterite at higher temperatures; the quenched phases contain Si, Mg, K and Cl, and the amount of quenched phases increases abruptly at the run temperatures of 1450°C, 1600 °C and 1650°C, respectively. Quenched liquid (qL) and quenched liquid (qL) are very similar in texture, but they can be differentiated from the amount of quenched phases (Figure 3-2). The quenched phases in small amounts are determined as qV and those in large amounts are determined as qL. The quenched phases in moderate amounts are difficult to distinguish as either quenched vapor or quenched liquid, so they are noted as quenched vapor and liquid (qV/qL). The coexistence of both vapor and liquid in one capsule is explained to be due to the existence of thermal gradient in the capsule.

Table 3-2. Experimental conditions and results.

| Run # | molar Cl/(Cl+$H_2O$ | *T* (℃) | Duration (h) | Results | *T* correction (℃) | | Ca in Ol (ppm) | | | Ca in Opx (ppm) | | |
|---|---|---|---|---|---|---|---|---|---|---|---|---|
| | | | | | *T'* | *R* | N | Av | SD | N | Av | SD |
| 3722 | 0 | 1100 | 12 | En+Fo+V | 1080 | 14 | 27 | 30 | 11 | 26 | 191 | 11 |
| 3710 | 0 | 1200 | 8 | En+Fo+V | 1178 | 12 | 20 | 29 | 7 | 15 | 220 | 29 |
| 3711 | 0 | 1250 | 12 | En+Fo+V/L | 1229 | 12 | 10 | 49 | 8 | 7 | 191 | 11 |
| 3709 | 0 | 1300 | 8 | En+Fo+L | 1285 | 11 | 16 | 29 | 7 | 14 | 128 | 6 |
| 3755 | 0 | 1350 | 12 | En+Fo+L | 1324 | 16 | 7 | 26 | 8 | 10 | 143 | 19 |
| 3765 | 0 | 1400 | 12 | En+Fo+L | 1379 | 9 | 15 | 74 | 43 | 18 | 160 | 26 |
| 3762 | 0 | 1450 | 12 | En+Fo+L | 1428 | 11 | 12 | 71 | 37 | 19 | 256 | 97 |
| 3771 | 0 | 1450 | 12 | En+Fo+L | 1425 | 11 | 48 | 26 | 6 | | | |
| 3770 | 0 | 1500 | 12 | En+Fo+L | 1478 | 13 | 14 | 31 | 5 | 37 | 193 | 140 |
| 3715 | 0.2 | 1300 | 12 | En+Fo+V | 1277 | 18 | 11 | 28 | 6 | 16 | 234 | 9 |
| 3753 | 0.2 | 1300 | 12 | En+Fo+V | 1276 | 11 | 19 | 30 | 9 | 9 | 223 | 16 |
| 3721 | 0.2 | 1400 | 12 | En+Fo+V/L | 1377 | 18 | 48 | 26 | 6 | 33 | 195 | 11 |
| 3750 | 0.2 | 1450 | 12 | Fo+L | 1428 | 12 | 19 | 47 | 12 | | | |
| 3727 | 0.2 | 1500 | 12 | Fo+L | 1480 | 14 | 56 | 20 | 6 | | | |
| 3737 | 0.2 | 1600 | 12 | Fo+L | 1580 | 10 | 11 | 25 | 4 | | | |
| 3761 | 0.2 | 1650 | 2 | L | 1629 | 10 | | | | | | |
| 3748 | 0.4 | 1400 | 12 | En+Fo+V | 1376 | 14 | 11 | 31 | 6 | 14 | 266 | 27 |
| 3728 | 0.4 | 1500 | 12 | En+Fo+V | 1476 | 17 | 28 | 37 | 4 | 11 | 219 | 7 |
| 3759 | 0.4 | 1550 | 12 | En+Fo+V/L | 1529 | 11 | 19 | 58 | 18 | 14 | 217 | 18 |
| 3744 | 0.4 | 1600 | 12 | Fo+L | 1584 | 8 | 26 | 31 | 11 | | | |
| 3763 | 0.4 | 1650 | 2 | Fo+L | 1627 | 15 | 14 | 83 | 16 | | | |
| 3747 | 0.4 | 1700 | 2 | L | 1676 | 13 | | | | | | |
| 3754 | 0.6 | 1500 | 12 | En+Fo+V | 1475 | 12 | 6 | 30 | 5 | 9 | 261 | 20 |
| 3739 | 0.6 | 1600 | 10 | En+Fo+V/L | 1581 | 10 | 17 | 40 | 7 | 9 | 250 | 60 |
| 3772 | 0.6 | 1650 | 2 | Fo+L | 1624 | 12 | 57 | 26 | 5 | | | |
| 3740 | 0.6 | 1700 | 2 | Fo+L | 1682 | 10 | 15 | 43 | 6 | | | |
| 3758 | 0.6 | 1700 | 2 | Fo+L | 1677 | 11 | 16 | 40 | 7 | | | |

Abbreviations: *T* temperature, *N* number of analysis, *R* temperature range in capsule, *Av* average, *SD* standard deviation, *En* enstatite, *Fo* forsterite, *V* vapor, *L* liquid.

T correction is done by $T' = T - \frac{1}{2}gh$ and $R = \frac{1}{2}gl$, where *g* is the thermal gradient in graphite furnace, *h* is the outer height of capsule, and *l* is the inner height of capsule.

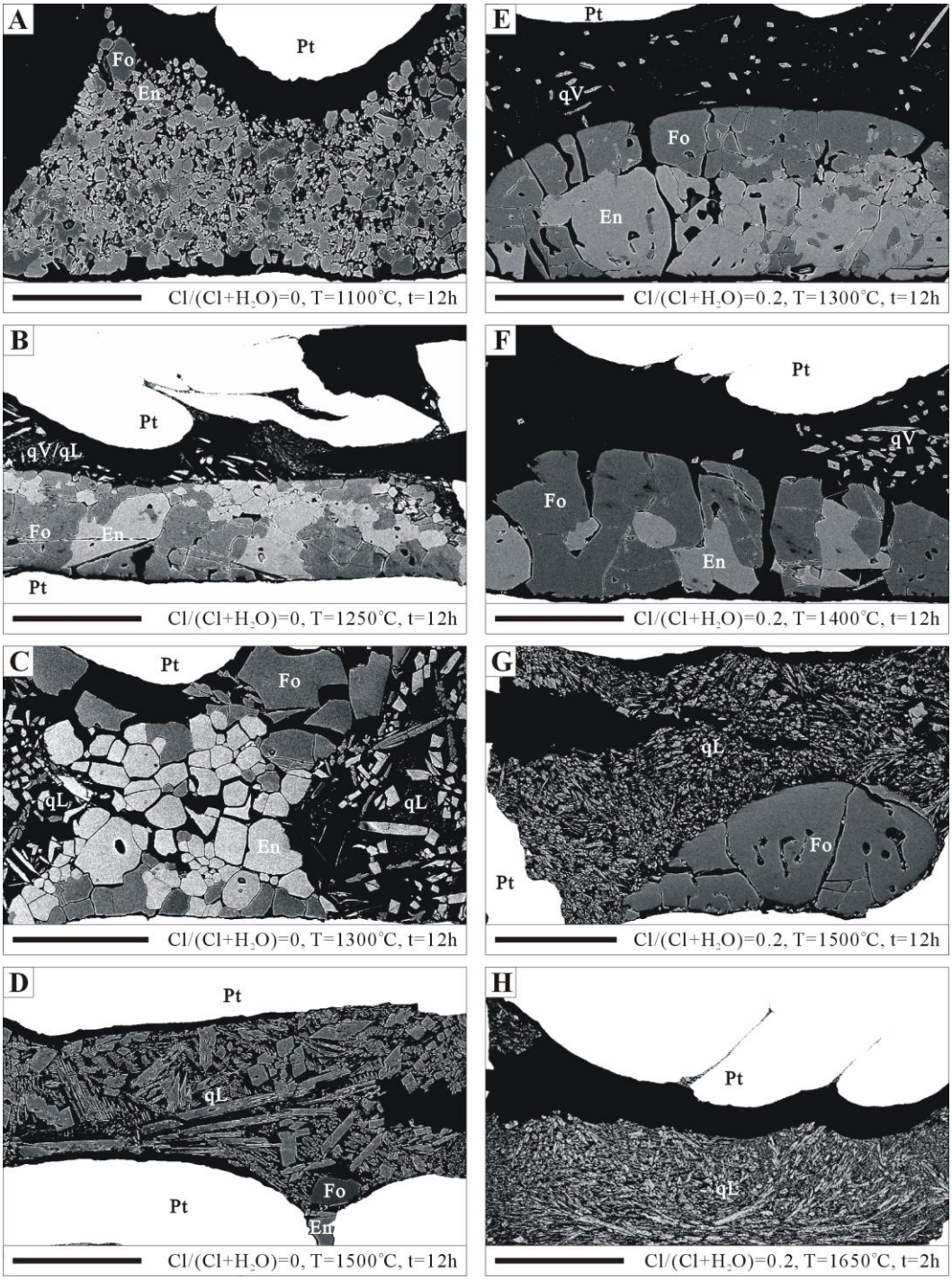


Figure 3-2. Backscattered electron images of run products.

A-D Run products of $Mg_2SiO_4$-$MgSiO_3$-$H_2O$ system, primary phases are forsterite and enstatite. E-F Run products of the $Mg_2SiO_4$-$MgSiO_3$-KCl-$H_2O$ system with Cl/(Cl+$H_2O$) ratio of 0.2, subsolidus primary phases are forsterite and enstatite, suprasolidus primary phases are forsterite, and the enstatite/forsterite modal ratio decreases as the temperature increases. Abbreviations: *Pt*, platinum capsule, *Fo*, forsterite, *En*, enstatite, *qV*, quenched vapor, *qL*, quenched liquid. Black scale bars at left bottom represent 400 μm.

For all systems, primary forsterite has Ca content of 20-83 ppm, and primary enstatite has Ca content of 128-226 ppm. The calcium in these experiments was probably derived from the reagent-grade $Mg(OH)_2$ starting material. In the $Mg_2SiO_4$-$MgSiO_3$-$H_2O$ system, forsterite has an obvious jump in Ca content around the temperature of 1229°C, and enstatite has a big drop in Ca content at the same temperature (Figure 3-3). In $Mg_2SiO_4$-$MgSiO_3$-KCl-$H_2O$ systems with $Cl/(Cl+H_2O)$ ratio of 0.2, 0.4 and 0.6, forsterite has jumps in Ca content at temperatures of 1428°C, 1529°C and 1581°C, respectively (Figure 3-4).

Abrupt increases in the amount of quenched phases and abrupt changes in Ca content of primary phases are interpreted to indicate the solidus, because transition from vapor to liquid will cause abrupt changes in the solubility of silicate in fluid and partitioning of trace elements between solid and vapor is different from that between solid and liquid. In the experiments on melting of peridotite-$CO_2$ system by Dasgupta and Hirschman (2006), the sodium content of the clinopyroxene dropped abruptly at the solidus, which suggests that the drop in content of minor element in pyroxene can indicate the position of solidus. In the $Mg_2SiO_4$-$MgSiO_3$-$H_2O$ system (Figure 3-3), the drop of Ca content in enstatite indicates the temperature of the solidus, and the jump of Ca content in olivine also happened at the same temperature. That forsterite and enstatite have different behaviors in changing Ca content at the temperature of solidus may be due to their different crystal structures, and both the drop of Ca content in enstatite and the jump of Ca content in olivine can be used in determine the solidus. Both the textural relationships and the Ca peaks give the same result for the

$Mg_2SiO_4$-$MgSiO_3$-$H_2O$ system and the $Mg_2SiO_4$-$MgSiO_3$-KCl-$H_2O$ systems with Cl/(Cl+$H_2O$) molar ratio of 0.2 and 0.4. Solidus of the $Mg_2SiO_4$-$MgSiO_3$-KCl-$H_2O$ system with Cl/(Cl+$H_2O$) molar ratio of 0.6 cannot be determined from textural relationships because the quenched material collapsed when large amount of water-soluble material was removed, and it is only determined by the Ca peak of forsterite.

The temperature of the solidus changing with Cl/(Cl+$H_2O$) molar ratio is shown in Figure 3-5. Above the solidus, both forsterite and enstatite coexist with melt in the $Mg_2SiO_4$-$MgSiO_3$-$H_2O$ system, which is consistent with a eutectic melting relationship of forsterite and enstatite at 5 GPa. In contrast, only forsterite coexists with melt in $Mg_2SiO_4$-$MgSiO_3$-KCl-$H_2O$ systems, which may reveal the incongruent melting of enstatite.

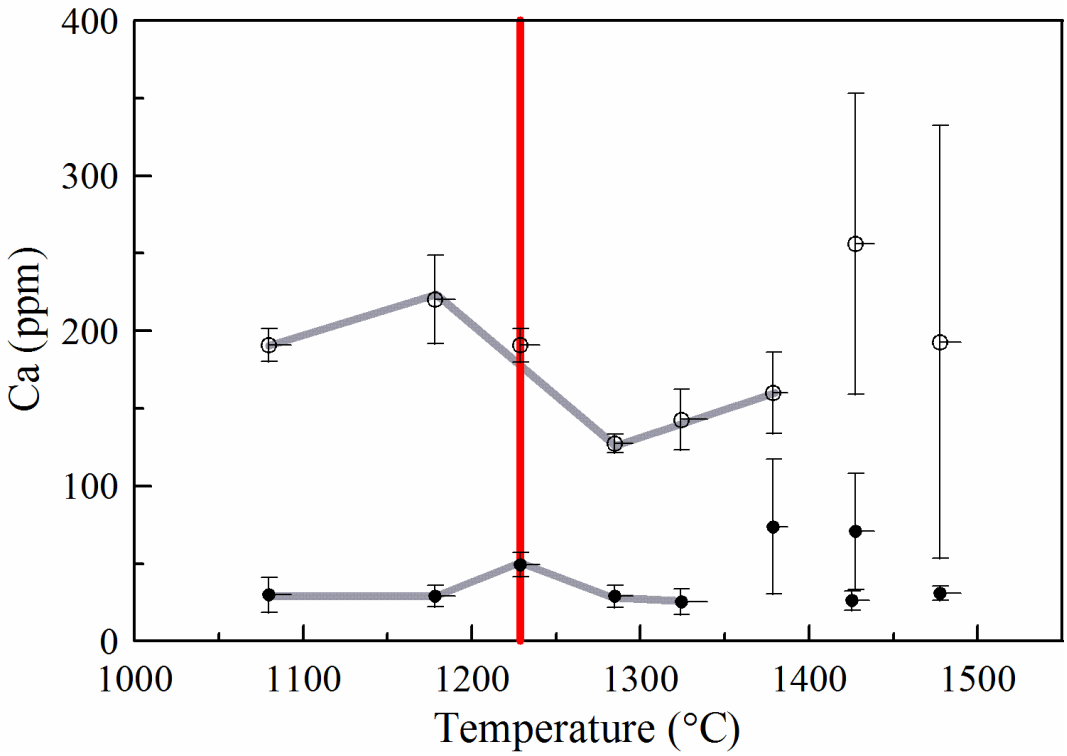


Figure 3-3. Ca contents of forsterite (filled circle) and enstatite (open circle) in the $Mg_2SiO_4$-$MgSiO_3$-$H_2O$ system as a function of temperature.

Error bars show temperature uncertainties in horizontal and 2 standard deviation of Ca content in vertical. The vertical line shows the inferred position of solidus. The big error bars for the Ca contents of forsterite and enstatite from high temperature experiments are because of the hardness in distinguishing primary phases from quenched phases.

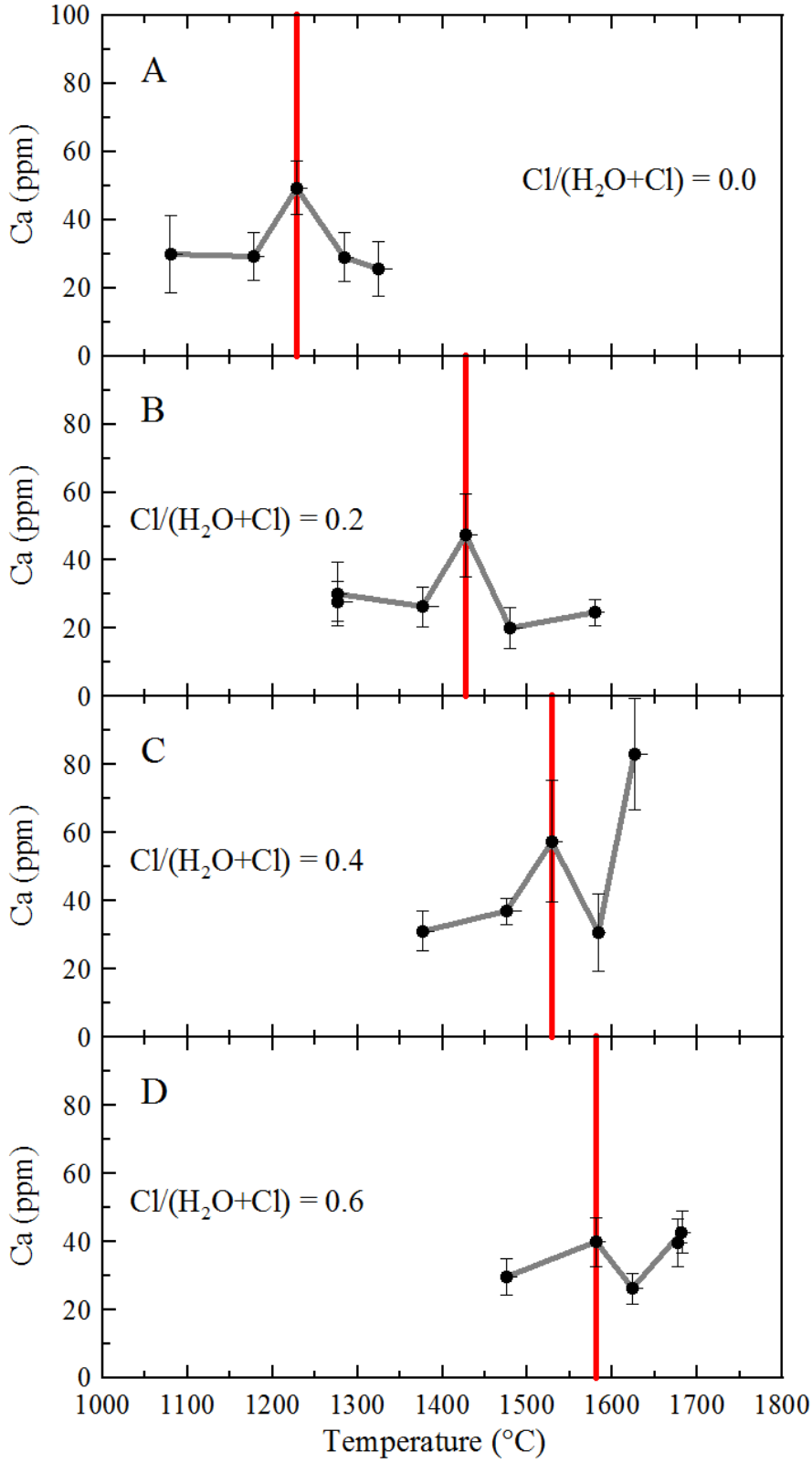


Figure 3-4. Ca contents of forsterite in the $Mg_2SiO_4$-$MgSiO_3$-$H_2O$ system and $Mg_2SiO_4$-$MgSiO_3$-KCl-$H_2O$ systems. Error bars show 2 standard deviation of Ca content. Vertical lines show positions of solidi.

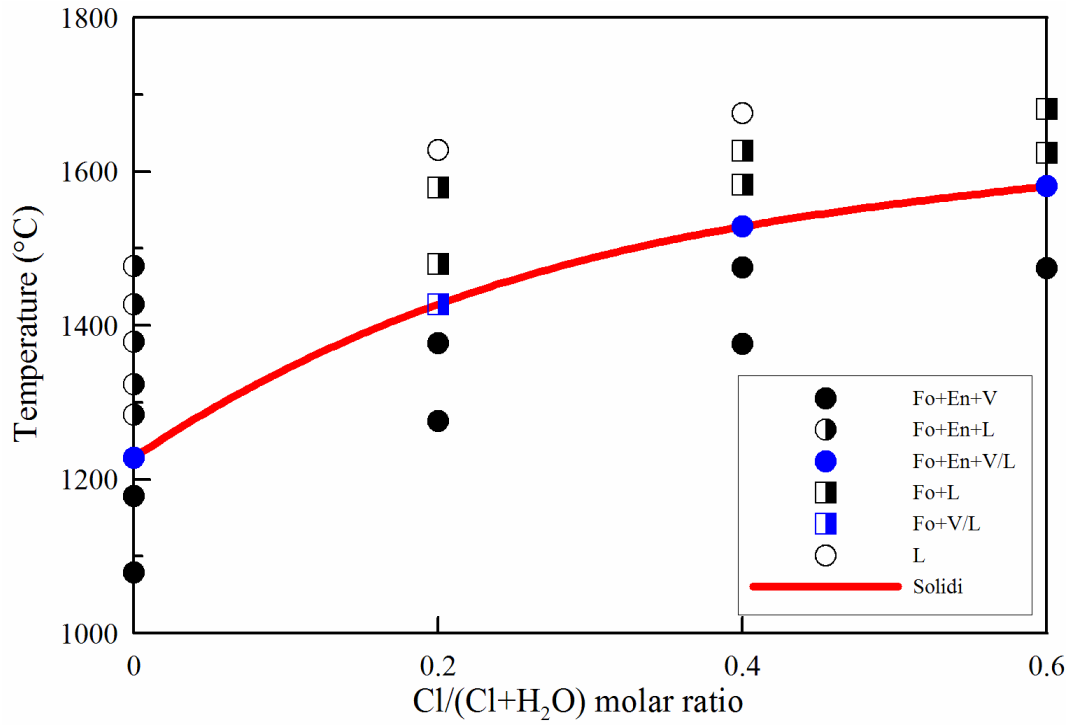


Figure 3-5. Phase relations of the $Mg_2SiO_4$-$MgSiO_3$-$H_2O$ system and $Mg_2SiO_4$-$MgSiO_3$-KCl-$H_2O$ systems at 5 GPa.

The curve shows the relation between solidi and Cl concentrations.

**Discussion**

Chloride can significantly reduce $H_2O$ activity in aqueous solutions, which was evidenced by measuring $H_2O$ activity in NaCl, KCl and NaCl-KCl solutions by the brucite-periclase equilibrium (Aranovich and Newton, 1996; Shmulovich and Graham, 1996; Aranovich and Newton, 1997). The experiments by Aranovich and Newton (1997) revealed that the $H_2O$ activity is nearly coincident with the square of its mole fraction in KCl solution at the pressure range from 4 to 15 kbar. Melting experiments of albite in NaCl solution by Shmulovich and Graham (1996) showed that the temperature of the vapor-saturated solidus of albite in a solution with NaCl mole fraction of 0.2 is ~100 ℃ higher than that in pure water at 9 kbar. Experiments on $Mg_2SiO_4$-$MgSiO_3$-KCl-$H_2O$ systems at 5 GPa in this study (Figure 3-5) show that temperatures of solidi of the systems with the $Cl/(Cl+H_2O)$ molar ratio of 0.2, 0.4 and 0.6 are, respectively, ~200 ℃, ~300 ℃ and ~350 ℃ higher than that with pure water, which indicates that chloride can also significantly reduce $H_2O$ activity in aqueous solution at pressure relevant to depth of ~160km in the Earth's mantle. Therefore, chlorine in the SCLM, evidenced by fluid inclusions in fibrous diamonds, can inhibit melting of the mantle by reducing the $H_2O$ activity in fluids, and the KCl-bearing fluids can be a robust agent of mantle metasomatism.

The absence of primary enstatite under suprasolidus conditions in $Mg_2SiO_4$-$MgSiO_3$-KCl-$H_2O$ systems may be due to the incongruent melting of enstatite. The incongruent melting of enstatite, discovered by Bowen and Andersen (1914) at 1 atm, has a significant bearing on the generation of

silica-saturated magmas from silica-undersaturated mantle rocks by partial melting or from silicate-undersaturated magmas by fractional crystallization (Kushiro et al., 1968), and thus potentially plays an important role in the Mg/Si differentiation of the planet. The incongruent melting of enstatite disappears at pressures higher than ~0.5 GPa under anhydrous conditions (Boyd et al., 1964) and at some pressure between 3 and 5.5 GPa under hydrous conditions (Kushiro et al., 1968; Inoue, 1994). The eutectic melting inferred in this study in the $Mg_2SiO_4$-$MgSiO_3$-$H_2O$ system at 5 GPa reveals that the incongruent melting of enstatite disappears at pressures less than 5 GPa. If the absence of primary enstatite under suprasolidus conditions in $Mg_2SiO_4$-$MgSiO_3$-KCl-$H_2O$ systems is due to the incongruent melting of enstatite, it will mean that the chlorine-rich brine can make the incongruent melting of enstatite happen at the pressure of 5 GPa or more.

**Conclusion**

KCl significantly elevates the solidus temperature of the $Mg_2SiO_4$-$MgSiO_3$-$H_2O$ system at 5 GPa by reducing the activity of $H_2O$ in the fluid. This indicates that chlorine can prevent melting in the SCLM and the KCl-bearing fluids can be a robust agent of mantle metasomatism. In $Mg_2SiO_4$-$MgSiO_3$-KCl-$H_2O$ systems, the absence of primary enstatite under suprasolidus conditions is probably due to the incongruent melting of enstatite, which needs to be defined by further experiments on the melting of the $MgSiO_3$-KCl-$H_2O$ system.

**References**

Aranovich, L.Y. and Newton, R.C., 1996, $H_2O$ activity in concentrated NaCl solutions at high pressures and temperatures measured by the brucite-periclase equilibrium: Contributions to Mineralogy and Petrology, v. 125, p. 200-212.

Aranovich, L.Y. and Newton, R.C., 1997, $H_2O$ activity in concentrated KCl and KCl-NaCl solutions at high temperatures and pressures measured by the brucite-periclase equilibrium: Contributions to Mineralogy and Petrology, v. 127, p. 261-271.

Aranovich, L.Y. and Newton, R.C., 1998, Reversed determination of the reaction: phlogopite + quartz = enstatite + potassium feldspar + $H_2O$ in the ranges 750-875 °C and 2-12 kbar at low $H_2O$ activity with concentrated KCl solutions: American Mineralogist, v. 83, p. 193-204.

Bowen, N.L. and Andersen, O., 1914, The binary system MgO-SiO2: The American Journal of Science, v. 37, p.487-500.

Boyd, F.R., England, J.L. and Davis, B.T.C., 1964, Effects of pressure on the melting and polymorphism of enstatite, $MgSiO_3$: Journal of Geophysical Research, v. 69, p. 2101-2109.

Dasgupta, R. and Hirschman, M.M., 2006, Melting in the Earth's deep upper mantle caused by carbon dioxide: Nature, v. 440, p. 659-662.

Grove, T.L., Chatterjee, N., Parman, S.W. and Médard, E., 2006, The influence of $H_2O$ on mantle wedge melting: Earth and Planetary Science Letters, v. 249, p. 74-89.

Inoue, T., 1994, Effect of water on melting phase relations and melt composition in the system $Mg_2SiO_4$-$MgSiO_3$-$H_2O$ up to 15 GPa: Physics of the Earth and Planetary Interiors, v. 85, p. 237-263.

Izraeli, E.S., Harris, J.W. and Navon, O., 2001, Brine inclusions in diamonds: a new upper mantle fluid: Earth and Planetary Science Letters, v. 187, p. 323-332.

Izraeli, E.S., Harris, J.W. and Navon, O., 2004, Fluid and mineral inclusions in cloudy diamonds from Koffiefontein, South Africa: Geochimica et Cosmochimica Acta, v. 68, p. 2561-2575.

Klein-BenDavid, O., Izraeli, E.S., Hauri, E.H. and Navon, O., 2007, Fluid inclusions in diamonds from the Diavik Mine, Canada and the evolution of diamond-forming fluids: Geochimica et Cosmochimica Acta, v. 71, p. 723-744.

Klein-BenDavid, O., Richard, W. and Navon, O., 2006, TEM imaging and analysis of microinclusions in diamonds; a close look at diamond-growing fluids: American Mineralogist, v. 91, p. 353-365.

Kushiro, I., Yoder, H.S. and Nishikawa, M., 1968, Effect of water on the melting of enstatite: Bulletin of the Geological Society of America, v. 79, p. 1685-1692.

Navon, O., Hutcheon, I.D., Rossman, G.R. and Wasserburg, G.J., 1988, Mantle-derived fluids in diamond micro-inclusions: Nature, v. 335, p. 784-789.

Potts, P.J., 1986, A handbook of silicate rock analysis, Chapman and Hall, New York, NY, p. 17.

Scott, V.D, Love, G., 1983, Quantitative Electron-Probe Microanalysis, Ellis Horwood Limited, p. 137-142.

Shmulovich, K.I. and Graham, C.M., 1996, Melting of albite and dehydration of brucite in $H_2O$-NaCl fluids to 9 kbars and 700-900°C: implications for partial melting and water activities during high pressure metamorphism: Contributions to Mineralogy and Petrology, v. 124, p. 370-382.

Tomlinson, E.L., Jones, A.P. and Harris, J.W., 2006, Co-existing fluid and silicate inclusions in mantle diamond: Earth and Planetary Science Letters, v. 250, p. 581-595.

Walter, M.J., Thibault, Y., Wei, K. and Luth, R.W., 1995, Characterizing experimental pressure and temperature conditions in multi-anvil apparatus: Canadian Journal of Physics, v. 73, p. 273-286.

## Chapter 4. General Discussion and Conclusions

The presence of chlorine in the subcratonic lithospheric mantle (SCLM) has been evaluated by compiling the compositional data of fluid inclusions in fibrous diamonds. It mainly associates with potassium, dissolving in water and forming a KCl-bearing brine with the $Cl/(Cl+H_2O)$ molar ratio of 0.05-0.68 mol%. To examine the effect of such a KCl-bearing brine on the melting behavior of the Earth's mantle, we conducted experiments in the $Mg_2SiO_4$-$MgSiO_3$-$H_2O$ and $Mg_2SiO_4$-$MgSiO_3$-KCl-$H_2O$ systems at 5 GPa and 1100-1700 ℃. In the $Mg_2SiO_4$-$MgSiO_3$-$H_2O$ system, the temperature of the fluid-saturated solidus is ~1230 ℃, and both forsterite and enstatite coexist with the liquid under suprasolidus conditions. In the $Mg_2SiO_4$-$MgSiO_3$-KCl-$H_2O$ systems with molar $Cl/(Cl+H_2O)$ ratios of 0.2, 0.4 and 0.6, the temperatures of the fluid-saturated solidus are ~1430 ℃, ~1530 ℃ and ~1580 ℃, respectively, and only forsterite coexists with liquid under suprasolidus conditions. The increase in the temperature of the solidus demonstrates the significant effect of KCl on elevating the solidus of the $Mg_2SiO_4$-$MgSiO_3$-$H_2O$ system by reducing the activity of $H_2O$ in the fluid. The change in the melting residues indicates that the incongruent melting of enstatite (enstatite = forsterite + silica-rich melt) could happen at pressures over 5 GPa in KCl-bearing systems, which needs to be verified by experiments on the $MgSiO_3$-KCl-$H_2O$ system in future work.

If KCl is present in the Earth's mantle, it will elevate the melting temperature of the $H_2O$-bearing mantle. In subduction zones, brine inclusions, with ~50 wt% NaCl and KCl, have been found in omphacite in eclogite (Scambelluri and

Philippot, 2001), which indicates the existence of chloride-rich brines in subducting slabs. Release of these brines, from subducting slabs to mantle wedges, will inhibit melting of the mantle wedges. In cratonic areas, fluid inclusions, with ~47 wt% KCl and NaCl, have been found in fibrous diamonds (Klein-BenDavid *et al*., 2007), which indicates the existence of chloride-rich fluids in the diamond stability field of the cratonic mantle. These fluids will inhibit melting at the $H_2O$-saturated solidus in the mantle, and the KCl-bearing brine can be a robust agent for mantle metasomatism at temperatures greater than that of the $H_2O$-saturated solidus. Accordingly, the brine-bearing fibrous diamonds are inferred to form from fluid rather than melt in the SCLM.

**References**

Klein-BenDavid, O., Izraeli, E.S., Hauri, E.H. and Navon, O., 2007, Fluid inclusions in diamonds from the Diavik Mine, Canada and the evolution of diamond-forming fluids: Geochimica et Cosmochimica Acta, v. 71, p. 723-744.

Scambelluri, M. and Philippot, P., 2001, Deep fluids in subduction zones: Lithos, v. 55, p. 213-227.

# Appendix. EPMA analysis of run products

| Run # | Analysis # | Phase | MgO (wt%) | $SiO_2$ (wt%) | CaO (wt%) | Total (wt%) |
|---|---|---|---|---|---|---|
| 3709 | LC3-1 | Fo | 56.027 | 40.022 | 0.0038 | 96.053 |
| 3709 | LC3-2 | Fo | 54.814 | 41.515 | 0.0033 | 96.332 |
| 3709 | LC3-3 | En | 39.339 | 59.713 | 0.0190 | 99.071 |
| 3709 | LC3-4 | En | 38.564 | 59.424 | 0.0164 | 98.005 |
| 3709 | LC3-5 | En | 37.989 | 58.777 | 0.0179 | 96.784 |
| 3709 | LC3-6 | En | 39.330 | 57.759 | 0.0180 | 97.107 |
| 3709 | LC3-7 | En | 38.469 | 57.237 | 0.0175 | 95.724 |
| 3709 | LC3-8 | En | 38.005 | 58.020 | 0.0165 | 96.042 |
| 3709 | LC3-9 | Fo | 52.589 | 39.617 | 0.0026 | 92.209 |
| 3709 | LC3-10 | Fo | 49.574 | 39.690 | 0.0032 | 89.267 |
| 3709 | LC3-11 | Fo | 49.974 | 41.070 | 0.0030 | 91.047 |
| 3709 | LC3-12 | En | 37.197 | 58.304 | 0.0188 | 95.520 |
| 3709 | LC3-13 | En | 37.139 | 59.185 | 0.0183 | 96.343 |
| 3709 | LC3-14 | En | 39.216 | 60.001 | 0.0163 | 99.234 |
| 3709 | LC3-15 | En | 39.937 | 61.031 | 0.0168 | 100.985 |
| 3709 | LC3-16 | En | 39.969 | 59.925 | 0.0162 | 99.911 |
| 3709 | LC3-17 | En | 40.183 | 60.432 | 0.0185 | 100.634 |
| 3709 | LC3-18 | En | 40.173 | 60.448 | 0.0179 | 100.639 |
| 3709 | LC3-19 | En | 39.443 | 59.216 | 0.0171 | 98.676 |
| 3709 | LC3-20 | Fo | 55.249 | 42.112 | 0.0031 | 97.364 |
| 3709 | LC3-21 | Fo | 47.822 | 37.529 | 0.0031 | 85.354 |
| 3709 | LC3-22 | Fo | 54.906 | 43.307 | 0.0042 | 98.217 |
| 3709 | LC3-23 | Fo | 54.451 | 41.216 | 0.0052 | 95.672 |
| 3709 | LC3-24 | Fo | 53.831 | 42.644 | 0.0039 | 96.479 |
| 3709 | LC3-25 | Fo | 53.932 | 41.960 | 0.0043 | 95.896 |
| 3709 | LC3-26 | Fo | 52.279 | 40.467 | 0.0050 | 92.751 |
| 3709 | LC3-27 | Fo | 54.593 | 41.903 | 0.0053 | 96.501 |
| 3709 | LC3-28 | Fo | 52.719 | 43.015 | 0.0059 | 95.740 |
| 3709 | LC3-29 | Fo | 54.627 | 41.846 | 0.0047 | 96.478 |
| 3709 | LC3-30 | Fo | 53.980 | 41.531 | 0.0050 | 95.516 |
| 3709 | LC3-31 | q | 39.091 | 57.950 | 0.0431 | 97.085 |
| 3709 | LC3-32 | q | 40.121 | 60.723 | 0.0453 | 100.890 |
| 3709 | LC3-33 | q | 39.519 | 58.801 | 0.0439 | 98.365 |
| 3709 | LC3-34 | q | 39.512 | 58.800 | 0.0493 | 98.362 |
| 3710 | LC4-1 | Fo | 53.724 | 40.576 | 0.0027 | 94.303 |
| 3710 | LC4-2 | Fo | 50.015 | 40.339 | 0.0045 | 90.359 |
| 3710 | LC4-3 | Fo | 53.463 | 41.314 | 0.0060 | 94.783 |
| 3710 | LC4-4 | En | 38.120 | 60.024 | 0.0272 | 98.172 |
| 3710 | LC4-5 | Fo | 50.316 | 42.232 | 0.0048 | 92.553 |
| 3710 | LC4-6 | Fo | 54.015 | 42.658 | 0.0031 | 96.676 |
| 3710 | LC4-7 | En | 36.849 | 60.911 | 0.0263 | 97.787 |
| 3710 | LC4-8 | En | 36.969 | 60.723 | 0.0278 | 97.721 |
| 3710 | LC4-9 | Fo | 53.967 | 43.200 | 0.0040 | 97.171 |
| 3710 | LC4-10 | Fo | 51.588 | 43.219 | 0.0041 | 94.811 |

| Run # | Analysis # | Phase | MgO (wt%) | $SiO_2$ (wt%) | CaO (wt%) | Total (wt%) |
|---|---|---|---|---|---|---|
| 3710 | LC4-11 | En | 36.163 | 60.589 | 0.0303 | 96.783 |
| 3710 | LC4-12 | Fo | 54.304 | 42.670 | 0.0034 | 96.978 |
| 3710 | LC4-13 | En | 37.255 | 61.269 | 0.0311 | 98.556 |
| 3710 | LC4-14 | En | 36.851 | 61.162 | 0.0390 | 98.053 |
| 3710 | LC4-15 | Fo | 53.283 | 43.330 | 0.0039 | 96.617 |
| 3710 | LC4-16 | Fo | 53.908 | 42.507 | 0.0039 | 96.419 |
| 3710 | LC4-17 | En | 38.122 | 59.661 | 0.0317 | 97.816 |
| 3710 | LC4-18 | Fo | 60.803 | 43.467 | 0.0042 | 104.274 |
| 3710 | LC4-19 | En | 40.225 | 60.182 | 0.0287 | 100.436 |
| 3710 | LC4-20 | En | 39.100 | 58.884 | 0.0281 | 98.013 |
| 3710 | LC4-21 | En | 39.650 | 59.839 | 0.0283 | 99.518 |
| 3710 | LC4-22 | Fo | 56.599 | 41.916 | 0.0044 | 98.519 |
| 3710 | LC4-23 | En | 39.624 | 59.285 | 0.0280 | 98.938 |
| 3710 | LC4-24 | Fo | 56.504 | 42.257 | 0.0033 | 98.764 |
| 3710 | LC4-25 | Fo | 56.291 | 41.728 | 0.0037 | 98.023 |
| 3710 | LC4-26 | Fo | 56.040 | 41.317 | 0.0035 | 97.361 |
| 3710 | LC4-27 | Fo | 55.966 | 41.777 | 0.0021 | 97.745 |
| 3710 | LC4-28 | Fo | 55.405 | 41.279 | 0.0044 | 96.688 |
| 3710 | LC4-29 | En | 41.037 | 55.965 | 0.0377 | 97.041 |
| 3710 | LC4-30 | En | 40.239 | 57.684 | 0.0263 | 97.950 |
| 3710 | LC4-31 | Fo | 58.579 | 40.356 | 0.0038 | 98.939 |
| 3710 | LC4-32 | Fo | 58.844 | 40.113 | 0.0063 | 98.963 |
| 3710 | LC4-33 | En | 40.239 | 58.608 | 0.0275 | 98.875 |
| 3710 | LC4-34 | Fo | 57.917 | 41.642 | 0.0047 | 99.564 |
| 3710 | LC4-35 | En | 41.600 | 57.815 | 0.0326 | 99.448 |
| 3710 | LC4-36 | q | 42.048 | 58.456 | 0.0892 | 100.595 |
| 3710 | LC4-37 | q | 40.597 | 57.402 | 0.1065 | 98.108 |
| 3710 | LC4-38 | q | 40.499 | 59.781 | 0.0834 | 100.365 |
| 3711 | LC5-1 | Fo | 60.803 | 40.439 | 0.0053 | 101.247 |
| 3711 | LC5-2 | En | 42.377 | 60.767 | 0.0273 | 103.172 |
| 3711 | LC5-3 | En | 40.993 | 61.267 | 0.0272 | 102.288 |
| 3711 | LC5-4 | Fo | 58.254 | 41.232 | 0.0061 | 99.492 |
| 3711 | LC5-5 | Fo | 57.690 | 42.293 | 0.0067 | 99.990 |
| 3711 | LC5-6 | En | 39.067 | 57.574 | 0.0792 | 96.722 |
| 3711 | LC5-7 | En | 39.839 | 60.377 | 0.0269 | 100.244 |
| 3711 | LC5-8 | En | 39.449 | 59.583 | 0.0731 | 99.107 |
| 3711 | LC5-9 | Fo | 54.003 | 40.050 | 0.0069 | 94.060 |
| 3711 | LC5-10 | Fo | 56.331 | 41.856 | 0.0090 | 98.196 |
| 3711 | LC5-11 | Fo | 59.100 | 44.480 | 0.0065 | 103.587 |
| 3711 | LC5-12 | En | 41.317 | 62.502 | 0.0257 | 103.845 |
| 3711 | LC5-13 | En | 56.406 | 42.404 | 0.0070 | 98.817 |
| 3711 | LC5-14 | En | 41.053 | 61.398 | 0.0263 | 102.478 |
| 3711 | LC5-15 | En | 39.992 | 59.799 | 0.0256 | 99.817 |
| 3711 | LC5-16 | En | 39.735 | 58.141 | 0.0342 | 97.911 |
| 3711 | LC5-17 | En | 40.180 | 60.995 | 0.0236 | 101.199 |
| 3711 | LC5-18 | Fo | 53.836 | 39.800 | 0.0079 | 93.644 |

| Run # | Analysis # | Phase | MgO (wt%) | $SiO_2$ (wt%) | CaO (wt%) | Total (wt%) |
|---|---|---|---|---|---|---|
| 3711 | LC5-19 | Fo | 58.654 | 44.506 | 0.0060 | 103.166 |
| 3711 | LC5-20 | Fo | 57.277 | 44.540 | 0.0069 | 101.824 |
| 3711 | LC5-21 | Fo | 50.662 | 40.957 | 0.0101 | 91.629 |
| 3711 | LC5-22 | En | 39.036 | 59.428 | 0.0298 | 98.495 |
| 3711 | LC5-23 | Fo | 52.753 | 38.998 | 0.0120 | 91.763 |
| 3711 | LC5-24 | En | 36.946 | 58.592 | 0.0324 | 95.571 |
| 3711 | LC5-25 | Fo | 52.786 | 40.491 | 0.0343 | 93.312 |
| 3711 | LC5-26 | En | 34.417 | 52.401 | 0.0324 | 86.851 |
| 3711 | LC5-27 | q | 37.931 | 61.210 | 0.2651 | 99.413 |
| 3711 | LC5-28 | q | 41.120 | 57.988 | 0.3266 | 99.442 |
| 3711 | LC5-29 | q | 40.980 | 56.517 | 0.5652 | 98.075 |
| 3711 | LC5-30 | q | 40.940 | 55.553 | 0.5518 | 97.058 |
| 3715 | LC7-1 | En | 39.536 | 55.522 | 0.0311 | 95.090 |
| 3715 | LC7-2 | Fo | 59.846 | 40.587 | 0.0034 | 100.436 |
| 3715 | LC7-3 | Fo | 61.756 | 42.280 | 0.0033 | 104.039 |
| 3715 | LC7-4 | Fo | 60.022 | 42.267 | 0.0037 | 102.293 |
| 3715 | LC7-5 | Fo | 60.257 | 42.675 | 0.0027 | 102.935 |
| 3715 | LC7-6 | Fo | 58.546 | 42.735 | 0.0043 | 101.285 |
| 3715 | LC7-7 | En | 40.341 | 58.614 | 0.0310 | 98.987 |
| 3715 | LC7-8 | En | 40.286 | 59.470 | 0.0334 | 99.790 |
| 3715 | LC7-9 | En | 40.338 | 59.860 | 0.0310 | 100.230 |
| 3715 | LC7-10 | En | 39.805 | 59.294 | 0.0334 | 99.133 |
| 3715 | LC7-11 | En | 39.852 | 58.885 | 0.0324 | 98.770 |
| 3715 | LC7-12 | En | 39.853 | 57.344 | 0.0313 | 97.229 |
| 3715 | LC7-13 | Fo | 60.201 | 42.707 | 0.0028 | 102.911 |
| 3715 | LC7-14 | En | 41.312 | 60.003 | 0.0318 | 101.348 |
| 3715 | LC7-15 | En | 41.008 | 59.735 | 0.0318 | 100.776 |
| 3715 | LC7-16 | En | 39.810 | 57.613 | 0.0319 | 97.456 |
| 3715 | LC7-17 | En | 40.385 | 58.329 | 0.0299 | 98.745 |
| 3715 | LC7-18 | En | 39.657 | 57.942 | 0.0309 | 97.631 |
| 3715 | LC7-19 | En | 38.676 | 56.932 | 0.0308 | 95.640 |
| 3715 | LC7-20 | En | 39.449 | 60.229 | 0.0301 | 99.709 |
| 3715 | LC7-21 | En | 38.149 | 57.395 | 0.0535 | 95.599 |
| 3715 | LC7-22 | En | 39.145 | 59.791 | 0.0331 | 98.970 |
| 3715 | LC7-23 | Fo | 55.826 | 42.213 | 0.0050 | 98.044 |
| 3715 | LC7-24 | Fo | 52.476 | 43.403 | 0.0053 | 95.884 |
| 3715 | LC7-25 | Fo | 53.554 | 44.052 | 0.0042 | 97.610 |
| 3715 | LC7-26 | Fo | 58.172 | 44.417 | 0.0044 | 102.593 |
| 3715 | LC7-27 | Fo | 60.290 | 45.462 | 0.0079 | 105.760 |
| 3715 | LC7-28 | Fo | 60.268 | 45.465 | 0.0046 | 105.738 |
| 3715 | LC7-29 | En | 40.184 | 60.351 | 0.0350 | 100.571 |
| 3715 | LC7-30 | q | 38.796 | 62.798 | 0.1160 | 101.713 |
| 3715 | LC7-31 | q | 39.831 | 58.967 | 0.1375 | 98.939 |
| 3715 | LC7-32 | q | 40.993 | 60.788 | 0.1182 | 101.902 |
| 3715 | LC7-33 | q | 41.080 | 61.168 | 0.1198 | 102.371 |
| 3721 | LC10-1 | En | 40.157 | 57.522 | 0.0269 | 97.707 |

| Run # | Analysis # | Phase | MgO (wt%) | $SiO_2$ (wt%) | CaO (wt%) | Total (wt%) |
|---|---|---|---|---|---|---|
| 3721 | LC10-2 | En | 39.931 | 57.678 | 0.0271 | 97.637 |
| 3721 | LC10-3 | En | 39.741 | 57.974 | 0.0273 | 97.743 |
| 3721 | LC10-4 | En | 39.585 | 58.072 | 0.0239 | 97.681 |
| 3721 | LC10-5 | En | 39.429 | 57.927 | 0.0251 | 97.382 |
| 3721 | LC10-6 | En | 39.421 | 57.647 | 0.0260 | 97.095 |
| 3721 | LC10-7 | En | 39.514 | 57.467 | 0.0268 | 97.008 |
| 3721 | LC10-8 | En | 39.628 | 57.197 | 0.0297 | 96.855 |
| 3721 | LC10-9 | En | 39.238 | 58.613 | 0.0281 | 97.880 |
| 3721 | LC10-10 | En | 39.288 | 58.631 | 0.0274 | 97.947 |
| 3721 | LC10-11 | En | 39.327 | 58.820 | 0.0281 | 98.176 |
| 3721 | LC10-12 | En | 39.168 | 58.738 | 0.0283 | 97.935 |
| 3721 | LC10-13 | En | 39.346 | 59.063 | 0.0254 | 98.435 |
| 3721 | LC10-14 | En | 39.388 | 58.684 | 0.0273 | 98.100 |
| 3721 | LC10-15 | En | 39.356 | 58.613 | 0.0284 | 97.998 |
| 3721 | LC10-16 | En | 39.337 | 58.520 | 0.0275 | 97.885 |
| 3721 | LC10-17 | En | 39.249 | 58.495 | 0.0273 | 97.772 |
| 3721 | LC10-18 | En | 38.945 | 58.316 | 0.0356 | 97.297 |
| 3721 | LC10-19 | En | 39.206 | 58.555 | 0.0262 | 97.788 |
| 3721 | LC10-20 | En | 39.328 | 58.726 | 0.0262 | 98.081 |
| 3721 | LC10-21 | En | 39.396 | 58.761 | 0.0261 | 98.184 |
| 3721 | LC10-22 | En | 39.395 | 58.741 | 0.0269 | 98.164 |
| 3721 | LC10-23 | En | 39.315 | 59.485 | 0.0362 | 98.837 |
| 3721 | LC10-24 | En | 39.109 | 59.105 | 0.0356 | 98.250 |
| 3721 | LC10-25 | En | 39.105 | 58.942 | 0.0324 | 98.080 |
| 3721 | LC10-26 | En | 39.649 | 59.868 | 0.0276 | 99.545 |
| 3721 | LC10-27 | En | 39.596 | 59.668 | 0.0265 | 99.291 |
| 3721 | LC10-28 | En | 39.527 | 59.638 | 0.0264 | 99.192 |
| 3721 | LC10-29 | En | 39.379 | 59.545 | 0.0273 | 98.952 |
| 3721 | LC10-30 | En | 39.217 | 59.403 | 0.0274 | 98.648 |
| 3721 | LC10-31 | En | 38.663 | 58.291 | 0.0278 | 96.982 |
| 3721 | LC10-32 | En | 38.661 | 58.870 | 0.0325 | 97.564 |
| 3721 | LC10-33 | En | 38.472 | 58.701 | 0.0263 | 97.200 |
| 3721 | LC10-34 | En | 38.950 | 59.282 | 0.0259 | 98.259 |
| 3721 | LC10-35 | En | 39.192 | 59.568 | 0.0241 | 98.785 |
| 3721 | LC10-36 | En | 39.353 | 59.755 | 0.0233 | 99.132 |
| 3721 | LC10-37 | En | 39.463 | 59.938 | 0.0236 | 99.425 |
| 3721 | LC10-38 | En | 39.577 | 60.023 | 0.0242 | 99.625 |
| 3721 | LC10-39 | Fo | 57.546 | 41.739 | 0.0033 | 99.288 |
| 3721 | LC10-40 | Fo | 57.134 | 41.753 | 0.0038 | 98.891 |
| 3721 | LC10-41 | Fo | 56.738 | 41.576 | 0.0028 | 98.317 |
| 3721 | LC10-42 | Fo | 56.139 | 41.412 | 0.0027 | 97.554 |
| 3721 | LC10-43 | Fo | 56.049 | 41.275 | 0.0029 | 97.327 |
| 3721 | LC10-44 | Fo | 55.576 | 41.019 | 0.0032 | 96.598 |
| 3721 | LC10-45 | Fo | 55.091 | 40.788 | 0.0033 | 95.882 |
| 3721 | LC10-46 | Fo | 55.132 | 41.157 | 0.0020 | 96.291 |
| 3721 | LC10-47 | Fo | 55.093 | 41.285 | 0.0031 | 96.381 |

| Run # | Analysis # | Phase | MgO (wt%) | $SiO_2$ (wt%) | CaO (wt%) | Total (wt%) |
|---|---|---|---|---|---|---|
| 3721 | LC10-48 | Fo | 55.410 | 41.596 | 0.0034 | 97.010 |
| 3721 | LC10-49 | Fo | 56.029 | 41.820 | 0.0040 | 97.853 |
| 3721 | LC10-50 | Fo | 56.533 | 42.099 | 0.0035 | 98.636 |
| 3721 | LC10-51 | Fo | 56.699 | 42.113 | 0.0036 | 98.816 |
| 3721 | LC10-52 | Fo | 57.322 | 42.401 | 0.0057 | 99.729 |
| 3721 | LC10-53 | Fo | 57.463 | 42.699 | 0.0047 | 100.167 |
| 3721 | LC10-54 | Fo | 57.676 | 42.861 | 0.0035 | 100.541 |
| 3721 | LC10-55 | Fo | 57.199 | 42.762 | 0.0047 | 99.966 |
| 3721 | LC10-56 | Fo | 56.731 | 42.572 | 0.0029 | 99.306 |
| 3721 | LC10-57 | Fo | 56.811 | 42.915 | 0.0029 | 99.729 |
| 3721 | LC10-58 | Fo | 56.748 | 42.732 | 0.0035 | 99.484 |
| 3721 | LC10-59 | Fo | 56.548 | 42.645 | 0.0029 | 99.196 |
| 3721 | LC10-60 | Fo | 56.446 | 42.471 | 0.0036 | 98.921 |
| 3721 | LC10-61 | Fo | 56.357 | 42.297 | 0.0061 | 98.660 |
| 3721 | LC10-62 | Fo | 56.174 | 42.228 | 0.0029 | 98.405 |
| 3721 | LC10-63 | Fo | 57.367 | 42.716 | 0.0037 | 100.087 |
| 3721 | LC10-64 | Fo | 57.935 | 43.350 | 0.0041 | 101.289 |
| 3721 | LC10-65 | Fo | 57.156 | 43.066 | 0.0084 | 100.231 |
| 3721 | LC10-66 | Fo | 57.095 | 42.647 | 0.0040 | 99.746 |
| 3721 | LC10-67 | Fo | 56.994 | 42.718 | 0.0052 | 99.717 |
| 3721 | LC10-68 | Fo | 56.816 | 42.713 | 0.0037 | 99.533 |
| 3721 | LC10-69 | Fo | 56.299 | 42.569 | 0.0037 | 98.872 |
| 3721 | LC10-70 | Fo | 56.122 | 42.602 | 0.0036 | 98.728 |
| 3721 | LC10-71 | Fo | 55.751 | 42.457 | 0.0037 | 98.212 |
| 3721 | LC10-72 | Fo | 56.553 | 42.553 | 0.0033 | 99.109 |
| 3721 | LC10-73 | Fo | 56.876 | 42.544 | 0.0027 | 99.423 |
| 3721 | LC10-74 | Fo | 57.246 | 42.639 | 0.0031 | 99.888 |
| 3721 | LC10-75 | Fo | 57.496 | 42.752 | 0.0032 | 100.251 |
| 3721 | LC10-76 | Fo | 57.088 | 43.135 | 0.0028 | 100.226 |
| 3721 | LC10-77 | Fo | 56.862 | 42.868 | 0.0040 | 99.734 |
| 3721 | LC10-78 | Fo | 56.313 | 42.904 | 0.0028 | 99.220 |
| 3721 | LC10-79 | Fo | 55.928 | 42.341 | 0.0167 | 98.286 |
| 3721 | LC10-80 | Fo | 55.787 | 42.168 | 0.0043 | 97.959 |
| 3721 | LC10-81 | Fo | 55.465 | 42.134 | 0.0042 | 97.603 |
| 3721 | LC10-82 | Fo | 57.244 | 42.982 | 0.0028 | 100.229 |
| 3721 | LC10-83 | Fo | 56.782 | 43.376 | 0.0038 | 100.162 |
| 3721 | LC10-84 | Fo | 56.318 | 43.561 | 0.0038 | 99.883 |
| 3721 | LC10-85 | Fo | 56.139 | 42.033 | 0.0027 | 98.175 |
| 3721 | LC10-86 | Fo | 55.599 | 41.861 | 0.0029 | 97.463 |
| 3721 | LC10-87 | Fo | 55.628 | 41.810 | 0.0039 | 97.442 |
| 3721 | LC10-88 | Fo | 55.133 | 42.094 | 0.0036 | 97.231 |
| 3722 | LC11-1 | Fo | 58.039 | 42.151 | 0.0034 | 100.193 |
| 3722 | LC11-2 | Fo | 57.506 | 42.019 | 0.0022 | 99.527 |
| 3722 | LC11-3 | En | 40.092 | 58.928 | 0.0235 | 99.044 |
| 3722 | LC11-4 | Fo | 56.752 | 42.085 | 0.0037 | 98.841 |
| 3722 | LC11-5 | Fo | 56.176 | 42.106 | 0.0054 | 98.287 |

| Run # | Analysis # | Phase | MgO (wt%) | $SiO_2$ (wt%) | CaO (wt%) | Total (wt%) |
|---|---|---|---|---|---|---|
| 3722 | LC11-6 | En | 40.186 | 60.477 | 0.0251 | 100.689 |
| 3722 | LC11-7 | En | 40.001 | 60.706 | 0.0250 | 100.733 |
| 3722 | LC11-8 | Fo | 57.018 | 42.984 | 0.0050 | 100.007 |
| 3722 | LC11-9 | En | 40.028 | 60.449 | 0.0268 | 100.504 |
| 3722 | LC11-10 | En | 39.793 | 60.394 | 0.0255 | 100.213 |
| 3722 | LC11-11 | Fo | 57.286 | 42.835 | 0.0050 | 100.126 |
| 3722 | LC11-12 | Fo | 57.294 | 42.906 | 0.0044 | 100.204 |
| 3722 | LC11-13 | Fo | 57.169 | 43.156 | 0.0049 | 100.330 |
| 3722 | LC11-14 | En | 39.742 | 60.384 | 0.0263 | 100.153 |
| 3722 | LC11-15 | En | 39.651 | 59.698 | 0.0262 | 99.376 |
| 3722 | LC11-16 | En | 39.420 | 60.155 | 0.0264 | 99.602 |
| 3722 | LC11-17 | En | 39.527 | 59.794 | 0.0279 | 99.350 |
| 3722 | LC11-18 | En | 40.128 | 59.957 | 0.0270 | 100.113 |
| 3722 | LC11-19 | En | 40.173 | 59.624 | 0.0372 | 99.835 |
| 3722 | LC11-20 | En | 39.894 | 59.639 | 0.0239 | 99.558 |
| 3722 | LC11-21 | En | 38.893 | 59.721 | 0.0449 | 98.660 |
| 3722 | LC11-22 | En | 39.940 | 59.656 | 0.0254 | 99.622 |
| 3722 | LC11-23 | En | 39.780 | 59.671 | 0.0285 | 99.480 |
| 3722 | LC11-24 | Fo | 57.922 | 42.161 | 0.0054 | 100.089 |
| 3722 | LC11-25 | En | 40.006 | 59.255 | 0.0237 | 99.285 |
| 3722 | LC11-26 | En | 40.383 | 59.280 | 0.0234 | 99.687 |
| 3722 | LC11-27 | Fo | 56.961 | 41.782 | 0.0036 | 98.747 |
| 3722 | LC11-28 | Fo | 56.959 | 42.158 | 0.0028 | 99.120 |
| 3722 | LC11-29 | Fo | 56.465 | 42.424 | 0.0016 | 98.891 |
| 3722 | LC11-30 | Fo | 56.899 | 42.479 | 0.0030 | 99.381 |
| 3722 | LC11-31 | Fo | 57.715 | 42.021 | 0.0033 | 99.739 |
| 3722 | LC11-32 | En | 39.337 | 60.170 | 0.0286 | 99.536 |
| 3722 | LC11-33 | Fo | 56.833 | 42.059 | 0.0027 | 98.895 |
| 3722 | LC11-34 | Fo | 56.583 | 42.241 | 0.0033 | 98.827 |
| 3722 | LC11-35 | En | 40.112 | 59.669 | 0.0271 | 99.809 |
| 3722 | LC11-36 | En | 40.032 | 59.293 | 0.0262 | 99.352 |
| 3722 | LC11-37 | En | 39.976 | 59.339 | 0.0266 | 99.342 |
| 3722 | LC11-38 | En | 40.521 | 60.086 | 0.0258 | 100.633 |
| 3722 | LC11-39 | En | 39.409 | 59.243 | 0.0283 | 98.681 |
| 3722 | LC11-40 | Fo | 56.308 | 42.326 | 0.0043 | 98.638 |
| 3722 | LC11-41 | Fo | 56.439 | 42.442 | 0.0070 | 98.888 |
| 3722 | LC11-42 | Fo | 56.426 | 42.271 | 0.0029 | 98.700 |
| 3722 | LC11-43 | En | 40.356 | 59.331 | 0.0265 | 99.714 |
| 3722 | LC11-44 | En | 39.368 | 58.728 | 0.0266 | 98.123 |
| 3722 | LC11-45 | Fo | 56.281 | 42.228 | 0.0029 | 98.512 |
| 3722 | LC11-46 | Fo | 56.515 | 42.309 | 0.0025 | 98.827 |
| 3722 | LC11-47 | Fo | 56.520 | 42.164 | 0.0028 | 98.687 |
| 3722 | LC11-48 | Fo | 55.958 | 41.938 | 0.0032 | 97.899 |
| 3722 | LC11-49 | En | 39.372 | 59.407 | 0.0251 | 98.805 |
| 3722 | LC11-50 | Fo | 55.741 | 41.231 | 0.0059 | 96.978 |
| 3722 | LC11-51 | Fo | 55.791 | 41.704 | 0.0064 | 97.502 |

| Run # | Analysis # | Phase | MgO (wt%) | $SiO_2$ (wt%) | CaO (wt%) | Total (wt%) |
|---|---|---|---|---|---|---|
| 3722 | LC11-52 | En | 39.403 | 59.516 | 0.0269 | 98.947 |
| 3722 | LC11-53 | Fo | 57.234 | 41.305 | 0.0068 | 98.546 |
| 3722 | LC11-54 | Fo | 56.692 | 41.228 | 0.0065 | 97.927 |
| 3722 | LC11-55 | En | 40.374 | 58.488 | 0.0256 | 98.888 |
| 3727 | LC12-1 | Fo | 56.406 | 38.017 | 0.0048 | 94.428 |
| 3727 | LC12-2 | Fo | 54.903 | 38.382 | 0.0030 | 93.288 |
| 3727 | LC12-3 | Fo | 56.155 | 39.387 | 0.0041 | 95.546 |
| 3727 | LC12-4 | Fo | 55.753 | 39.397 | 0.0026 | 95.153 |
| 3727 | LC12-5 | Fo | 55.003 | 39.310 | 0.0028 | 94.316 |
| 3727 | LC12-6 | Fo | 55.068 | 39.776 | 0.0034 | 94.847 |
| 3727 | LC12-7 | Fo | 54.506 | 39.107 | 0.0020 | 93.615 |
| 3727 | LC12-8 | Fo | 54.720 | 39.578 | 0.0031 | 94.301 |
| 3727 | LC12-9 | Fo | 54.676 | 39.852 | 0.0031 | 94.531 |
| 3727 | LC12-10 | Fo | 53.879 | 39.894 | 0.0034 | 93.776 |
| 3727 | LC12-11 | Fo | 53.370 | 40.241 | 0.0032 | 93.614 |
| 3727 | LC12-12 | Fo | 52.305 | 39.356 | 0.0032 | 91.664 |
| 3727 | LC12-13 | Fo | 51.496 | 37.980 | 0.0031 | 89.479 |
| 3727 | LC12-14 | Fo | 52.330 | 38.401 | 0.0024 | 90.733 |
| 3727 | LC12-15 | Fo | 59.577 | 40.494 | 0.0027 | 100.074 |
| 3727 | LC12-16 | Fo | 59.214 | 40.635 | 0.0029 | 99.852 |
| 3727 | LC12-17 | Fo | 58.626 | 40.721 | 0.0034 | 99.350 |
| 3727 | LC12-18 | Fo | 58.064 | 40.856 | 0.0036 | 98.924 |
| 3727 | LC12-19 | Fo | 57.672 | 41.022 | 0.0014 | 98.695 |
| 3727 | LC12-20 | Fo | 57.881 | 41.380 | 0.0014 | 99.262 |
| 3727 | LC12-21 | Fo | 57.260 | 41.484 | 0.0024 | 98.746 |
| 3727 | LC12-22 | Fo | 57.319 | 41.641 | 0.0021 | 98.962 |
| 3727 | LC12-23 | Fo | 57.086 | 41.979 | 0.0017 | 99.067 |
| 3727 | LC12-24 | Fo | 57.125 | 42.149 | 0.0024 | 99.276 |
| 3727 | LC12-25 | Fo | 56.888 | 42.151 | 0.0036 | 99.043 |
| 3727 | LC12-26 | Fo | 56.626 | 42.240 | 0.0018 | 98.868 |
| 3727 | LC12-27 | Fo | 56.492 | 42.421 | 0.0017 | 98.915 |
| 3727 | LC12-28 | Fo | 56.458 | 42.848 | 0.0011 | 99.307 |
| 3727 | LC12-29 | Fo | 54.880 | 41.578 | 0.0035 | 96.462 |
| 3727 | LC12-30 | Fo | 54.615 | 41.134 | 0.0024 | 95.751 |
| 3727 | LC12-31 | Fo | 54.313 | 40.851 | 0.0025 | 95.167 |
| 3727 | LC12-32 | Fo | 54.087 | 40.568 | 0.0033 | 94.658 |
| 3727 | LC12-33 | Fo | 53.866 | 40.358 | 0.0022 | 94.226 |
| 3727 | LC12-34 | Fo | 53.813 | 40.163 | 0.0032 | 93.979 |
| 3727 | LC12-35 | Fo | 52.776 | 39.978 | 0.0029 | 92.757 |
| 3727 | LC12-36 | Fo | 53.136 | 40.370 | 0.0035 | 93.510 |
| 3727 | LC12-37 | Fo | 54.251 | 40.860 | 0.0026 | 95.114 |
| 3727 | LC12-38 | Fo | 54.285 | 41.062 | 0.0020 | 95.349 |
| 3727 | LC12-39 | Fo | 54.068 | 41.425 | 0.0023 | 95.495 |
| 3727 | LC12-40 | Fo | 53.774 | 41.613 | 0.0031 | 95.390 |
| 3727 | LC12-41 | Fo | 53.412 | 41.861 | 0.0022 | 95.275 |
| 3727 | LC12-42 | Fo | 54.423 | 42.150 | 0.0027 | 96.576 |

| Run # | Analysis # | Phase | MgO (wt%) | $SiO_2$ (wt%) | CaO (wt%) | Total (wt%) |
|---|---|---|---|---|---|---|
| 3727 | LC12-43 | Fo | 54.712 | 42.565 | 0.0022 | 97.279 |
| 3727 | LC12-44 | Fo | 52.321 | 43.219 | 0.0027 | 95.543 |
| 3727 | LC12-45 | Fo | 51.810 | 43.580 | 0.0025 | 95.393 |
| 3727 | LC12-46 | Fo | 52.445 | 44.083 | 0.0030 | 96.531 |
| 3727 | LC12-47 | Fo | 49.880 | 44.260 | 0.0033 | 94.143 |
| 3727 | LC12-48 | Fo | 48.873 | 43.275 | 0.0050 | 92.153 |
| 3727 | LC12-49 | Fo | 48.814 | 42.841 | 0.0031 | 91.658 |
| 3727 | LC12-50 | Fo | 48.986 | 42.049 | 0.0023 | 91.037 |
| 3727 | LC12-51 | Fo | 47.681 | 41.122 | 0.0033 | 88.806 |
| 3727 | LC12-52 | Fo | 44.727 | 39.094 | 0.0028 | 83.824 |
| 3727 | LC12-53 | Fo | 44.607 | 38.985 | 0.0027 | 83.595 |
| 3727 | LC12-54 | Fo | 44.862 | 38.087 | 0.0036 | 82.953 |
| 3727 | LC12-55 | Fo | 50.542 | 41.357 | 0.0033 | 91.902 |
| 3727 | LC12-56 | Fo | 52.329 | 41.121 | 0.0026 | 93.453 |
| 3727 | LC12-57 | q | 38.335 | 60.043 | 0.0419 | 98.421 |
| 3727 | LC12-58 | q | 36.385 | 61.785 | 0.0433 | 98.214 |
| 3727 | LC12-59 | q | 37.214 | 62.076 | 0.0496 | 99.341 |
| 3728 | LC13-1 | Fo | 59.947 | 41.131 | 0.0110 | 101.089 |
| 3728 | LC13-2 | Fo | 60.225 | 41.248 | 0.0102 | 101.483 |
| 3728 | LC13-3 | Fo | 58.992 | 41.441 | 0.0096 | 100.443 |
| 3728 | LC13-4 | Fo | 57.048 | 41.268 | 0.0097 | 98.326 |
| 3728 | LC13-5 | Fo | 57.461 | 41.672 | 0.0098 | 99.143 |
| 3728 | LC13-6 | Fo | 56.183 | 40.217 | 0.0057 | 96.406 |
| 3728 | LC13-7 | Fo | 56.760 | 40.323 | 0.0056 | 97.089 |
| 3728 | LC13-8 | Fo | 57.131 | 40.459 | 0.0054 | 97.595 |
| 3728 | LC13-9 | Fo | 57.017 | 40.622 | 0.0055 | 97.645 |
| 3728 | LC13-10 | Fo | 57.028 | 40.746 | 0.0052 | 97.779 |
| 3728 | LC13-11 | Fo | 57.476 | 40.768 | 0.0054 | 98.250 |
| 3728 | LC13-12 | Fo | 58.192 | 40.794 | 0.0049 | 98.991 |
| 3728 | LC13-13 | Fo | 57.197 | 41.166 | 0.0053 | 98.368 |
| 3728 | LC13-14 | Fo | 56.653 | 40.588 | 0.0047 | 97.246 |
| 3728 | LC13-15 | Fo | 56.683 | 40.915 | 0.0053 | 97.603 |
| 3728 | LC13-16 | Fo | 56.776 | 41.079 | 0.0050 | 97.860 |
| 3728 | LC13-17 | Fo | 56.773 | 41.116 | 0.0046 | 97.894 |
| 3728 | LC13-18 | Fo | 57.153 | 41.295 | 0.0044 | 98.453 |
| 3728 | LC13-19 | Fo | 56.519 | 41.700 | 0.0048 | 98.224 |
| 3728 | LC13-20 | Fo | 56.654 | 41.893 | 0.0048 | 98.552 |
| 3728 | LC13-21 | Fo | 56.895 | 41.979 | 0.0051 | 98.879 |
| 3728 | LC13-22 | Fo | 57.531 | 41.992 | 0.0047 | 99.528 |
| 3728 | LC13-23 | Fo | 57.591 | 42.235 | 0.0049 | 99.831 |
| 3728 | LC13-24 | Fo | 57.252 | 42.394 | 0.0056 | 99.652 |
| 3728 | LC13-25 | Fo | 57.300 | 42.600 | 0.0044 | 99.904 |
| 3728 | LC13-26 | Fo | 57.842 | 42.181 | 0.0044 | 100.027 |
| 3728 | LC13-27 | Fo | 57.922 | 42.125 | 0.0046 | 100.052 |
| 3728 | LC13-28 | Fo | 57.540 | 42.492 | 0.0058 | 100.038 |
| 3728 | LC13-29 | Fo | 57.232 | 41.297 | 0.0052 | 98.534 |

| Run # | Analysis # | Phase | MgO (wt%) | $SiO_2$ (wt%) | CaO (wt%) | Total (wt%) |
|---|---|---|---|---|---|---|
| 3728 | LC13-30 | Fo | 57.173 | 41.929 | 0.0052 | 99.107 |
| 3728 | LC13-31 | Fo | 57.767 | 41.377 | 0.0061 | 99.150 |
| 3728 | LC13-32 | Fo | 57.892 | 41.684 | 0.0052 | 99.581 |
| 3728 | LC13-33 | Fo | 58.272 | 41.355 | 0.0045 | 99.632 |
| 3728 | LC13-34 | En | 41.027 | 56.190 | 0.0297 | 97.247 |
| 3728 | LC13-35 | En | 41.047 | 56.044 | 0.0300 | 97.122 |
| 3728 | LC13-36 | En | 40.836 | 55.528 | 0.0308 | 96.396 |
| 3728 | LC13-37 | En | 40.838 | 55.656 | 0.0297 | 96.524 |
| 3728 | LC13-38 | En | 40.776 | 55.407 | 0.0306 | 96.214 |
| 3728 | LC13-39 | En | 40.874 | 55.527 | 0.0300 | 96.432 |
| 3728 | LC13-40 | En | 41.054 | 57.350 | 0.0281 | 98.433 |
| 3728 | LC13-41 | En | 41.768 | 57.333 | 0.0307 | 99.132 |
| 3728 | LC13-42 | En | 42.015 | 56.989 | 0.0315 | 99.036 |
| 3728 | LC13-43 | En | 41.230 | 57.193 | 0.0295 | 98.453 |
| 3728 | LC13-44 | En | 41.227 | 57.008 | 0.0296 | 98.265 |
| 3737 | LC17-1 | Fo | 56.529 | 42.277 | 0.0039 | 98.810 |
| 3737 | LC17-2 | Fo | 55.962 | 42.233 | 0.0043 | 98.199 |
| 3737 | LC17-3 | Fo | 56.331 | 42.178 | 0.0030 | 98.512 |
| 3737 | LC17-4 | Fo | 55.841 | 42.128 | 0.0041 | 97.973 |
| 3737 | LC17-5 | Fo | 55.718 | 42.085 | 0.0034 | 97.806 |
| 3737 | LC17-6 | Fo | 55.674 | 42.159 | 0.0029 | 97.836 |
| 3737 | LC17-7 | Fo | 55.155 | 41.648 | 0.0034 | 96.806 |
| 3737 | LC17-8 | Fo | 55.495 | 41.580 | 0.0031 | 97.078 |
| 3737 | LC17-9 | Fo | 55.631 | 41.616 | 0.0030 | 97.250 |
| 3737 | LC17-10 | Fo | 55.660 | 41.470 | 0.0040 | 97.134 |
| 3737 | LC17-11 | Fo | 55.752 | 41.579 | 0.0035 | 97.335 |
| 3739 | LC18-2 | Fo | 57.202 | 41.876 | 0.0064 | 99.085 |
| 3739 | LC18-3 | Fo | 57.382 | 42.069 | 0.0069 | 99.458 |
| 3739 | LC18-4 | Fo | 57.225 | 42.527 | 0.0053 | 99.757 |
| 3739 | LC18-6 | Fo | 56.002 | 41.620 | 0.0074 | 97.630 |
| 3739 | LC18-7 | Fo | 56.046 | 41.976 | 0.0051 | 98.027 |
| 3739 | LC18-8 | Fo | 56.527 | 41.386 | 0.0046 | 97.918 |
| 3739 | LC18-9 | Fo | 56.648 | 41.739 | 0.0042 | 98.391 |
| 3739 | LC18-10 | Fo | 54.942 | 41.733 | 0.0047 | 96.680 |
| 3739 | LC18-12 | Fo | 55.324 | 42.019 | 0.0057 | 97.349 |
| 3739 | LC18-13 | Fo | 55.214 | 42.127 | 0.0048 | 97.346 |
| 3739 | LC18-14 | Fo | 54.731 | 42.086 | 0.0050 | 96.822 |
| 3739 | LC18-15 | Fo | 55.754 | 42.922 | 0.0047 | 98.681 |
| 3739 | LC18-16 | Fo | 56.593 | 42.648 | 0.0053 | 99.246 |
| 3739 | LC18-17 | Fo | 57.103 | 42.344 | 0.0055 | 99.453 |
| 3739 | LC18-18 | Fo | 55.846 | 42.098 | 0.0047 | 97.949 |
| 3739 | LC18-19 | Fo | 57.112 | 42.206 | 0.0059 | 99.324 |
| 3739 | LC18-22 | Fo | 56.058 | 42.942 | 0.0054 | 99.006 |
| 3740 | LC19-5 | Fo | 55.856 | 42.653 | 0.0072 | 98.516 |
| 3740 | LC19-6 | Fo | 56.193 | 42.567 | 0.0060 | 98.766 |
| 3740 | LC19-7 | Fo | 56.601 | 42.666 | 0.0054 | 99.273 |

| Run # | Analysis # | Phase | MgO (wt%) | $SiO_2$ (wt%) | CaO (wt%) | Total (wt%) |
|---|---|---|---|---|---|---|
| 3740 | LC19-8 | Fo | 56.919 | 42.535 | 0.0066 | 99.461 |
| 3740 | LC19-9 | Fo | 56.956 | 42.495 | 0.0060 | 99.457 |
| 3740 | LC19-10 | Fo | 56.370 | 42.423 | 0.0055 | 98.799 |
| 3740 | LC19-11 | Fo | 56.322 | 42.578 | 0.0059 | 98.906 |
| 3740 | LC19-12 | Fo | 55.733 | 42.545 | 0.0061 | 98.284 |
| 3740 | LC19-13 | Fo | 57.139 | 42.745 | 0.0044 | 99.889 |
| 3740 | LC19-14 | Fo | 57.145 | 42.476 | 0.0078 | 99.629 |
| 3740 | LC19-19 | Fo | 56.143 | 42.922 | 0.0059 | 99.071 |
| 3740 | LC19-20 | Fo | 56.224 | 42.702 | 0.0049 | 98.931 |
| 3740 | LC19-21 | Fo | 56.907 | 42.876 | 0.0045 | 99.788 |
| 3740 | LC19-22 | Fo | 57.118 | 42.622 | 0.0046 | 99.745 |
| 3740 | LC19-23 | Fo | 57.367 | 42.380 | 0.0055 | 99.753 |
| 3744 | LC21-1 | Fo | 58.771 | 41.917 | 0.0042 | 100.692 |
| 3744 | LC21-2 | Fo | 58.670 | 42.200 | 0.0023 | 100.872 |
| 3744 | LC21-3 | Fo | 58.402 | 42.299 | 0.0031 | 100.704 |
| 3744 | LC21-4 | Fo | 58.128 | 42.460 | 0.0031 | 100.591 |
| 3744 | LC21-5 | Fo | 58.147 | 42.620 | 0.0037 | 100.771 |
| 3744 | LC21-9 | Fo | 56.095 | 41.358 | 0.0045 | 97.458 |
| 3744 | LC21-10 | Fo | 55.881 | 41.478 | 0.0043 | 97.363 |
| 3744 | LC21-11 | Fo | 55.881 | 41.515 | 0.0035 | 97.400 |
| 3744 | LC21-13 | Fo | 59.095 | 42.283 | 0.0059 | 101.384 |
| 3744 | LC21-14 | Fo | 58.699 | 42.494 | 0.0074 | 101.201 |
| 3744 | LC21-15 | Fo | 58.841 | 42.943 | 0.0062 | 101.790 |
| 3744 | LC21-16 | Fo | 56.313 | 41.340 | 0.0060 | 97.659 |
| 3744 | LC21-17 | Fo | 56.867 | 41.666 | 0.0078 | 98.541 |
| 3744 | LC21-22 | Fo | 55.440 | 41.217 | 0.0042 | 96.661 |
| 3744 | LC21-23 | Fo | 55.052 | 41.470 | 0.0039 | 96.526 |
| 3744 | LC21-24 | Fo | 57.564 | 42.649 | 0.0024 | 100.215 |
| 3744 | LC21-25 | Fo | 57.711 | 43.136 | 0.0030 | 100.850 |
| 3744 | LC21-26 | Fo | 56.611 | 42.709 | 0.0034 | 99.323 |
| 3744 | LC21-27 | Fo | 55.810 | 42.498 | 0.0030 | 98.311 |
| 3744 | LC21-28 | Fo | 55.445 | 42.564 | 0.0035 | 98.013 |
| 3744 | LC21-29 | Fo | 55.537 | 42.826 | 0.0030 | 98.366 |
| 3744 | LC21-30 | Fo | 57.303 | 41.897 | 0.0036 | 99.204 |
| 3744 | LC21-31 | Fo | 57.007 | 42.539 | 0.0038 | 99.550 |
| 3744 | LC21-32 | Fo | 56.689 | 42.345 | 0.0042 | 99.038 |
| 3744 | LC21-33 | Fo | 56.613 | 42.634 | 0.0054 | 99.253 |
| 3744 | LC21-34 | Fo | 56.115 | 42.606 | 0.0050 | 98.726 |
| 3748 | LC24-4 | Fo | 58.128 | 41.442 | 0.0050 | 99.575 |
| 3748 | LC24-5 | En | 40.209 | 60.308 | 0.0355 | 100.553 |
| 3748 | LC24-6 | En | 39.324 | 59.865 | 0.0378 | 99.228 |
| 3748 | LC24-7 | En | 39.489 | 59.427 | 0.0378 | 98.955 |
| 3748 | LC24-8 | En | 39.612 | 59.236 | 0.0387 | 98.888 |
| 3748 | LC24-9 | En | 39.971 | 59.076 | 0.0384 | 99.086 |
| 3748 | LC24-10 | En | 40.460 | 59.347 | 0.0332 | 99.841 |
| 3748 | LC24-11 | En | 40.241 | 59.718 | 0.0326 | 99.992 |

| Run # | Analysis # | Phase | MgO (wt%) | $SiO_2$ (wt%) | CaO (wt%) | Total (wt%) |
|---|---|---|---|---|---|---|
| 3748 | LC24-12 | En | 39.989 | 60.148 | 0.0328 | 100.171 |
| 3748 | LC24-13 | En | 39.779 | 60.339 | 0.0320 | 100.151 |
| 3748 | LC24-14 | En | 38.855 | 59.326 | 0.0424 | 98.224 |
| 3748 | LC24-15 | En | 39.847 | 59.408 | 0.0436 | 99.300 |
| 3748 | LC24-16 | En | 39.385 | 59.966 | 0.0335 | 99.385 |
| 3748 | LC24-17 | En | 39.483 | 59.541 | 0.0364 | 99.061 |
| 3748 | LC24-18 | En | 39.787 | 58.636 | 0.0353 | 98.459 |
| 3748 | LC24-19 | Fo | 56.803 | 41.560 | 0.0040 | 98.367 |
| 3748 | LC24-22 | Fo | 55.988 | 42.487 | 0.0091 | 98.484 |
| 3748 | LC24-23 | Fo | 56.239 | 42.121 | 0.0108 | 98.371 |
| 3748 | LC24-24 | Fo | 56.334 | 41.793 | 0.0044 | 98.131 |
| 3748 | LC24-25 | Fo | 57.989 | 41.360 | 0.0042 | 99.353 |
| 3748 | LC24-26 | Fo | 57.742 | 41.857 | 0.0038 | 99.603 |
| 3748 | LC24-27 | Fo | 56.999 | 42.403 | 0.0058 | 99.408 |
| 3748 | LC24-28 | Fo | 55.791 | 42.006 | 0.0031 | 97.800 |
| 3748 | LC24-29 | Fo | 56.389 | 41.297 | 0.0046 | 97.691 |
| 3748 | LC24-32 | Fo | 57.950 | 42.060 | 0.0039 | 100.014 |
| 3748 | LC24-33 | Fo | 57.092 | 42.522 | 0.0049 | 99.619 |
| 3748 | LC24-34 | Fo | 56.920 | 42.544 | 0.0042 | 99.468 |
| 3750 | LC26-9 | Fo | 56.674 | 43.638 | 0.0044 | 100.317 |
| 3750 | LC26-10 | Fo | 55.839 | 43.563 | 0.0049 | 99.407 |
| 3750 | LC26-11 | Fo | 55.391 | 42.906 | 0.0054 | 98.303 |
| 3750 | LC26-12 | Fo | 55.811 | 42.460 | 0.0050 | 98.276 |
| 3750 | LC26-13 | Fo | 55.961 | 42.645 | 0.0043 | 98.610 |
| 3750 | LC26-14 | Fo | 56.823 | 42.111 | 0.0048 | 98.939 |
| 3750 | LC26-15 | Fo | 57.335 | 42.079 | 0.0063 | 99.420 |
| 3750 | LC26-16 | Fo | 56.536 | 43.752 | 0.0081 | 100.296 |
| 3750 | LC26-17 | Fo | 55.792 | 43.172 | 0.0066 | 98.971 |
| 3750 | LC26-18 | Fo | 55.571 | 42.592 | 0.0069 | 98.170 |
| 3750 | LC26-19 | Fo | 56.025 | 42.020 | 0.0068 | 98.052 |
| 3750 | LC26-20 | Fo | 56.898 | 42.521 | 0.0056 | 99.425 |
| 3750 | LC26-21 | Fo | 57.545 | 42.559 | 0.0086 | 100.113 |
| 3750 | LC26-22 | Fo | 58.146 | 42.694 | 0.0069 | 100.847 |
| 3750 | LC26-23 | Fo | 57.006 | 41.649 | 0.0109 | 98.666 |
| 3750 | LC26-24 | Fo | 56.165 | 41.724 | 0.0085 | 97.898 |
| 3750 | LC26-25 | Fo | 57.093 | 42.595 | 0.0064 | 99.695 |
| 3750 | LC26-26 | Fo | 57.163 | 42.109 | 0.0057 | 99.278 |
| 3750 | LC26-27 | Fo | 57.381 | 42.523 | 0.0060 | 99.910 |
| 3750 | LC26-28 | q | 39.695 | 59.044 | 0.0396 | 98.780 |
| 3750 | LC26-29 | q | 39.526 | 59.262 | 0.0412 | 98.830 |
| 3750 | LC26-30 | q | 55.737 | 42.034 | 0.0527 | 97.825 |
| 3750 | LC26-31 | q | 40.269 | 59.437 | 0.0265 | 99.733 |
| 3750 | LC26-32 | q | 40.142 | 59.366 | 0.0343 | 99.543 |
| 3750 | LC26-33 | q | 39.672 | 59.316 | 0.0416 | 99.031 |
| 3750 | LC26-34 | q | 40.774 | 59.137 | 0.0389 | 99.951 |
| 3753 | LC29-1 | Fo | 57.525 | 42.504 | 0.0038 | 100.033 |

| Run # | Analysis # | Phase | MgO (wt%) | $SiO_2$ (wt%) | CaO (wt%) | Total (wt%) |
|---|---|---|---|---|---|---|
| 3753 | LC29-2 | Fo | 56.338 | 42.772 | 0.0037 | 99.114 |
| 3753 | LC29-3 | Fo | 56.302 | 43.231 | 0.0030 | 99.536 |
| 3753 | LC29-4 | Fo | 55.968 | 42.315 | 0.0029 | 98.286 |
| 3753 | LC29-5 | Fo | 55.937 | 42.410 | 0.0034 | 98.350 |
| 3753 | LC29-6 | Fo | 56.569 | 42.502 | 0.0033 | 99.074 |
| 3753 | LC29-7 | Fo | 57.064 | 41.955 | 0.0045 | 99.024 |
| 3753 | LC29-8 | Fo | 56.668 | 41.779 | 0.0041 | 98.451 |
| 3753 | LC29-9 | Fo | 56.194 | 42.383 | 0.0040 | 98.581 |
| 3753 | LC29-10 | Fo | 55.622 | 42.211 | 0.0034 | 97.836 |
| 3753 | LC29-11 | Fo | 56.370 | 41.439 | 0.0030 | 97.812 |
| 3753 | LC29-12 | Fo | 55.648 | 42.454 | 0.0025 | 98.105 |
| 3753 | LC29-13 | Fo | 56.879 | 42.786 | 0.0035 | 99.669 |
| 3753 | LC29-14 | Fo | 56.803 | 42.985 | 0.0040 | 99.792 |
| 3753 | LC29-15 | Fo | 56.707 | 42.591 | 0.0045 | 99.303 |
| 3753 | LC29-16 | Fo | 56.995 | 43.059 | 0.0053 | 100.059 |
| 3753 | LC29-17 | Fo | 57.317 | 42.218 | 0.0056 | 99.541 |
| 3753 | LC29-18 | Fo | 56.438 | 42.760 | 0.0066 | 99.205 |
| 3753 | LC29-19 | Fo | 57.214 | 42.512 | 0.0067 | 99.733 |
| 3753 | LC29-20 | En | 39.690 | 59.489 | 0.0307 | 99.210 |
| 3753 | LC29-21 | En | 40.059 | 59.986 | 0.0330 | 100.079 |
| 3753 | LC29-22 | En | 40.279 | 59.897 | 0.0309 | 100.208 |
| 3753 | LC29-23 | En | 40.287 | 60.200 | 0.0288 | 100.517 |
| 3753 | LC29-24 | En | 39.880 | 60.001 | 0.0259 | 99.908 |
| 3753 | LC29-25 | En | 39.707 | 60.315 | 0.0287 | 100.051 |
| 3753 | LC29-26 | En | 39.494 | 59.816 | 0.0309 | 99.342 |
| 3753 | LC29-27 | En | 39.096 | 60.417 | 0.0309 | 99.545 |
| 3753 | LC29-28 | En | 39.501 | 60.203 | 0.0332 | 99.738 |
| 3754 | LC30-1 | En | 39.739 | 59.948 | 0.0374 | 99.725 |
| 3754 | LC30-2 | En | 39.341 | 60.085 | 0.0358 | 99.463 |
| 3754 | LC30-3 | En | 39.007 | 59.503 | 0.0340 | 98.545 |
| 3754 | LC30-4 | En | 39.338 | 59.754 | 0.0331 | 99.126 |
| 3754 | LC30-5 | En | 39.096 | 59.964 | 0.0341 | 99.095 |
| 3754 | LC30-6 | En | 39.559 | 60.350 | 0.0327 | 99.943 |
| 3754 | LC30-7 | En | 39.415 | 60.567 | 0.0422 | 100.025 |
| 3754 | LC30-8 | En | 39.916 | 60.291 | 0.0356 | 100.243 |
| 3754 | LC30-9 | En | 39.628 | 60.693 | 0.0359 | 100.358 |
| 3754 | LC30-10 | Fo | 57.349 | 42.560 | 0.0048 | 99.914 |
| 3754 | LC30-11 | Fo | 57.254 | 43.174 | 0.0039 | 100.432 |
| 3754 | LC30-12 | Fo | 56.477 | 43.403 | 0.0036 | 99.884 |
| 3754 | LC30-13 | Fo | 56.382 | 43.087 | 0.0026 | 99.472 |
| 3754 | LC30-14 | Fo | 56.075 | 43.479 | 0.0045 | 99.559 |
| 3754 | LC30-15 | Fo | 56.444 | 42.835 | 0.0042 | 99.283 |
| 3758 | LC31-1 | Fo | 56.813 | 41.706 | 0.0039 | 98.523 |
| 3758 | LC31-2 | Fo | 56.518 | 41.925 | 0.0043 | 98.447 |
| 3758 | LC31-3 | Fo | 56.711 | 42.116 | 0.0040 | 98.831 |
| 3758 | LC31-4 | Fo | 57.430 | 41.845 | 0.0056 | 99.281 |

| Run # | Analysis # | Phase | MgO (wt%) | $SiO_2$ (wt%) | CaO (wt%) | Total (wt%) |
|---|---|---|---|---|---|---|
| 3758 | LC31-5 | Fo | 57.531 | 41.918 | 0.0062 | 99.455 |
| 3758 | LC31-6 | Fo | 57.280 | 41.944 | 0.0058 | 99.230 |
| 3758 | LC31-7 | Fo | 56.962 | 42.056 | 0.0052 | 99.023 |
| 3758 | LC31-8 | Fo | 57.051 | 42.097 | 0.0058 | 99.154 |
| 3758 | LC31-9 | Fo | 57.397 | 41.862 | 0.0044 | 99.264 |
| 3758 | LC31-10 | Fo | 58.479 | 42.379 | 0.0058 | 100.864 |
| 3758 | LC31-11 | Fo | 57.008 | 41.953 | 0.0062 | 98.967 |
| 3758 | LC31-12 | Fo | 58.045 | 41.886 | 0.0050 | 99.936 |
| 3758 | LC31-13 | Fo | 58.311 | 41.673 | 0.0056 | 99.990 |
| 3758 | LC31-14 | Fo | 56.863 | 42.318 | 0.0066 | 99.188 |
| 3758 | LC31-15 | Fo | 57.654 | 42.329 | 0.0070 | 99.990 |
| 3758 | LC31-16 | Fo | 58.173 | 42.774 | 0.0061 | 100.953 |
| 3755 | LC32-1 | En | 39.711 | 61.251 | 0.0189 | 100.981 |
| 3755 | LC32-2 | En | 40.007 | 60.250 | 0.0184 | 100.276 |
| 3755 | LC32-3 | En | 40.423 | 60.088 | 0.0184 | 100.530 |
| 3755 | LC32-4 | En | 40.058 | 60.234 | 0.0171 | 100.310 |
| 3755 | LC32-5 | En | 38.924 | 59.361 | 0.0215 | 98.307 |
| 3755 | LC32-6 | En | 39.095 | 60.687 | 0.0174 | 99.800 |
| 3755 | LC32-7 | En | 38.715 | 59.832 | 0.0181 | 98.566 |
| 3755 | LC32-8 | En | 39.326 | 60.318 | 0.0260 | 99.671 |
| 3755 | LC32-9 | En | 39.924 | 59.823 | 0.0387 | 99.787 |
| 3755 | LC32-10 | Fo | 56.302 | 42.364 | 0.0026 | 98.669 |
| 3755 | LC32-11 | Fo | 56.158 | 42.656 | 0.0027 | 98.817 |
| 3755 | LC32-12 | Fo | 56.206 | 42.728 | 0.0025 | 98.937 |
| 3755 | LC32-13 | Fo | 56.393 | 42.745 | 0.0039 | 99.142 |
| 3755 | LC32-14 | Fo | 55.858 | 42.687 | 0.0048 | 98.550 |
| 3755 | LC32-15 | Fo | 56.578 | 43.104 | 0.0054 | 99.687 |
| 3755 | LC32-16 | Fo | 55.708 | 43.332 | 0.0024 | 99.042 |
| 3755 | LC32-17 | En | 38.896 | 60.076 | 0.0181 | 98.991 |
| 3755 | LC32-18 | En | 38.854 | 59.609 | 0.0444 | 98.508 |
| 3755 | LC32-19 | En | 39.682 | 59.257 | 0.0194 | 98.959 |
| 3759 | LC35-1 | Fo | 58.413 | 41.838 | 0.0070 | 100.258 |
| 3759 | LC35-2 | Fo | 58.657 | 41.744 | 0.0076 | 100.409 |
| 3759 | LC35-3 | Fo | 58.895 | 41.826 | 0.0069 | 100.728 |
| 3759 | LC35-4 | Fo | 58.146 | 42.493 | 0.0074 | 100.646 |
| 3759 | LC35-5 | Fo | 57.825 | 42.356 | 0.0078 | 100.189 |
| 3759 | LC35-6 | Fo | 57.314 | 41.971 | 0.0069 | 99.292 |
| 3759 | LC35-7 | Fo | 57.615 | 42.636 | 0.0063 | 100.257 |
| 3759 | LC35-8 | Fo | 57.507 | 42.349 | 0.0056 | 99.862 |
| 3759 | LC35-9 | Fo | 56.838 | 41.961 | 0.0074 | 98.807 |
| 3759 | LC35-10 | Fo | 57.267 | 42.082 | 0.0118 | 99.361 |
| 3759 | LC35-11 | En | 40.523 | 60.136 | 0.0299 | 100.690 |
| 3759 | LC35-12 | En | 40.485 | 59.711 | 0.0289 | 100.226 |
| 3759 | LC35-13 | En | 40.623 | 59.836 | 0.0311 | 100.491 |
| 3759 | LC35-14 | En | 40.374 | 59.935 | 0.0274 | 100.337 |
| 3759 | LC35-15 | En | 40.323 | 60.110 | 0.0254 | 100.459 |

| Run # | Analysis # | Phase | MgO (wt%) | $SiO_2$ (wt%) | CaO (wt%) | Total (wt%) |
|---|---|---|---|---|---|---|
| 3759 | LC35-16 | Fo | 56.466 | 42.821 | 0.0063 | 99.293 |
| 3759 | LC35-17 | En | 40.261 | 60.201 | 0.0269 | 100.490 |
| 3759 | LC35-18 | En | 40.274 | 59.966 | 0.0273 | 100.268 |
| 3759 | LC35-19 | En | 40.483 | 59.875 | 0.0321 | 100.391 |
| 3759 | LC35-20 | En | 40.615 | 59.411 | 0.0317 | 100.058 |
| 3759 | LC35-21 | En | 40.312 | 59.080 | 0.0317 | 99.425 |
| 3759 | LC35-22 | En | 40.106 | 58.275 | 0.0302 | 98.412 |
| 3759 | LC35-23 | En | 39.583 | 57.682 | 0.0325 | 97.298 |
| 3759 | LC35-24 | Fo | 56.285 | 41.194 | 0.0090 | 97.488 |
| 3759 | LC35-25 | En | 39.531 | 58.842 | 0.0324 | 98.406 |
| 3759 | LC35-26 | En | 39.308 | 59.199 | 0.0260 | 98.534 |
| 3759 | LC35-27 | Fo | 56.072 | 41.219 | 0.0050 | 97.296 |
| 3759 | LC35-28 | Fo | 55.301 | 41.812 | 0.0063 | 97.119 |
| 3759 | LC35-29 | Fo | 56.067 | 41.806 | 0.0051 | 97.878 |
| 3759 | LC35-30 | Fo | 56.041 | 42.177 | 0.0089 | 98.227 |
| 3759 | LC35-31 | Fo | 55.890 | 42.227 | 0.0114 | 98.129 |
| 3759 | LC35-32 | Fo | 56.409 | 41.949 | 0.0113 | 98.370 |
| 3759 | LC35-33 | Fo | 56.207 | 42.142 | 0.0130 | 98.362 |
| 3759 | LC35-34 | Fo | 54.316 | 42.137 | 0.0178 | 96.471 |
| 3759 | LC35-35 | En | 39.428 | 59.358 | 0.0417 | 98.829 |
| 3763 | LC36-1 | Fo | 55.054 | 41.784 | 0.0137 | 96.852 |
| 3763 | LC36-2 | Fo | 56.490 | 42.171 | 0.0118 | 98.673 |
| 3763 | LC36-3 | Fo | 56.705 | 42.141 | 0.0127 | 98.859 |
| 3763 | LC36-4 | Fo | 56.857 | 42.423 | 0.0139 | 99.294 |
| 3763 | LC36-5 | Fo | 57.228 | 42.397 | 0.0125 | 99.638 |
| 3763 | LC36-6 | Fo | 57.904 | 42.263 | 0.0101 | 100.177 |
| 3763 | LC36-7 | Fo | 56.945 | 42.801 | 0.0118 | 99.758 |
| 3763 | LC36-8 | Fo | 56.984 | 42.639 | 0.0110 | 99.634 |
| 3763 | LC36-9 | Fo | 57.456 | 42.547 | 0.0093 | 100.012 |
| 3763 | LC36-10 | Fo | 57.357 | 42.268 | 0.0095 | 99.635 |
| 3763 | LC36-11 | Fo | 57.616 | 42.703 | 0.0103 | 100.330 |
| 3763 | LC36-12 | Fo | 56.068 | 41.953 | 0.0155 | 98.037 |
| 3763 | LC36-13 | Fo | 58.867 | 42.797 | 0.0072 | 101.671 |
| 3763 | LC36-14 | Fo | 57.866 | 42.361 | 0.0206 | 100.248 |
| 3763 | LC36-15 | Fo | 56.989 | 41.808 | 0.0112 | 98.808 |
| 3763 | LC36-16 | Fo | 56.900 | 41.994 | 0.0030 | 98.897 |
| 3763 | LC36-17 | Fo | 57.975 | 42.336 | 0.0020 | 100.313 |
| 3762 | LC37-1 | En | 40.178 | 58.729 | 0.0286 | 98.936 |
| 3762 | LC37-2 | En | 40.624 | 58.968 | 0.0217 | 99.614 |
| 3762 | LC37-3 | En | 40.945 | 58.988 | 0.0227 | 99.956 |
| 3762 | LC37-4 | En | 41.244 | 57.855 | 0.0232 | 99.123 |
| 3762 | LC37-5 | En | 40.788 | 58.466 | 0.0192 | 99.274 |
| 3762 | LC37-6 | En | 39.963 | 58.695 | 0.0230 | 98.682 |
| 3762 | LC37-7 | En | 39.688 | 58.444 | 0.0259 | 98.159 |
| 3762 | LC37-8 | En | 39.231 | 58.505 | 0.0263 | 97.763 |
| 3762 | LC37-9 | En | 39.514 | 58.814 | 0.0237 | 98.352 |

| Run # | Analysis # | Phase | MgO (wt%) | $SiO_2$ (wt%) | CaO (wt%) | Total (wt%) |
|---|---|---|---|---|---|---|
| 3762 | LC37-10 | Fo | 55.234 | 41.906 | 0.0221 | 97.163 |
| 3762 | LC37-11 | Fo | 56.642 | 42.118 | 0.0157 | 98.776 |
| 3762 | LC37-12 | Fo | 57.477 | 42.087 | 0.0111 | 99.575 |
| 3762 | LC37-13 | Fo | 58.246 | 42.127 | 0.0123 | 100.385 |
| 3762 | LC37-14 | Fo | 57.332 | 42.445 | 0.0112 | 99.788 |
| 3762 | LC37-15 | Fo | 58.575 | 42.581 | 0.0066 | 101.163 |
| 3762 | LC37-16 | Fo | 57.174 | 42.642 | 0.0065 | 99.823 |
| 3762 | LC37-17 | Fo | 57.368 | 42.971 | 0.0083 | 100.347 |
| 3762 | LC37-18 | Fo | 58.260 | 42.719 | 0.0073 | 100.986 |
| 3762 | LC37-19 | Fo | 57.859 | 42.934 | 0.0073 | 100.800 |
| 3762 | LC37-20 | Fo | 58.209 | 42.598 | 0.0061 | 100.813 |
| 3762 | LC37-21 | Fo | 57.284 | 42.798 | 0.0043 | 100.086 |
| 3762 | LC37-22 | En | 40.738 | 60.132 | 0.0515 | 100.923 |
| 3762 | LC37-23 | En | 40.644 | 60.188 | 0.0514 | 100.885 |
| 3762 | LC37-24 | En | 40.771 | 60.216 | 0.0522 | 101.040 |
| 3762 | LC37-25 | En | 41.155 | 59.709 | 0.0501 | 100.915 |
| 3762 | LC37-26 | En | 41.209 | 59.725 | 0.0485 | 100.984 |
| 3762 | LC37-27 | En | 41.426 | 59.581 | 0.0448 | 101.053 |
| 3762 | LC37-28 | En | 41.368 | 59.649 | 0.0458 | 101.064 |
| 3762 | LC37-29 | En | 41.439 | 59.276 | 0.0426 | 100.759 |
| 3762 | LC37-30 | En | 41.515 | 59.261 | 0.0461 | 100.823 |
| 3762 | LC37-31 | En | 41.393 | 59.109 | 0.0167 | 100.519 |
| 3762 | LC37-32 | En | 41.620 | 59.164 | 0.0147 | 100.799 |
| 3762 | LC37-33 | q | 41.463 | 59.466 | 0.0251 | 100.955 |
| 3762 | LC37-34 | q | 39.990 | 58.741 | 0.0342 | 98.766 |
| 3762 | LC37-35 | q | 40.832 | 59.792 | 0.0491 | 100.674 |
| 3762 | LC37-36 | q | 39.823 | 58.933 | 0.0331 | 98.790 |
| 3762 | LC37-37 | q | 39.242 | 58.741 | 0.0356 | 98.019 |
| 3762 | LC37-38 | q | 39.461 | 58.649 | 0.0245 | 98.135 |
| 3762 | LC37-39 | q | 40.381 | 58.226 | 0.0267 | 98.634 |
| 3762 | LC37-40 | q | 39.481 | 58.609 | 0.0281 | 98.119 |
| 3762 | LC37-41 | q | 39.933 | 57.704 | 0.0300 | 97.668 |
| 3762 | LC37-42 | q | 56.779 | 40.664 | 0.0092 | 97.452 |
| 3762 | LC37-43 | q | 40.731 | 57.785 | 0.0278 | 98.544 |
| 3765 | LC38-1 | En | 40.899 | 59.571 | 0.0199 | 100.490 |
| 3765 | LC38-2 | En | 40.700 | 58.696 | 0.0200 | 99.417 |
| 3765 | LC38-3 | En | 40.926 | 58.335 | 0.0207 | 99.282 |
| 3765 | LC38-4 | En | 40.546 | 58.083 | 0.0220 | 98.652 |
| 3765 | LC38-5 | En | 39.698 | 58.249 | 0.0226 | 97.970 |
| 3765 | LC38-6 | En | 40.327 | 58.790 | 0.0204 | 99.138 |
| 3765 | LC38-7 | En | 39.815 | 58.719 | 0.0217 | 98.556 |
| 3765 | LC38-8 | Fo | 57.741 | 42.094 | 0.0110 | 99.846 |
| 3765 | LC38-9 | En | 39.910 | 58.560 | 0.0226 | 98.493 |
| 3765 | LC38-10 | En | 40.137 | 59.352 | 0.0221 | 99.512 |
| 3765 | LC38-11 | En | 39.976 | 59.677 | 0.0261 | 99.680 |
| 3765 | LC38-12 | En | 39.039 | 58.214 | 0.0208 | 97.274 |

| Run # | Analysis # | Phase | MgO (wt%) | $SiO_2$ (wt%) | CaO (wt%) | Total (wt%) |
|---|---|---|---|---|---|---|
| 3765 | LC38-13 | En | 39.292 | 58.853 | 0.0229 | 98.168 |
| 3765 | LC38-14 | En | 39.547 | 59.250 | 0.0222 | 98.820 |
| 3765 | LC38-15 | En | 39.383 | 58.851 | 0.0170 | 98.251 |
| 3765 | LC38-16 | En | 39.407 | 57.877 | 0.0278 | 97.312 |
| 3765 | LC38-17 | En | 39.957 | 59.817 | 0.0313 | 99.806 |
| 3765 | LC38-18 | En | 39.750 | 59.975 | 0.0178 | 99.743 |
| 3765 | LC38-19 | En | 39.152 | 59.289 | 0.0177 | 98.459 |
| 3765 | LC38-20 | Fo | 55.254 | 41.367 | 0.0036 | 96.625 |
| 3765 | LC38-21 | Fo | 55.831 | 41.156 | 0.0057 | 96.993 |
| 3765 | LC38-22 | Fo | 55.365 | 42.039 | 0.0231 | 97.428 |
| 3765 | LC38-23 | Fo | 55.323 | 41.789 | 0.0187 | 97.131 |
| 3765 | LC38-24 | Fo | 55.467 | 41.339 | 0.0081 | 96.814 |
| 3765 | LC38-25 | Fo | 57.095 | 41.378 | 0.0054 | 98.479 |
| 3765 | LC38-26 | Fo | 56.532 | 41.629 | 0.0050 | 98.166 |
| 3765 | LC38-27 | Fo | 56.426 | 42.035 | 0.0076 | 98.469 |
| 3765 | LC38-28 | Fo | 55.374 | 41.456 | 0.0029 | 96.833 |
| 3765 | LC38-29 | Fo | 55.718 | 41.196 | 0.0048 | 96.919 |
| 3765 | LC38-30 | Fo | 56.122 | 41.178 | 0.0150 | 97.315 |
| 3765 | LC38-31 | Fo | 56.740 | 41.722 | 0.0137 | 98.476 |
| 3765 | LC38-32 | Fo | 55.367 | 41.198 | 0.0139 | 96.579 |
| 3765 | LC38-33 | Fo | 57.157 | 41.753 | 0.0129 | 98.923 |
| 3765 | LC38-34 | q | 37.210 | 61.305 | 0.0317 | 98.548 |
| 3765 | LC38-35 | q | 38.896 | 60.545 | 0.0460 | 99.488 |
| 3765 | LC38-36 | q | 39.052 | 59.810 | 0.0295 | 98.892 |
| 3765 | LC38-37 | q | 39.405 | 59.500 | 0.0334 | 98.939 |
| 3770 | LC39-1 | En | 38.234 | 59.395 | 0.0146 | 97.644 |
| 3770 | LC39-2 | En | 37.813 | 58.953 | 0.0150 | 96.781 |
| 3770 | LC39-3 | En | 39.155 | 58.820 | 0.0142 | 97.989 |
| 3770 | LC39-4 | En | 39.596 | 58.913 | 0.0133 | 98.523 |
| 3770 | LC39-5 | En | 39.603 | 59.529 | 0.0131 | 99.145 |
| 3770 | LC39-6 | En | 40.410 | 59.608 | 0.0128 | 100.031 |
| 3770 | LC39-7 | En | 39.172 | 60.069 | 0.0131 | 99.254 |
| 3770 | LC39-8 | En | 39.360 | 60.252 | 0.0138 | 99.626 |
| 3770 | LC39-9 | En | 38.575 | 59.984 | 0.0135 | 98.573 |
| 3770 | LC39-10 | En | 38.251 | 59.247 | 0.0141 | 97.512 |
| 3770 | LC39-11 | En | 38.398 | 59.246 | 0.0136 | 97.658 |
| 3770 | LC39-12 | En | 38.444 | 59.531 | 0.0145 | 97.990 |
| 3770 | LC39-13 | En | 38.478 | 59.538 | 0.0140 | 98.030 |
| 3770 | LC39-14 | En | 38.528 | 59.594 | 0.0157 | 98.138 |
| 3770 | LC39-15 | En | 38.744 | 59.688 | 0.0162 | 98.449 |
| 3770 | LC39-16 | En | 39.404 | 59.736 | 0.0162 | 99.157 |
| 3770 | LC39-17 | En | 39.833 | 59.440 | 0.0164 | 99.290 |
| 3770 | LC39-18 | Fo | 56.596 | 41.596 | 0.0042 | 98.196 |
| 3770 | LC39-19 | Fo | 55.413 | 42.006 | 0.0051 | 97.424 |
| 3770 | LC39-20 | Fo | 54.836 | 42.089 | 0.0036 | 96.929 |
| 3770 | LC39-21 | Fo | 55.058 | 42.561 | 0.0030 | 97.622 |

| Run # | Analysis # | Phase | MgO (wt%) | $SiO_2$ (wt%) | CaO (wt%) | Total (wt%) |
|---|---|---|---|---|---|---|
| 3770 | LC39-22 | Fo | 55.516 | 42.796 | 0.0054 | 98.317 |
| 3770 | LC39-23 | Fo | 55.763 | 42.668 | 0.0043 | 98.435 |
| 3770 | LC39-24 | Fo | 56.250 | 42.825 | 0.0047 | 99.080 |
| 3770 | LC39-25 | Fo | 56.771 | 42.725 | 0.0043 | 99.500 |
| 3770 | LC39-26 | Fo | 57.467 | 42.825 | 0.0038 | 100.296 |
| 3770 | LC39-27 | Fo | 57.642 | 42.432 | 0.0038 | 100.078 |
| 3770 | LC39-28 | Fo | 57.295 | 43.069 | 0.0048 | 100.369 |
| 3770 | LC39-29 | Fo | 56.673 | 43.197 | 0.0049 | 99.875 |
| 3770 | LC39-30 | Fo | 56.346 | 43.203 | 0.0049 | 99.554 |
| 3770 | LC39-31 | Fo | 55.809 | 43.172 | 0.0037 | 98.985 |
| 3770 | LC39-32 | q | 40.488 | 59.741 | 0.0261 | 100.256 |
| 3770 | LC39-33 | q | 40.023 | 55.048 | 0.0927 | 95.166 |
| 3770 | LC39-34 | q | 39.655 | 59.032 | 0.0273 | 98.715 |
| 3770 | LC39-35 | q | 40.091 | 60.536 | 0.0218 | 100.649 |
| 3770 | LC39-36 | q | 39.985 | 61.839 | 0.0367 | 101.862 |
| 3770 | LC39-37 | q | 39.530 | 60.028 | 0.0232 | 99.582 |
| 3770 | LC39-38 | q | 39.378 | 58.750 | 0.0719 | 98.202 |
| 3770 | LC39-39 | q | 39.581 | 58.781 | 0.0209 | 98.383 |
| 3770 | LC39-40 | q | 40.283 | 61.809 | 0.0389 | 102.132 |
| 3770 | LC39-41 | q | 39.422 | 61.361 | 0.0273 | 100.811 |
| 3770 | LC39-42 | q | 38.457 | 60.851 | 0.0202 | 99.329 |
| 3770 | LC39-43 | q | 39.566 | 60.576 | 0.0649 | 100.208 |
| 3770 | LC39-44 | q | 39.178 | 61.108 | 0.0659 | 100.354 |
| 3770 | LC39-45 | q | 40.106 | 61.405 | 0.0190 | 101.531 |
| 3770 | LC39-46 | q | 39.741 | 61.163 | 0.0476 | 100.953 |
| 3770 | LC39-47 | q | 39.088 | 61.286 | 0.0211 | 100.396 |
| 3770 | LC39-48 | q | 39.725 | 60.745 | 0.0206 | 100.491 |
| 3770 | LC39-49 | q | 39.838 | 60.495 | 0.0218 | 100.355 |
| 3770 | LC39-50 | q | 40.805 | 59.468 | 0.0287 | 100.302 |
| 3770 | LC39-51 | q | 39.976 | 59.330 | 0.0341 | 99.341 |
| 3771 | LC40-1 | Fo | 52.987 | 41.263 | 0.0031 | 94.253 |
| 3771 | LC40-2 | Fo | 53.841 | 42.015 | 0.0023 | 95.858 |
| 3771 | LC40-3 | Fo | 53.707 | 42.416 | 0.0026 | 96.126 |
| 3771 | LC40-4 | Fo | 54.036 | 42.665 | 0.0027 | 96.704 |
| 3771 | LC40-5 | Fo | 54.469 | 43.213 | 0.0030 | 97.685 |
| 3771 | LC40-6 | Fo | 55.827 | 42.440 | 0.0022 | 98.269 |
| 3771 | LC40-7 | q | 38.539 | 60.513 | 0.0834 | 99.137 |
| 3771 | LC40-8 | Fo | 56.168 | 42.730 | 0.0026 | 98.901 |
| 3771 | LC40-9 | Fo | 54.885 | 42.124 | 0.0035 | 97.013 |
| 3771 | LC40-10 | Fo | 55.355 | 42.288 | 0.0027 | 97.646 |
| 3771 | LC40-11 | Fo | 55.638 | 42.440 | 0.0030 | 98.081 |
| 3771 | LC40-12 | Fo | 55.836 | 42.461 | 0.0033 | 98.300 |
| 3771 | LC40-13 | Fo | 56.218 | 42.594 | 0.0031 | 98.815 |
| 3771 | LC40-14 | Fo | 56.621 | 42.461 | 0.0036 | 99.086 |
| 3771 | LC40-15 | Fo | 56.981 | 42.452 | 0.0036 | 99.437 |
| 3771 | LC40-16 | Fo | 57.428 | 42.446 | 0.0036 | 99.878 |

| Run # | Analysis # | Phase | MgO (wt%) | $SiO_2$ (wt%) | CaO (wt%) | Total (wt%) |
|---|---|---|---|---|---|---|
| 3771 | LC40-17 | Fo | 57.588 | 42.709 | 0.0035 | 100.301 |
| 3771 | LC40-18 | Fo | 57.148 | 42.973 | 0.0038 | 100.125 |
| 3771 | LC40-19 | Fo | 56.181 | 43.209 | 0.0029 | 99.393 |
| 3771 | LC40-20 | Fo | 55.733 | 43.165 | 0.0042 | 98.902 |
| 3771 | LC40-21 | Fo | 55.164 | 43.147 | 0.0033 | 98.314 |
| 3771 | LC40-22 | Fo | 54.539 | 43.595 | 0.0028 | 98.137 |
| 3771 | LC40-23 | Fo | 55.132 | 43.882 | 0.0032 | 99.017 |
| 3771 | LC40-24 | Fo | 55.601 | 43.992 | 0.0040 | 99.597 |
| 3771 | LC40-25 | q | 38.592 | 61.471 | 0.0601 | 100.125 |
| 3771 | LC40-26 | q | 38.681 | 61.525 | 0.0572 | 100.265 |
| 3771 | LC40-27 | q | 38.561 | 61.262 | 0.0757 | 99.901 |
| 3771 | LC40-28 | Fo | 55.584 | 42.323 | 0.0049 | 97.912 |
| 3771 | LC40-29 | Fo | 55.667 | 42.840 | 0.0039 | 98.511 |
| 3771 | LC40-30 | Fo | 55.811 | 42.919 | 0.0039 | 98.734 |
| 3771 | LC40-31 | Fo | 55.775 | 42.999 | 0.0036 | 98.778 |
| 3771 | LC40-32 | Fo | 55.156 | 43.121 | 0.0054 | 98.283 |
| 3771 | LC40-33 | Fo | 56.853 | 41.893 | 0.0045 | 98.751 |
| 3771 | LC40-34 | Fo | 56.102 | 42.439 | 0.0036 | 98.545 |
| 3771 | LC40-35 | Fo | 56.848 | 42.647 | 0.0038 | 99.499 |
| 3771 | LC40-36 | Fo | 56.933 | 42.207 | 0.0032 | 99.143 |
| 3771 | LC40-37 | Fo | 57.130 | 42.279 | 0.0035 | 99.413 |
| 3771 | LC40-38 | Fo | 56.502 | 42.586 | 0.0032 | 99.091 |
| 3771 | LC40-39 | Fo | 56.631 | 42.686 | 0.0030 | 99.320 |
| 3771 | LC40-40 | Fo | 56.694 | 42.836 | 0.0022 | 99.532 |
| 3771 | LC40-41 | Fo | 56.747 | 43.005 | 0.0035 | 99.756 |
| 3771 | LC40-42 | Fo | 56.806 | 42.888 | 0.0038 | 99.698 |
| 3771 | LC40-43 | Fo | 56.384 | 43.041 | 0.0033 | 99.428 |
| 3771 | LC40-44 | Fo | 56.464 | 43.076 | 0.0039 | 99.544 |
| 3771 | LC40-45 | Fo | 56.711 | 42.985 | 0.0038 | 99.700 |
| 3771 | LC40-46 | Fo | 56.635 | 43.159 | 0.0043 | 99.798 |
| 3771 | LC40-47 | Fo | 56.593 | 43.155 | 0.0055 | 99.754 |
| 3771 | LC40-48 | Fo | 56.905 | 43.148 | 0.0050 | 100.058 |
| 3771 | LC40-49 | Fo | 56.786 | 43.230 | 0.0042 | 100.020 |
| 3771 | LC40-50 | Fo | 56.647 | 43.335 | 0.0034 | 99.985 |
| 3771 | LC40-51 | Fo | 56.167 | 43.528 | 0.0041 | 99.699 |
| 3771 | LC40-52 | Fo | 57.625 | 43.416 | 0.0047 | 101.046 |
| 3771 | LC40-53 | q | 40.209 | 59.541 | 0.0892 | 99.841 |
| 3771 | LC40-54 | q | 39.857 | 59.696 | 0.0939 | 99.649 |
| 3771 | LC40-55 | q | 40.891 | 59.689 | 0.0782 | 100.660 |
| 3771 | LC40-56 | q | 43.776 | 53.220 | 0.0612 | 97.059 |
| 3771 | LC40-57 | q | 39.790 | 59.328 | 0.0607 | 99.180 |
| 3771 | LC40-58 | q | 40.399 | 60.736 | 0.0217 | 101.157 |
| 3771 | LC40-59 | q | 41.346 | 60.158 | 0.0309 | 101.536 |
| 3771 | LC40-60 | q | 40.178 | 60.472 | 0.0222 | 100.673 |
| 3771 | LC40-61 | q | 41.289 | 60.328 | 0.0222 | 101.640 |
| 3771 | LC40-62 | q | 39.495 | 61.010 | 0.0727 | 100.579 |

| Run # | Analysis # | Phase | MgO (wt%) | $SiO_2$ (wt%) | CaO (wt%) | Total (wt%) |
|---|---|---|---|---|---|---|
| 3772 | LC41-1 | Fo | 58.131 | 44.784 | 0.0038 | 102.919 |
| 3772 | LC41-2 | Fo | 57.574 | 44.600 | 0.0043 | 102.178 |
| 3772 | LC41-3 | Fo | 57.137 | 44.741 | 0.0036 | 101.882 |
| 3772 | LC41-4 | Fo | 56.476 | 44.717 | 0.0039 | 101.197 |
| 3772 | LC41-5 | Fo | 55.871 | 44.495 | 0.0034 | 100.369 |
| 3772 | LC41-6 | Fo | 55.176 | 44.384 | 0.0029 | 99.563 |
| 3772 | LC41-7 | Fo | 54.170 | 44.358 | 0.0034 | 98.531 |
| 3772 | LC41-8 | Fo | 53.888 | 44.273 | 0.0036 | 98.165 |
| 3772 | LC41-9 | Fo | 59.359 | 43.615 | 0.0039 | 102.978 |
| 3772 | LC41-10 | Fo | 59.661 | 43.364 | 0.0040 | 103.029 |
| 3772 | LC41-11 | Fo | 59.135 | 43.201 | 0.0042 | 102.340 |
| 3772 | LC41-12 | Fo | 58.813 | 43.077 | 0.0043 | 101.894 |
| 3772 | LC41-13 | Fo | 60.326 | 42.929 | 0.0041 | 103.259 |
| 3772 | LC41-14 | Fo | 60.214 | 42.842 | 0.0050 | 103.061 |
| 3772 | LC41-15 | Fo | 60.042 | 42.715 | 0.0035 | 102.761 |
| 3772 | LC41-16 | Fo | 60.089 | 42.637 | 0.0043 | 102.730 |
| 3772 | LC41-17 | Fo | 60.247 | 42.467 | 0.0046 | 102.719 |
| 3772 | LC41-18 | Fo | 60.501 | 42.102 | 0.0044 | 102.607 |
| 3772 | LC41-19 | Fo | 58.941 | 42.111 | 0.0037 | 101.056 |
| 3772 | LC41-20 | Fo | 59.237 | 41.468 | 0.0033 | 100.708 |
| 3772 | LC41-21 | Fo | 58.585 | 41.799 | 0.0036 | 100.388 |
| 3772 | LC41-22 | Fo | 57.451 | 42.156 | 0.0040 | 99.611 |
| 3772 | LC41-23 | Fo | 56.066 | 41.883 | 0.0028 | 97.952 |
| 3772 | LC41-24 | Fo | 56.656 | 42.466 | 0.0036 | 99.126 |
| 3772 | LC41-25 | Fo | 56.831 | 42.531 | 0.0033 | 99.365 |
| 3772 | LC41-26 | Fo | 56.935 | 42.521 | 0.0044 | 99.460 |
| 3772 | LC41-27 | Fo | 57.030 | 42.469 | 0.0039 | 99.503 |
| 3772 | LC41-28 | Fo | 56.696 | 42.449 | 0.0042 | 99.149 |
| 3772 | LC41-29 | Fo | 56.830 | 42.557 | 0.0034 | 99.390 |
| 3772 | LC41-30 | Fo | 57.333 | 42.781 | 0.0030 | 100.117 |
| 3772 | LC41-31 | Fo | 56.489 | 42.844 | 0.0028 | 99.336 |
| 3772 | LC41-32 | Fo | 56.987 | 42.992 | 0.0037 | 99.983 |
| 3772 | LC41-33 | Fo | 56.749 | 43.160 | 0.0043 | 99.913 |
| 3772 | LC41-34 | Fo | 52.059 | 42.210 | 0.0044 | 94.273 |
| 3772 | LC41-35 | Fo | 51.200 | 41.812 | 0.0039 | 93.016 |
| 3772 | LC41-36 | Fo | 56.234 | 42.610 | 0.0032 | 98.847 |
| 3772 | LC41-37 | Fo | 56.082 | 42.208 | 0.0043 | 98.294 |
| 3772 | LC41-38 | Fo | 56.977 | 44.071 | 0.0030 | 101.051 |
| 3772 | LC41-39 | Fo | 56.268 | 43.735 | 0.0032 | 100.006 |
| 3772 | LC41-40 | Fo | 56.588 | 43.691 | 0.0037 | 100.283 |
| 3772 | LC41-41 | Fo | 56.854 | 43.532 | 0.0019 | 100.388 |
| 3772 | LC41-42 | Fo | 57.102 | 43.167 | 0.0039 | 100.273 |
| 3772 | LC41-43 | Fo | 57.318 | 42.999 | 0.0029 | 100.320 |
| 3772 | LC41-44 | Fo | 56.968 | 42.827 | 0.0032 | 99.798 |
| 3772 | LC41-45 | Fo | 57.004 | 42.327 | 0.0036 | 99.335 |
| 3772 | LC41-46 | Fo | 56.760 | 42.996 | 0.0033 | 99.759 |

| Run # | Analysis # | Phase | MgO (wt%) | $SiO_2$ (wt%) | CaO (wt%) | Total (wt%) |
|---|---|---|---|---|---|---|
| 3772 | LC41-47 | Fo | 56.965 | 42.763 | 0.0031 | 99.731 |
| 3772 | LC41-48 | Fo | 55.983 | 42.489 | 0.0031 | 98.475 |
| 3772 | LC41-49 | Fo | 55.395 | 42.287 | 0.0035 | 97.686 |
| 3772 | LC41-50 | Fo | 57.093 | 42.129 | 0.0041 | 99.226 |
| 3772 | LC41-51 | Fo | 56.725 | 42.055 | 0.0045 | 98.785 |
| 3772 | LC41-52 | Fo | 57.277 | 41.878 | 0.0030 | 99.158 |
| 3772 | LC41-53 | Fo | 57.497 | 42.731 | 0.0033 | 100.231 |
| 3772 | LC41-54 | Fo | 58.002 | 42.180 | 0.0027 | 100.185 |
| 3772 | LC41-55 | Fo | 57.757 | 41.568 | 0.0041 | 99.329 |
| 3772 | LC41-56 | Fo | 57.337 | 40.896 | 0.0040 | 98.237 |
| 3772 | LC41-57 | Fo | 57.257 | 40.891 | 0.0046 | 98.153 |

Abbreviations: *En* enstatite in primary phase, *Fo* forsterite in primary phase, *q* quenched phases.

Note: CaO (wt%) is calculated from counts reported by microprobe.